Ecological differentiation and local adaptation mediate incipient speciation in the *Gladiolus carneus* (Iridaceae) species complex

THESIS

Submitted in fulfilment of the requirements for the degree of

MASTER OF SCIENCE

In Botany

at

RHODES UNIVERSITY

by

Katharine L. Khoury

February 2024

Under the supervision of Dr Ethan Newman

PREFACE

The research contained in '**Ecological differentiation and local adaptation mediate incipient speciation in the *Gladiolus carneus* (Iridaceae) species complex**' was completed by the candidate while based in the Discipline of Evolutionary Ecology, Department of Botany, Rhodes University, Makhanda, South Africa. The research was financially supported by the Botanical Education Trust (KLK) and NRF-Thuthuka Grant TTK210211585733 (ELN).

The contents of this work have not been submitted in any form to another university and, except where the work of others is acknowledged in the text, the results reported are due to investigations by the candidate.

Supervisor: Dr Ethan Newman

Signed:

Date: 14 February 2025

PLAGIARISM DECLARATION

I, Katharine L. Khoury, declare that:

(i) the research reported in this dissertation, except where otherwise indicated or acknowledged, is my original work;

(ii) this dissertation has not been submitted in full or in part for any degree or examination to any other university;

(iii) this dissertation does not contain other persons' data, pictures, graphs or other information, unless specifically acknowledged as being sourced from other persons;

(iv) this dissertation does not contain other persons' writing, unless specifically acknowledged as being sourced from other researchers. Where other written sources have been quoted, then:

a) their words have been re-written but the general information attributed to them has been referenced;

b) where their exact words have been used, their writing has been placed inside quotation marks, and referenced;

(v) where I have used material for which publications followed, I have indicated in detail my role in the work;

(vi) this dissertation is primarily a collection of material, prepared by myself, published as journal articles or presented as a poster and oral presentations at conferences. In some cases, additional material has been included;

(vii) this dissertation does not contain text, graphics or tables copied and pasted from the Internet, unless specifically acknowledged, and the source being detailed in the dissertation and in the references sections.

Candidate: Katharine L. Khoury

Signed: 

Date of submission: 14 February 2025

PUBLICATIONS

Chapter 2 and 3 were written for publication in appropriate journals.

Chapter 2 has been published in *Annals of Botany*.

Khoury, K. L., Edwards, S., & Newman, E. L. (in press). Ecological niche differentiation mediates near complete premating reproductive isolation within the *Gladiolus carneus* (Iridaceae) species complex. *Annals of Botany*, https://doi.org/10.1093/aob/mcaf172

The author contributions are as follows: E.N. and K.L.K. conceptualized the study. K.L.K. and E.N. collected the data. K.L.K. analysed all data and wrote the paper with input from E.N. All authors provided input on editing the manuscript.

Chapter 3 of this thesis has been submitted for publication.

The author contributions are as follows: KLK and EN conceptualised the study. KLK collected and analysed the data. KLK wrote the paper with input from EN.

ABSTRACT

Ecological speciation is the process whereby ecologically-based divergent natural selection acting on populations results in the formation of new species. In the hyper-diverse Cape Floristic Region (CFR), the interactions between topographic, climatic, edaphic and biotic heterogeneity at fine-spatial scales is hypothesised to be a major driver of ecological speciation. However, investigations into the mechanisms mediating this diversity has largely focused on either identifying macroevolutionary drivers in a phylogenetic context or by documenting trait-by-environment associations between closely related taxa that are suggestive of local adaptation. To date, there has been relatively few studies that directly test whether ecologically-driven divergence causes local adaptation or reproductive isolation in the CFR. In this thesis, I use *Gladiolus carneus*, a polymorphic geophyte that occurs along the entire elevational gradient of the CFR, to investigate whether ecological niche differentiation causes local adaptation and premating reproductive isolation.

Specifically, in Chapter 2, I investigate whether ecological niche differentiation of the putative ecotypes of *G. carneus* causes strong premating reproductive isolation across the species complex. I found that the ecotypes of *G. carneus* are morphologically distinct and that they occupy distinct predicted and realised abiotic niches, resulting in, with only a few exceptions, strong ecogeographic isolation. I further found that the ecotypes occupy distinct phenological niches leading to moderate phenological isolation. For the pollinator niche, I found that all sampled populations were associated with a single highly effective functional pollinator, but at the ecotypic level, there were no consistent trends resulting in varying strengths of pollinator-mediated isolation. The strength of the ecogeographic, phenological and pollinator isolation lead to near complete premating reproductive isolation across the species

complex. This chapter showcases that ecological niche differentiation can cause reproductive isolation between recently diverged taxa in the CFR.

In Chapter 3, I used a common garden and a multi-year reciprocal translocation to test whether ecotypes of *G. carneus* that occur along an elevational gradient were locally adapted to their edaphic niche. In the common garden experiment, I found evidence that the ecotypes occupying the most extreme edaphic niches had a fitness advantage on their native soil. In the reciprocal translocations, I found that all ecotypes showed evidence of local adaptation. The two most elevationally extreme ecotypes had a fitness advantage both on their native soil, and at their native site. These results suggest that edaphic properties, along with other abiotic factors, can cause local adaptation in the CFR.

Overall, my thesis provides evidence that niche differentiation can cause local adaptation and premating reproductive isolation between recently diverged taxa and that abiotic niche differentiation is likely a major driver of the early stages of speciation in the CFR.

ACKNOWLEDGEMENTS

Firstly and most importantly, I thank my supervisor, Ethan Newman, for guiding me through this journey. Your unending enthusiasm, passion and knowledge has inspired me. Thank you for your constant belief, patience, and support. You have been the best possible mentor through this journey.

Secondly, I would like to thank the Department of Botany. The academic, technical and administrative staff along with the postgraduates have been instrumental in creating a welcoming and productive environment. I would particularly like to thank Craig Peter for always making time to answer my questions. I would also like to thank Riaan Strauss and Barry Hartley for technical assistance.

Thank you to Cindy Fourie and Marelise Faul for assisting with data collection, and Connal Eardley for providing bee identifications. I would like to thank Jamie Venter, Josie Makkink, the Newman family and the Hansford family for accommodation during field work.

To Kaelin du Plessis, Zoë Landsberg, Jordan McCullough, Mallory Hansford, and Tafadzwa Thabethe – thank you for being an incredible support system in the last few years. Thank you for helping with field work, data collection, accommodation and most importantly, endless emotional support.

To my family, thank you for your lifelong support. Robyn Khoury, thank you for always having an open door for me. To my parents, Chris and Gill Khoury, you are my rock and biggest cheerleaders.

Finally, I thank the Ada and Bertie Levenstein Fund and the Botanical Education Trust for providing personal and research funding, and Cape Nature (CN35-87-18949; CN44-87-18954) and SANPARKS (CRC/2022-2023/018--2021/V1) for providing permits to conduct this research.

TABLE OF CONTENTS

LIST OF FIGURES

LIST OF TABLES

CHAPTER 1:

Ecological speciation in the Cape Floristic Region

ECOLOGICAL SPECIATION

Ecological speciation is the process whereby new species form due to ecologically-based divergent selection and is largely considered to be the major driver of speciation (Schluter, 2000, Schluter, 2001, Coyne and Orr, 2004, Rundle and Nosil, 2005, Sobel *et al.*, 2010). The process starts when ecologically-based divergent selection acts on populations resulting in phenotypic differences that give those populations a fitness advantage in their native habitat, resulting in local adaptation and ecotype formation (Kawecki and Ebert, 2004). This divergent selection is often imposed by shifts in ecological niches which encompass both abiotic and biotic factors (E.g.: pollinators) (Godsoe, 2010, Johnson, 2010). Shifts in divergent ecological niches can cause a variety of gene flow barriers which are commonly, although not exclusively, premating reproductive isolation barriers (Schluter, 2001, Coyne and Orr, 2004, Rundle and Nosil, 2005), which either prevent taxa from co-occurring or reduce gene flow between co-occurring heterospecific and conspecific taxa (Sobel and Chen, 2014). Premating barriers are often the strongest forms of reproductive isolation between taxa (Christie *et al.*, 2022) and can lead to near complete gene flow cessation (Ramsey *et al.*, 2003, Kay, 2006, Briscoe Runquist *et al.*, 2014, Sobel and Streisfeld, 2015, Newman and Johnson, 2024), potentially resulting in 'good species' (Lowry, 2012). However, this is debated (*see* Lowry, 2012), as some argue that speciation is not complete until taxa can stably coexist in sympatry (Coyne and Orr, 2004, Mallet and Mullen, 2022) or exhibit strong postzygotic isolation (Lowry, 2012). While divergent selection and ecotype formation are essential steps that act early in the ecological speciation process, they do not necessarily result in strong reproductive isolation as ongoing gene flow can cause introgression and the breakdown of species barriers (Lowry, 2012). These variations on the biological species concept reflect that speciation is a fundamentally continuous processes (Thompson, 2013). Therefore, by linking ecological divergence and local

adaptation to the strength of reproductive isolation, we can start to understand divergence at the earliest stages the speciation.

ECOLOGICAL SPECIATION IN THE CAPE FLORISTIC REGION

The Cape Floristic Region (CFR) is one of the most biodiverse areas in the world, with more than 9000 species in an area of only 90 000km^2 with 69% of all species being endemic (Goldblatt and Manning, 2002, Manning and Goldblatt, 2012). Interestingly, the diversity in the CFR is restricted to relatively few lineages, with 33 'Cape Floral Clades' accounting for nearly half of all species (Goldblatt and Manning, 2002, Linder, 2003). The exceptional diversity has long been attributed to a combination of high speciation rates, caused by complex topography and environmental heterogeneity, accompanied by low extinction rates, likely due to the climatic stability in the Pleistocene (Linder, 2003, Ellis *et al.*, 2014). Speciation in the CFR has likely been driven by ecologically-imposed divergent selection created by a complex set of interactions between topography, climate, fire, and edaphic heterogeneity at fine spatial scales (Linder, 2003, Ellis *et al.*, 2014).

The CFR is characterised by sets of folded mountain belts that run parallel to the coast. Two of which run along the Indian Ocean coast and one along the Atlantic coast (Linder, 2003). The mountain peaks generally reach 1500m with only the highest peaks exceeding 2000m (Linder, 2003). These peaks are high enough for freezing winter temperatures to affect local vegetation (Manning and Goldblatt, 2012). The erosion-resistant sandstone of the mountain ranges gives rise to the most nutrient-poor soils currently recorded on earth (Cramer *et al.*, 2014), with particularly low phosphorus concentrations (Linder, 2003, Cramer *et al.*, 2014). However, the soils in the coastal planes and intermontane valleys are generally derived from

shale and are moderately fertile (Cramer *et al.*, 2014), creating a mosaic of edaphic conditions. Rainfall in the CFR varies along both an east-west and topographic gradient. In the west, there is a strongly seasonal Mediterranean climate with winter rainfall and hot, dry summers, while in the east, the climate is much more aseasonal with rainfall throughout the year (Manning and Goldblatt, 2012). Further variation is created by steep mountainous landscapes, resulting in orographic rainfall (Manning and Goldblatt, 2012). Additionally, fires occur roughly every 10 to 20 years in the CFR, creating disturbance in an already heterogenous environment (Kraaij and van Wilgen, 2014). These conditions have facilitated complex biotic and abiotic interactions at fine-spatial scales. Despite this ecological complexity, most research has focussed on relatively few drivers, including topographic and climatic heterogeneity, edaphic heterogeneity and pollinator-mediated divergence (Linder, 2003, van der Niet and Johnson, 2009, Schnitzler *et al.*, 2011, Ellis *et al.*, 2014).

Topographic and climatic heterogeneity

The complex topography of the Cape Fold Mountains is thought to create steep selective gradients that have allowed for adaptive diversification (Linder, 2003, Ellis *et al.*, 2014). A myriad of techniques, including phylogenetics, population genetics, field experiments and environmental niche models, have been used to test whether habitat transitions (caused specifically by differences in climate and topography) are associated with the diversification of plant lineages within the CFR. Population genetic analyses have provided evidence that topographic and climatic factors prevent gene flow between *Protea repens* populations (Prunier *et al.*, 2017) and phylogenetic evidence has shown habitat transitions are frequently associated with speciation events in the CFR (van der Niet and Johnson, 2009, Bouchenak-Khelladi and Linder, 2017).

There are a number of studies that test for trait-by-environment associations along environmental gradients. Mitchell *et al.* (2015) found both parallel and genus-specific associations between functional traits and climatic variables in *Protea* and *Pelargonium*. Furthermore, within *Protea*, trait-by-environment associations have been shown across climatic (Carlson *et al.*, 2011) and aridity gradients (Carlson *et al.*, 2016). These trait-by-environment associations are largely consistent with the patterns expected by local adaptation, however, explicit tests of local adaptation in the CFR are rare. These tests can take the form of reciprocal translocations or common garden experiments which test whether local genotypes have a fitness advantage over immigrant genotypes (*see* Kawecki and Ebert, 2004). The reciprocal translocations are used to identify whether specific populations are locally adapted in the field, while the common gardens are used to isolate the environmental agents of selection causing local adaptation (Kawecki and Ebert, 2004). Latimer *et al.* (2009), which used a reciprocal translocation to identify the factors limiting the distribution of *Protea* species along an environmental gradient, is the only study to date that has tested for local adaptation in contrasting abiotic niches in the CFR. Although Latimer *et al.* (2009) found a home-site advantage for all species, they also found that the *Protea* species could maintain positive growth rates at sites outside of their current distributions, suggesting that their current range limits were not solely due to abiotic factors.

Another approach that can determine if closely related taxa can occupy the same abiotic niches is environmental niche modelling. These niche models can be used to measure ecogeographic isolation, an early acting gene flow barrier caused by a reduction in encounter rates between taxa due to spatial separation resulting from intrinsic biological differences (Sobel, 2014). Unfortunately, these models have rarely been used to test for differences in the abiotic niche between closely related taxa in the CFR (*but see* Duffy and Johnson, 2017, Shaik,

2019, Newman and Johnson, 2024). This is somewhat surprising considering that these models can be built using occurrence records (GBIF, iNaturalist), bioclimatic variables (Fick and Hijmans, 2017), global (Hengl *et al.*, 2017) and regional soil layers (Cramer *et al.*, 2019) that are all publicly available. Despite topographical and climatic heterogeneity being hypothesised as a major driver of speciation, the lack of formal tests of local adaptation and niche overlap leaves major gaps in our understanding of the early stages of speciation in the CFR. Furthermore, ecogeographic isolation and immigrant inviability, the gene flow barriers linked to niche overlap and local adaptation, have been shown as the strongest gene flow barriers across seed plants (Christie *et al.*, 2022), and are likely to play major roles as isolating mechanisms at the early stages of speciation.

Edaphic heterogeneity

Although most soils in the CFR are highly leached and infertile, complex geological and geomorphic processes have led to widespread edaphic heterogeneity (Cramer *et al.*, 2014). This heterogeneity is hypothesised to be another major driver of diversification, however, the extent of its contribution has long been questioned (Ellis *et al.*, 2014). Many Cape clades are restricted to a specific soil types (*Mesembryanthemum*, *Oxalis* and Scrophylariaceae are largely found on shale-derived soils; and Restionaceae, Ericaceae, and Proteaceae on sandstone-derived soils), which results in an ecological filter (Linder, 2003). This filter has been demonstrated by Verboom *et al.* (2017) which found that Cape lineages showing specialisation to extremely nutrient-poor fynbos soils had reduced evolutionary lability in their nutritional traits. This ecological filter makes edaphically driven speciation unlikely in fynbos-specialist lineages.

The phylogenetic evidence provides mixed support for the frequency of edaphic shifts in the CFR. van der Niet and Johnson (2009) showed edaphic shifts in only 17% of sister

species pairs from eight Cape clades, and further found that habitat shifts, pollinator and fire-survival strategy shifts, occurred more frequently than edaphic shifts. This was further corroborated by Forest *et al.* (2014) which also showed that pollinator shifts were more common than edaphic shifts in *Lapeirousia*. In contrast, Schnitzler *et al.* (2011) showed edaphic shifts between 20 - 72% of sister species from four Cape clades making edaphic shifts the most frequent in three of the clades.

There is limited experimental evidence for edaphic shifts driving the diversification of the CFR. The best evidence comes from Verboom *et al.* (2004) which showed that seedlings from eight *Ehrharta* species grown under controlled nutrient-rich conditions differed in their relative growth rates and were associated with different adult-stage growth forms. The authors further showed shifts from the slow to the fast growth form only occurred after transitioning from nutrient-poor, sandstone-derived soils to richer, shale and granite-derived soils. Similar associations between life history traits, climate and substrate have also been further demonstrated in *Ehrharta* and *Pentameris* sp. (Verboom *et al.*, 2012). Despite edaphic shifts potentially playing a major role in the diversification of the CFR, there are currently no examples testing for local adaptation on contrasting edaphic niches. The only examples testing for local adaptation between contrasting edaphic environments within the Greater Cape Floristic Region (GCFR) are from the Succulent Karoo (Ellis and Weis, 2006, Musker *et al.*, 2021) and are not necessarily applicable to the CFR, due to paleoenvironmental differences between fynbos and succulent karoo biomes (Verboom *et al.*, 2009). Further experimental tests, including those testing for edaphic shifts and local adaptation, are needed to ascertain the role of edaphic heterogeneity in the early stages of speciation in the CFR.

Pollinator-driven divergence

Pollinator-driven divergence is the most well tested driver of diversification in the CFR. It was initially proposed as a major mechanism of divergence, as many Cape lineages display substantial floral diversity, but limited vegetative diversity (Johnson, 1996). There are a number of different mechanisms that can lead to floral divergence (Johnson, 2010) including, pollinator shifts (Johnson and Steiner, 1997), differential use of the same pollinator (Anderson *et al.*, 2016, Minnaar *et al.*, 2019), coevolution (Pauw *et al.*, 2009), trait tracking (Anderson *et al.*, 2014), and mimicry of different model flowers (Newman *et al.*, 2012, Newman and Johnson, 2024). The basis of these mechanisms are associated with spatio-temporal variation in pollinator-mediated selection on floral traits that have been imposed through the behaviours and morphology of pollinators (Johnson, 2025). Although these mechanisms have been demonstrated in the CFR, they have rarely been conclusively linked to local adaptation, or the strength of reproductive isolation (Ellis *et al.*, 2014).

The best evidence for pollinator-driven speciation in the CFR comes from phylogenetic studies showing pollinator shifts across lineages (van der Niet and Johnson, 2009, Valente *et al.*, 2012, Forest *et al.*, 2014), however the frequency of these shifts has been questioned (Schnitzler *et al.*, 2011). Although pollinator shifts in particular have been frequently demonstrated in the CFR, there are only a few studies that have used reciprocal translocations to test whether these shifts result in local adaptation (Waterman *et al.*, 2011, Newman *et al.*, 2012, Newman *et al.*, 2015). The best evidence in the CFR comes from Newman *et al.* (2015) which showed that reciprocally transplanted *Nerine humilis* populations with divergent pollinator communities had a higher seed set at their home site. Furthermore, Waterman *et al.* (2011), showed that reciprocally transplanted *Pterygodium* sp., pollinated by oil-collecting bees had higher pollination rates at their home sites, and Newman *et al.* (2012) showed that when the orange and red forms of *Disa ferruginea* were reciprocally transplanted, their sole

pollinator *Aeropetes tulbaghia,* visited the local phenotypes at higher rates. These studies show that pollinator shifts can result in local adaptation and ecotype formation.

Nevertheless, there have also been few studies that link floral divergence to reproductive isolation, which is particularly pertinent as there are a number of different mechanisms that can cause pollinator-mediated isolation. For example, Minnaar *et al.* (2019) showed that divergent floral tube lengths in *Lapeirousia anceps* lead to differential pollen placement on its pollinator, *Moegistorhynchus longirostris*, causing strong mechanical isolation. Furthermore, Newman and Johnson (2024) demonstrated complete behavioural isolation between sympatric closely-related non-rewarding *Disa* sp. that mimic different rewarding model species. These studies demonstrate that different mechanisms, such as differential use of the same pollinator and mimicry of different model species, can cause floral divergence and pollinator-mediated reproductive isolation.

Research gaps in ecologically-driven diversification of the CFR

Overall, there is strong phylogenetic evidence of ecological speciation in the CFR (van der Niet and Johnson, 2009, Schnitzler *et al.*, 2011, Forest *et al.*, 2014). There is also evidence of trait divergence linked to ecological differences (Verboom *et al.*, 2004, Carlson *et al.*, 2011, Mitchell *et al.*, 2015, Newman *et al.*, 2015), although this evidence has rarely been directly linked to local adaptation. Furthermore, there are very few examples that link ecologically-based divergence to gene flow reduction and the evolution of reproductive isolation in the CFR. Further evidence should link ecological divergence to phenotypic selection experiments, local adaptation and reproductive isolation to investigate the early drivers of speciation in the CFR.

SPECIATION OF IRIDACEAE AND THE GENUS *GLADIOLUS* IN THE CAPE FLORISTIC REGION

Within the CFR, the Iridaceae is the third largest family (Goldblatt and Manning, 2002, Manning and Goldblatt, 2012) with 78% of species, and more than 20% of genera being endemic (Manning and Goldblatt, 2012). With an estimated 94% of sub-Saharan Iridaceae having specialised pollination syndromes (Goldblatt and Manning, 2006), the investigations into the mechanisms driving this immense diversity have largely focussed on the role of pollinators. Frequent pollinator shifts have been documented across the sub-Saharan Iridaceae (Goldblatt and Manning, 2006) and within genera in the CFR (Manning and Goldblatt, 2005, Forest *et al.*, 2014). Furthermore, a phylogenetic study comparing the frequency of pollinator and substrate shifts in *Lapeirousia*, a well-represented genus in the GCFR, found that pollinator shifts were more frequent, demonstrating the importance of pollinator shifts in the diversification of the genus (Forest *et al.*, 2014). Although pollinator shifts have been frequently documented in the Iridaceae, the extent of this diversity is unlikely to be a result of a single driver, and further investigations are needed to examine the contribution of abiotic drivers.

Gladiolus is the second largest genus within the Iridaceae (Goldblatt and Manning, 2008) and one of the largest genera in the CFR (Goldblatt and Manning, 2002). The monophyletic genus originated in the Miocene in southern Africa with the centre of diversity in the GCFR (Valente *et al.*, 2011). The number of species in the GCFR (106 species) far outpaces the number of species in the comparable Mediterranean basin (7 species). This disparity is largely due to two interacting factors, namely the genus's southern Africa origin, allowing for more time for the species to diverge (Valente *et al.*, 2011), and the high ongoing diversification in the GCFR (Rymer *et al.*, 2010, Valente *et al.*, 2011). This diversification has,

at least in part, been due to frequent pollinator shifts, often between highly specialised pollinators (Goldblatt and Manning, 1999, Goldblatt *et al.*, 2001). In particular, Valente *et al.* (2012) estimated that one-third of lineage splitting events were caused by pollinator shifts in southern African *Gladioli.* Despite pollinators playing a large role in the diversification of the species, other drivers of diversification, including abiotic factors have not been adequately investigated.

GLADIOLUS CARNEUS SPECIES COMPLEX

Gladiolus carneus D. Delaroche (Iridaceae) is a polymorphic cormous geophyte endemic to the CFR (Figure 1.1). The species occupies a wide geographic range and occurs along the entire elevational gradient in the CFR, with populations occurring from sea level along the Kleinmond coast to 1000m above sea level on the peaks of the Southern and South Western Cape mountains. Specifically, the species occurs through the Cape Peninsula, up to Ceres and through the Southern Cape, and has also been documented at high elevations in the Hottentots-holland, Drakenstein, Riviersonderend, Langeberg and Outeniqua Mountain ranges. The species flowers between August and January (K. Khoury personal observation) with the peak flowering during October and November (Goldblatt and Manning, 1998). *G. carneus* populations are also visited by a diverse array of pollinators, including long-tonged flies in the genus *Philoliche* and *Prosoeca* (Goldblatt and Manning, 1999, Goldblatt *et al.*, 2001), and solitary bees (K. Khoury, personal observation).

The species has been described under at least 20 different taxonomic names in the past, which usually has referred to specific populations or forms of the species (Goldblatt and Manning, 1998). Lewis *et al.* (1972) eventually sunk the different taxa into a single species, which also included *Gladiolus pappei*, a late flowering, high altitude species in the *Blandus*

series. Goldblatt and Manning (1998) described the taxon as a separate species based on differing morphology and ecology. Specifically, *G. pappei* is a peninsula endemic with deep pink flowers, and relatively narrow leaves with a slender growth form, compared to the more robust *G. carneus*. Based on Goldblatt and Manning (1998)'s designation of *G. pappei*, it has been excluded from this study. The *G. carneus* complex can be divided into distinct morphs, which likely represent 'putative ecotypes,' based on their morphology and geographic distribution (Delpierre and du Plessis, 1974). In this thesis, the putative ecotypes include *albidus*, *blandus*, *callistus*, *macowanianus*, and *prismatosiphon* as defined by the morphology and localities described by Delpierre and du Plessis (1974). The *G. carneus* populations in the Langeberg and Outeniqua mountains have previously been grouped with both *blandus* and *prismatosiphon*, however these populations are treated as a distinct *langeberg* ecotype. This distinction has been made as all sampled populations in the Langeberg Mountain range have nectar guides with UV properties that differ from all other ecotypes (*see chapter 2 for detailed analyses*). The populations at the top of the Hottentots-holland, Drakenstein and Riviersonderend mountains are treated as a *high-altitude* ecotype. These *high-altitude* populations have been included in the *G. carneus* complex rather than in *G. pappei*, as they have much wider leaves, and nectar guides more characteristic with that of *G. carneus*.

Albidus, which is identified by their white flowers with pale yellow markings on the lower tepals, is found from Paarl to Somerset West, and through to Hermanus. *Blandus* is found along the Kleinmond coast, up the Palmiet river and into the Koegelberg Nature Reserve. *Callistus*, often found in wet or marshy areas in the Southern Cape, has spooned lower tepals that lack any nectar guides and instead has a deep purple gullet. *Macowanianus* is the most well-documented of the species, and occurs throughout the Cape Peninsula and Southern Cape, with well-developed red nectar guides on the lower tepals. *Prismatosiphon* is a form often

found on rocky outcrops near Bredasdorp, with well-developed white and red nectar guides on the lower tepals. The *langeberg* form, occurs throughout the Langeberg and into the Outeniqua Mountain range while the *high-altitude* ecotype exclusively occurs on mountain peaks in the Southern and south western Cape, and are often exposed to freezing temperatures in the winter.

THESIS AIMS

In this thesis, I investigate the early acting barriers to gene flow that contribute to ecological speciation in the *G. carneus* species complex. Using a combination of modelling, field sampling, common garden, and field experiments, I examine how ecological niche differentiation and local adaptation result in reproductive isolation at the earliest stages of diversification (*see Figure 1.2 for all sites sampled in this thesis*).

Chapter 2 will address whether ecological niche differentiation causes strong premating reproductive isolation. First, I quantified the differences in functional floral and vegetative morphology between all *G. carneus* putative ecotypes and found evidence for ecotype status. Second, I quantified the predicted and realized abiotic niche, phenological niche and pollinator niches of the ecotypes. Third, I linked niche differentiation between the ecotypes to the strength of corresponding premating reproductive isolation barriers both between ecotypes and across the species complex. This chapter will address which forms of niche differentiation causes the strongest reproductive isolation, whether the strongest barriers are consistent across the species complex, and therefore, which barriers are most important in driving the diversification of the species complex.

As strong niche differentiation between ecotypes should result in local adaptation, in Chapter 3, I tested whether *G. carneus* populations are locally adapted to their edaphic niche, a fundamental part of their abiotic niche. In this chapter, I focused on three focal populations

of *G. carneus* representing ecotypes occupying the most distinct abiotic niches along an elevational gradient (Figure 1.2). First, I tested whether all *G. carneus* ecotypes and the focal populations occupy distinct edaphic niches. Second, I used a common garden to test whether the *G. carneus* populations are locally adapted to their edaphic niche, and third, I used a reciprocal translocation to test for local adaptation along an elevational gradient. This chapter will address whether shifts in niches are a reliable predictor of local adaptation and whether adaptation to edaphic niches or other abiotic factors contribute to local adaptation in the species complex.

In Chapter 4, I synthesise the results of the previous chapters and assess the role of niche differentiation and local adaptation in the diversification of the species complex. I further explore how these findings contribute to our understanding of ecological speciation in the CFR. Overall, this thesis will address key theoretical and experimental gaps at the earliest stages of speciation, including the role of ecological niche differentiation, the extent of premating reproductive isolation and the role of local adaptation in driving the diversification of the CFR.

LITERATURE CITED

Anderson B, Pauw A, Cole WW, Barrett SC. 2016. Pollination, mating and reproductive fitness in a plant population with bimodal floral-tube length. *Journal of Evolutionary Biology*, **29**: 1631-1642.

Anderson B, Ros P, Wiese TJ, Ellis AG. 2014. Intraspecific divergence and convergence of floral tube length in specialized pollination interactions. *Proceedings of the Royal Society B: Biological Sciences*, **281**: 20141420.

Bouchenak-Khelladi Y, Linder HP. 2017. Frequent and parallel habitat transitions as driver of unbounded radiations in the Cape flora. *Evolution*, **71**: 2548-2561.

Briscoe Runquist RD, Chu E, Iverson JL, Kopp JC, Moeller DA. 2014. Rapid evolution of reproductive isolation between incipient outcrossing and selfing *Clarkia* species. *Evolution,* **68**: 2885-900.

Carlson JE, Adams CA, Holsinger KE. 2016. Intraspecific variation in stomatal traits, leaf traits and physiology reflects adaptation along aridity gradients in a South African shrub. *Annals of Botany,* **117**: 195-207.

Carlson JE, Holsinger KE, Prunier R. 2011. Plant responses to climate in the Cape Floristic Region of South Africa: evidence for adaptive differentiation in the Proteaceae. *Evolution,* **65**: 108-124.

Christie K, Fraser LS, Lowry DB. 2022. The strength of reproductive isolating barriers in seed plants: insights from studies quantifying premating and postmating reproductive barriers over the past 15 years. *Evolution,* **76**: 2228-2243.

Coyne JA, Orr HA. 2004. *Speciation.* Sunderland, MA: Sinauer Associates.

Cramer MD, West AG, Power SC, Skelton R, Stock WD. 2014. Plant ecophysiological diversity. In: Allsopp N, Colville JF, Verboom GA, eds. *Fynbos: ecology, evolution and conservation of a megadiverse region*. Oxford: Oxford University Press.

Cramer MD, Wootton LM, Mazijk R, Verboom GA. 2019. New regionally modelled soil layers improve prediction of vegetation type relative to that based on global soil models. *Diversity and Distributions,* **25**: 1736-1750.

Delpierre GR, du Plessis NM. 1974. *The winter-growing Gladioli of South Africa.* London: Nasionale Bokhandel Ltd.

Duffy KJ, Johnson SD. 2017. Specialized mutualisms may constrain the geographical distribution of flowering plants. *Proceedings of the Royal Society B: Biological Sciences,* **284**: 1-7.

Ellis AG, Verboom GA, van der Niet T, Johnson SD, Linder HP. 2014. Speciation and extinction in the Greater Cape Floristic Region. In: Allsopp N, Colville JF, Verboom GA, eds. *Fynbos: ecology, evolution and conservation of a megadiverse region.* Oxford: Oxford University Press.

Ellis AG, Weis AE. 2006. Coexistence and differentiation of 'flowering stones': the role of local adaptation to soil microenvironment. *Journal of Ecology,* **94**: 322-335.

Fick SE, Hijmans RJ. 2017. WorldClim 2: new 1-km spatial resolution climate surfaces for global land areas. *International Journal of Climatology,* **37**: 4302-4315.

Forest F, Goldblatt P, Manning JC, *et al.* 2014. Pollinator shifts as triggers of speciation in painted petal irises (*Lapeirousia*: Iridaceae). *Annals of Botany,* **113**: 357-371.

Godsoe W. 2010. I can't define the niche but I know it when I see it: a formal link between statistical theory and the ecological niche. *Oikos,* **119**: 53-60.

Goldblatt P, Manning J. 1998. *Gladiolus in Southern Africa.* Vlaeberg: Fernwood Press.

Goldblatt P, Manning J. 2002. Plant diversity of the Cape region of southern Africa. *Annals of the Missouri Botanical Garden,* **89**: 281–302.

Goldblatt P, Manning JC. 1999. The long-proboscid fly pollination system in *Gladiolus* (Iridaceae). *Annals of the Missouri Botanical Garden,* **86**: 758-774.

Goldblatt P, Manning JC. 2006. Radiation of pollination systems in the Iridaceae of sub-Saharan Africa. *Annals of Botany,* **97**: 317-44.

Goldblatt P, Manning JC. 2008. *The Iris family: natural history & classification.* London: Timber Press.

Goldblatt P, Manning JC, Bernhardt P. 2001. Radiation of pollination systems in *Gladiolus* (Iridaceae: Crocoideae) in southern Africa. *Annals of the Missouri Botanical Garden,* **88**: 713-734.

Hengl T, Mendes de Jesus J, Heuvelink GB, *et al.* 2017. SoilGrids250m: Global gridded soil information based on machine learning. *PLoS one,* **12**: e0169748.

Johnson SD. 1996. Pollination, adaptation and speciation models in the Cape flora of South Africa. *Taxon,* **45**: 59-66.

Johnson SD. 2010. The pollination niche and its role in the diversification and maintenance of the southern African flora. *Philosophical Transactions of the Royal Society B,* **365**: 499-516.

Johnson SD. 2025. Pollination ecotypes and the origin of plant species. *Proceedings of the Royal Society B,* **292**: 20242787.

Johnson SD, Steiner KE. 1997. Long-tongued fly pollination and evolution of floral spur length in the *Disa draconis* complex (Orchidaceae). *Evolution,* **51**: 45-53.

Kawecki TJ, Ebert D. 2004. Conceptual issues in local adaptation. *Ecology Letters,* **7**: 1225-1241.

Kay KM. 2006. Reproductive isolation between two closely related hummingbird-pollinated neotropical gingers. *Evolution,* **60**: 538-552.

Kraaij T, van Wilgen BW. 2014. Drivers, ecology, and management of fire in fynbos. In: Allsopp N, Colville JF, Verboom GA, eds. *Fynbos: ecology, evolution, and conservation of a megadiverse region.* Oxford: Oxford University Press.

Latimer AM, Silander Jr. JA, Rebelo AG, Midgley GF. 2009. Experimental biogeography: the role of environmental gradients in high geographic diversity in Cape Proteaceae. *Oecologia,* **160**: 151-162.

Lewis GJ, Obermeyer AA, Barnard TT. 1972. *Gladiolus a revision of the South African species.* Cape Town: Purnell & Sons.

Linder HP. 2003. The radiation of the Cape flora, southern Africa. *Biological Reviews,* **78**: 597–638.

Lowry DB. 2012. Ecotypes and the controversy of stages in the formation of new species. *Biological Journal of the Linnean Society*, **106**: 241–257.

Mallet J, Mullen SP. 2022. Reproductive isolation is a heuristic, not a measure: a commentary on Westram et al., 2022. *Journal of Evolutionary Biology,* **35**: 1175-1182.

Manning J, Goldblatt P. 2012. *Plants of the Greater Cape Floristic Region 1: the core Cape flora.* Pretoria: Strelitzia 29.

Manning JC, Goldblatt P. 2005. Radiation of pollination systems in the Cape genus *Tritoniopsis* (Iridaceae: Crocoideae) and the development of bimodal pollination strategies. *International Journal of Plant Sciences,* **166**: 459-474.

Minnaar C, de Jager ML, Anderson B. 2019. Intraspecific divergence in floral-tube length promotes asymmetric pollen movement and reproductive isolation. *New Phytologist,* **224**: 1160-1170.

Mitchell N, Moore TE, Mollmann HK, *et al.* 2015. Functional traits in parallel evolutionary radiations and trait-environment associations in the Cape Floristic Region of South Africa. *The American Naturalist,* **185**: 525-537.

Musker SD, Ellis AG, Schlebusch SA, Verboom GA. 2021. Niche specificity influences gene flow across fine-scale habitat mosaics in Succulent Karoo plants. *Molecular Ecology,* **30**: 175-192.

Newman E, Anderson B, Johnson SD. 2012. Flower colour adaptation in a mimetic orchid. *Proceedings of the Royal Society B,* **279**: 2309-2313.

Newman E, Johnson SD. 2024. Pollinator-mediated isolation promotes coexistence of closely related food-deceptive orchids. *Journal of Evolutionary Biology,* **38**: 190-201.

Newman E, Manning J, Anderson B. 2015. Local adaptation: mechanical fit between floral ecotypes of *Nerine humilis* (Amaryllidaceae) and pollinator communities. *Evolution,* **69**: 2262-2275.

Pauw A, Stofberg J, Waterman RJ. 2009. Flies and flowers in Darwin's race. *Evolution,* **63**: 268-279.

Prunier R, Akman M, Kremer CT, *et al.* 2017. Isolation by distance and isolation by environment contribute to population differentiation in *Protea repens* (Proteaceae L.), a widespread South African species. *American Journal of Botany,* **104**: 674-684.

Ramsey J, Bradshaw HD, Schemske DW. 2003. Components of reproductive isolation between the monkeyflowers *Mimulus lewisii* and *M. cardinalis* (Phrymaceae). *Evolution,* **57**: 1520-1534.

Rundle HD, Nosil P. 2005. Ecological speciation. *Ecology Letters,* **8**: 336-352.

Rymer PD, Manning JC, Goldblatt P, Powell MP, Savolainen V. 2010. Evidence of recent and continuous speciation in a biodiversity hotspot: a population genetic approach in southern African *gladioli* (*Gladiolus*; Iridaceae). *Molecular Ecology,* **19**: 4765-4782.

Schluter D. 2000. *The ecology of adaptive radiation.* New York: OUP Oxford.

Schluter D. 2001. Ecology and the origin of species. *Trends in Ecology & Evolution,* **16**: 372-380.

Schnitzler J, Barraclough TG, Boatwright JS, *et al.* 2011. Causes of plant diversification in the Cape biodiversity hotspot of South Africa. *Systematic Biology,* **60**: 343-357.

Shaik Z. 2019. *Species delimitation and speciation process in the Seriphium plumosum L. complex (Gnaphalieae: Asteraceae) in South Africa,* MSc Thesis, University of Cape Town.

Sobel JM. 2014. Ecogeographic isolation and speciation in the genus *Mimulus*. *The American Naturalist,* **184**: 565-579.

Sobel JM, Chen GF. 2014. Unification of methods for estimating the strength of reproductive isolation. *Evolution,* **68**: 1511-1522.

Sobel JM, Chen GF, Watt LR, Schemske DW. 2010. The biology of speciation. *Evolution,* **64**: 295-315.

Sobel JM, Streisfeld MA. 2015. Strong premating reproductive isolation drives incipient speciation in *Mimulus aurantiacus*. *Evolution,* **69**: 447-461.

Thompson JN. 2013. *Relentless evolution*: University of Chicago Press.

Valente LM, Manning JC, Goldblatt P, Vargas P. 2012. Did pollination shifts drive diversification in southern African *Gladiolus*? Evaluating the model of pollinator-driven speciation. *The American Naturalist,* **180**: 83-98.

Valente LM, Savolainen V, Manning JC, Goldblatt P, Vargas P. 2011. Explaining disparities in species richness between Mediterranean floristic regions: a case study in *Gladiolus* (Iridaceae). *Global Ecology and Biogeography,* **20**: 881-892.

van der Niet T, Johnson SD. 2009. Patterns of plant speciation in the Cape Floristic Region. *Molecular Phylogenetics and Evolution,* **51**: 85-93.

Verboom GA, Archibald JK, Bakker FT, *et al.* 2009. Origin and diversification of the Greater Cape flora: ancient species repository, hot-bed of recent radiation, or both? *Molecular Phylogenetics and Evolution,* **51**: 44-53.

Verboom GA, Linder HP, Stock WD. 2004. Testing the adaptive nature of radiation: growth form and life history divergence in the African grass genus *Ehrharta* (Poaceae: Ehrhartoideae). *American Journal of Botany,* **91**: 1364-1370.

Verboom GA, Moore TE, Hoffmann V, Cramer MD. 2012. The roles of climate and soil nutrients in shaping the life histories of grasses native to the Cape Floristic Region. *Plant Soil*, **355**: 323–340.

Verboom GA, Stock WD, Cramer MD. 2017. Specialization to extremely low-nutrient soils limits the nutritional adaptability of plant lineages. *The American Naturalist*, **189**: 684-699.

Waterman RJ, Bidartondo MI, Stofberg J, *et al.* 2011. The effects of above- and belowground mutualisms on orchid speciation and coexistence. *The American Naturalist*, **177**: E54-68.

FIGURES

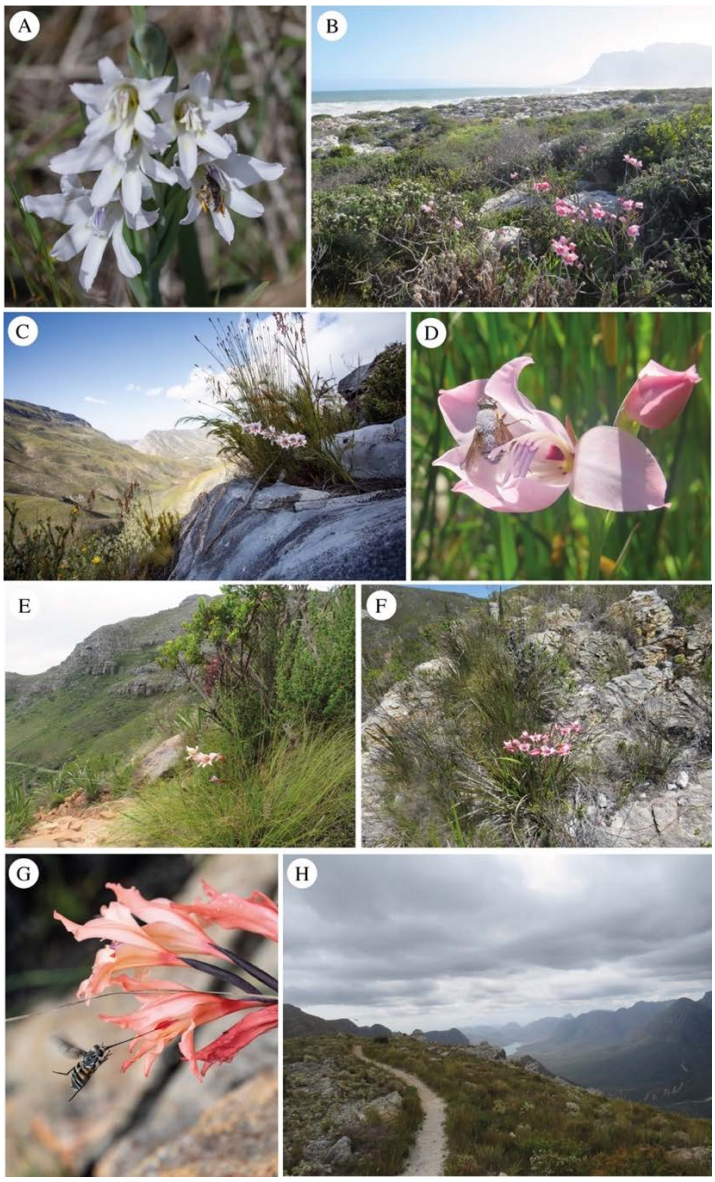

Figure 1.1. Abiotic and biotic niches of the *Gladiolus carneus* putative ecotypes. These putative ecotypes include (A) *albidus* being pollinated by a *Anthophora diversipes* at Limietberg, (B) *blandus* flowering on the Kleinmond coastline, (C) the *langeberg* ecotype growing in Garcia's pass, (D) *callistus* being pollinated by *Philoliche lateralis* at Brodie-Link, (E) *macowanianus* flowering in Table Mountain National Park, (F) *prismatosiphon* flowering on a rocky outcrop in Grootbos, (G) the *high-altitude* ecotype being pollinated by *Philoliche rostrata* at Jonaskop, (H) and the habitat of the *high-altitude* population at Mont Rochelle. Photos: B, D, E, F, H: Katharine Khoury; A, C, G: Ethan Newman

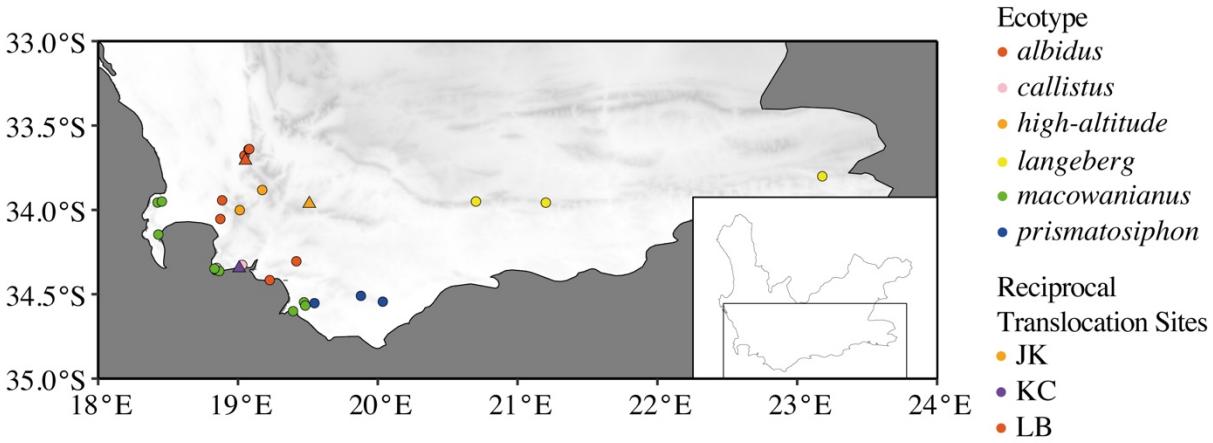

Figure 1.2. *Gladiolus carneus* study sites sampled along the elevational gradient of the Western Cape of South Africa. Different colours denote the *G. carneus* ecotypes. All sites were sampled in Chapter 2. The triangles represent the reciprocal translocation sites in Chapter 3.

CHAPTER 2:

Ecological niche differentiation mediates near complete premating reproductive isolation within the *Gladiolus carneus* (Iridaceae) species complex

Katharine L. Khoury[1, *], Shelley Edwards[2] and Ethan Newman[1]

[1]Department of Botany, Rhodes University, Makhanda, South Africa

[2]Department of Zoology and Entomology, Rhodes University, Makhanda, South Africa

*For correspondence: E-mail katharinekhoury@gmail.com

ABSTRACT

Ecological niche differentiation is well associated with intraspecific divergence of functional traits, which may lead to the evolution of premating reproductive isolation. However, the link between the ecological niches, trait divergence, and premating isolation remains poorly understood. This is particularly pertinent in hyper-diverse areas such as the Cape Floristic Region (CFR) of South Africa, where fine-scale ecological heterogeneity has been hypothesised as a major driver of speciation. Using the polymorphic geophyte *Gladiolus carneus,* endemic to the CFR, we test whether ecological niche differentiation mediates premating reproductive isolation. We first tested whether putative ecotypes of *G. carneus* were distinct based on their floral and vegetative morphology. Next, we documented each putative ecotypes' abiotic niche, flowering phenology and pollination niche and further tested whether any resulting niche differentiation causes premating reproductive isolation. Seven distinct ecotypes were identified. Using niche modelling and multivariate analyses, we found that these ecotypes occupied distinct abiotic niches, resulting in strong ecogeographic isolation. They also had distinct flowering times, causing varying strengths of phenological isolation. For the pollinator niche, we found that all sampled populations were pollinated by one of three highly effective functional pollinators; however, at the ecotypic level, there were no consistent trends leading to varying strengths in pollinator-mediated isolation. Across all ecotypes, ecogeographic isolation was the strongest gene flow barrier, which combined with phenological and pollinator-mediated isolation, caused near complete premating reproductive isolation. These results suggest that ecological niche differentiation between *G. carneus* ecotypes may be contributing to incipient speciation within the species complex and further suggests that ecological niche differentiation may be a major driver of speciation in the hyper-diverse Cape Floristic Region.

Key words: niche differentiation, premating reproductive isolation, ecogeographic isolation, pollinator-mediated isolation, phenological isolation, Cape Floristic Region

INTRODUCTION

At the early stages of ecological speciation, ecologically-based divergent selection is key in producing phenotypes that often associate with distinct biotic and abiotic niches (Schluter, 2000, Schluter, 2001, Rundle and Nosil, 2005). These divergent niches, which distinct phenotypes occupy, are often directly associated with gene flow barriers that act before mating (Coyne and Orr, 2004, Rundle and Nosil, 2005). In seed plants, these premating barriers are thought to be important in completing reproductive isolation, especially in recently diverged taxa or ecotypes (Christie *et al.*, 2022), making it pertinent to disentangle the ecological shifts underlying barrier effectiveness when studying lineage diversification. For example, if shifts in abiotic factors cause divergent selection on the functional traits of a plant in different parts of its range, it will likely result in ecogeographic isolation, which is defined as a reduction in encounter rates due to spatial separation as a result of genetically based differences (Sobel, 2014). Similarly, closely related taxa associated with distinct pollinator niches may have divergent floral phenotypes that promote pollinator-mediated isolation (Kay, 2006, Sobel and Streisfeld, 2015, Minnaar *et al.*, 2019). Specifically, this may occur when niche differentiation is associated with functional pollinator groups that differ in their sensory systems, causing pollinator-mediated isolation through attraction traits (e.g., flower colour) (Grant, 1994, Lunau *et al.*, 2011, Newman *et al.*, 2012). Alternatively, differences in pollinator dimensions may cause pollinator-mediated isolation through morphological-fit floral traits (e.g., corolla tube length), which may be accompanied with or without differential pollen placement (Minnaar *et al.*, 2019, Newman and Anderson, 2020). Here, a reduction in gene flow is directly linked to differences in pollinator functional groups and how they interact with the floral traits of closely related taxa, making it pertinent to study both the pollinator niche, and their functional fit with floral traits. Phenotypic shifts, such as flowering times, are difficult to associate with any single biotic or abiotic driver. Shifts in flowering phenology can be due to either selection by biotic

and abiotic factors (Elzinga *et al.*, 2007, Munguia-Rosas *et al.*, 2011), or by plastic responses to the abiotic environment (Elzinga *et al.*, 2007). Regardless of the causes of the shift in flowering times, it can result in phenological isolation (Paudel *et al.*, 2018, Ramirez-Aguirre *et al.*, 2019), which is a reduction in gene flow due to a mismatch in flowering times (Coyne and Orr, 2004).

Although ecological shifts in association with early lineage diversification have been well documented (Grossenbacher *et al.*, 2014, Dellinger *et al.*, 2024, Fernandez-Mazuecos and Glover, 2024), this is rarely placed in a reproductive isolation context (*but see* Sandstedt *et al.*, 2021, Boucher *et al.*, 2023, Farnitano and Sweigart, 2023). Usually, reproductive isolation is studied by either quantifying the strength of multiple barriers between sister taxa (*see* Ramsey *et al.*, 2003, Kay, 2006, Sobel and Streisfeld, 2015, Ostevik *et al.*, 2016, Christie and Strauss, 2019, Ivey *et al.*, 2023) or by focussing on a single barrier across multiple taxa pairs (Sobel, 2014). The first approach provides valuable information on the relative strength of barriers between taxa pairs, while the second approach shows the role of single barriers in driving wider trends in reproductive isolation within and between lineages. If these approaches were combined, where multiple gene flow barriers were quantified to test their relative importance across multiple taxa pairs, it would show which barriers played the largest role in maintaining reproductive isolation and driving the diversification of lineages as a whole. This approach has highlighted the role of multiple postpollination barriers (particularly hybrid seed inviability) in reducing gene flow between *Mimulus* species in the section *Eunanus* (Farnitano and Sweigart, 2023), for postzygotic barriers completing reproductive isolation in the *Mimulus tilingii* species complex (Sandstedt *et al.*, 2021), and for showing that geographic and phenological isolation maintain species boundaries within the genus *Argyroderma* (Boucher *et al.*, 2023).

Documenting ecological niche differentiation in association with premating isolation is particularly pertinent in hyper-diverse areas such as the Cape Floristic Region (CFR), where interactions between topography, soils, climate, and pollinators have generated ecological heterogeneity that has facilitated the diversification of plant lineages (Ellis *et al.*, 2014). Specifically, the CFR is characterised by folded mountain belts that run parallel to the Indian and Atlantic ocean coasts (Linder, 2003), which gave rise to some of the most nutrient-poor soils currently recorded on Earth (Cramer *et al.*, 2014). However, these soils contrast with the moderately fertile, shale-derived soils in coastal planes and intermontane valleys (Cramer *et al.*, 2014), which have created a mosaic of edaphic conditions in the CFR. Rainfall varies along both an east-west and elevational gradient. In the west, there is a strongly seasonal Mediterranean climate, while in the east, the climate is much more aseasonal with rainfall throughout the year (Manning and Goldblatt, 2012). Further variation is created by steep mountainous landscapes, resulting in orographic rainfall (Manning and Goldblatt, 2012). These interacting conditions have created a heterogenous abiotic selective landscape that has facilitated frequent ecological speciation in the CFR (van der Niet and Johnson, 2009, Schnitzler *et al.*, 2011, Ellis *et al.*, 2014). Apart from diverse abiotic niches that have contributed to lineage diversification, shifts in biotic niches associated with pollinators are also thought to be important drivers of lineage diversification in the Cape (van der Niet and Johnson, 2009, Valente *et al.*, 2012). These ecological shifts considering both biotic and abiotic niches have been shown at a macroevolutionary scale, focusing on species-level phylogenies of the major Cape clades (van der Niet and Johnson, 2009, Schnitzler *et al.*, 2011, Valente *et al.*, 2012), as well as through trait-by-environment associations (Carlson *et al.*, 2011, Mitchell *et al.*, 2015, Newman *et al.*, 2015). However, few of these ecological shifts have been directly linked to the strength of corresponding premating isolation barriers in the CFR (*but see*

Newman and Johnson, 2024) to elucidate the relative importance of individual gene flow barriers to lineage diversification.

Gladiolus carneus Delaroche (Iridaceae) is a geophyte endemic to the CFR (Figure 2.1). The species complex is polymorphic and is made up of at least seven distinct forms that differ in both their functional traits and geographic distributions (Lewis *et al.*, 1972, Delpierre and du Plessis, 1974), representing putative ecotypes (Turesson, 1922). This provides an opportunity to explore the relationship between trait divergence, ecological niche differentiation, and premating reproductive isolation in a diverging species complex within the CFR. Using the *G. carneus* study system, we tested (1) whether putative ecotypes are morphologically distinct from one another, (2) whether they occupy distinct abiotic, phenological and pollinator niches, and (3) whether differences in these ecological niches results in premating reproductive isolation.

MATERIALS AND METHODS

Study species

Gladiolus carneus is a deciduous cormous geophyte endemic to the CFR. The species occurs from Ceres, south into the Cape peninsula, and east along the Southern Cape coast and then inland into the Langeberg and Outeniqua Mountains (Goldblatt and Manning, 1998). *Gladiolus carneus* occurs along the entire elevational gradient of the CFR, with populations occurring from sea level along the rocky Kleinmond coast, up to the high peaks of the South-Western and Southern Cape over 1000 meters above sea level. The species flowers from August into early January (Lewis *et al.*, 1972). *Philoliche rostrata* (Tabanidae) and *Prosoeca nitidula* (Nemestrinidae), both long-tongued flies, have been documented pollinating the species (Goldblatt and Manning, 1999, Goldblatt *et al.*, 2001) while *Amegilla spilostoma* (Apidae), a

solitary bee, is a documented nectar thief (Goldblatt *et al.*, 2001). However, these observations were only conducted at two sites (Devil's Peak and Silvermine) and our own preliminary observations suggest that both long-tongued flies and solitary bees are legitimate pollinators of *G. carneus*.

Gladiolus carneus has been described under at least 20 different names, with many of those taxonomic distinctions referring to specific populations or forms of the species. These forms were eventually sunk into the single species, *G. carneus,* by Lewis *et al.* (1972). However, these forms likely represent 'putative ecotypes' based on their distinctive morphology and geographic distributions, and we provide empirical evidence for ecotype status in the manuscript. In the methods, we refer to the different forms as 'putative ecotypes,' and provide evidence in the results. The results of this study provides evidence for seven ecotypes, five of which have been previously included in Delpierre and du Plessis (1974) as varieties, and we provide evidence for a further two. The putative ecotypes include *albidus, blandus, callistus, macowanianus,* and *prismatosiphon* as defined by morphology and localities described by Delpierre and du Plessis (1974). The form of *G. carneus* that has been found in the Langeberg mountains has been previously grouped in both *blandus* (Delpierre and du Plessis, 1974) and *prismatosiphon* (Lewis *et al.*, 1972). However, due to its distinct geographic range and floral morphology (this study), the Langeberg form of *G. carneus* has been treated as a separate putative ecotype. Similarly, the late-flowering, high-altitude forms of *G. carneus* in the Drakenstein, Hottentots-Holland and Riviersonderend mountain ranges were treated as a *high-altitude* putative ecotype.

Albidus (Figure 2.1A) occurs in Paarl, Stellenbosch, and south into Hermanus (Delpierre and du Plessis, 1974). The ecotype can be identified by the white flowers with pale

yellow markings on the lower tepals (Delpierre and du Plessis, 1974). *Blandus* (Figure 2.1B) is found near Kleinmond (Delpierre and du Plessis, 1974). *Callistus* (Figure 2.1C) lacks any nectar guides and instead has a deep purple gullet (Delpierre and du Plessis, 1974). The *high-altitude* ecotype includes all late-flowering populations occurring on the top of the Drakenstein, Hottentots-Holland, and Riviersonderend mountain ranges (Figure 2.1D), which are frequently exposed to summer cloud cover and freezing temperatures in winter. The *langeberg* ecotype of *G. carneus* is found in the Langeberg and Outeniqua mountains (Figure 2.1E). *Macowanianus* is the most well documented ecotype (Figure 2.1F), found in the Southern Cape and along the Cape peninsula (Delpierre and du Plessis, 1974), and is identified by its distinct dark nectar guides. *Prismatosiphon* (Figure 2.1G) is restricted to the Agulhas Plain, and is found predominantly on rocky outcrops (Delpierre and du Plessis, 1974).

Are the putative ecotypes of *Gladiolus carneus* morphologically distinct?

Morphological differences between putative ecotypes of Gladiolus carneus

To test whether *G. carneus* separates into distinct ecotypes based on morphology, we measured morphological traits in a total of 29 populations (eight *albidus*, one *blandus*, three *callistus*, three *high-altitude*, three *langeberg*, eight *macowanianus* and three *prismatosiphon*) (*see Table S2.1 for site coordinates*) representing the entirety of the geographic and morphological variation within the species complex (*see Table S2.2 for sample sizes*). Voucher specimens were collected from 14 populations representing six of the seven putative ecotypes which were deposited at the Selmar Schonland Herbarium (GRA) (Table S2.1). At each population, we chose between five and 40 individuals during their peak flowering season for morphological measurements. To avoid pseudoreplication, all floral and vegetative measurements were taken from a single flower and leaf per individual. Some or all of the following morphological traits were measured on each individual using digital callipers (0-200 mm, TA): floral tube length,

flower gape, petal size, flower width, and width of the longest leaf, while inflorescence height and the length of the longest leaf was measured using a measuring tape (Figure S2.1A-C). Flower gape was measured from the lowest anther to the lower median tepal directly underneath (Figure S2.1A). Flower width was the distance between the tips of the lateral tepals (Figure S2.1A). Floral tube length was measured from the top of the ovary to the notch connecting the corolla to the lower tepals (Figure S2.1B). Petal size was measured from the tip to the base of the dorsal tepal (Figure S2.1B). Inflorescence height was measured from the base of the inflorescence to the top of the display (Figure S2.1C). Leaf length was measured as the distance from the ground to the tip of the longest leaf (Figure S2.1C), whereas leaf width was measured as the widest point on the longest leaf (Figure S2.1C). Finally, we documented the total number of flowers, which included all buds, open and senesced flowers, and the total number of leaves starting from the base of the fan during the peak flowering period.

All data analysis was conducted in R v.4.1.2 (R Core Team, 2021). We used a series of Principal Component Analyses (PCA's) to determine if different putative ecotypes cluster separately based on their vegetative and floral morphology. We implemented the PCAs using the *prcomp* function from the '*stats*' package (R Core Team, 2021) and tested whether the putative ecotypes cluster separately using a permutation MANOVA (999 permutations). We then used a pairwise permutation MANOVA with a Bonferroni correction for pairwise comparisons between putative ecotypes. The permutation MANOVA was implemented using the *adonis2* function in the package '*vegan*' (Oksanen *et al.*, 2020) and we used *pairwise.perm.manova* from the '*RVAideMemoire*' package (Herve, 2023). We used this procedure to test whether the putative ecotypes separate based on their floral traits, vegetative traits, and all morphological traits.

We further determined if there were significant differences between putative ecotypes using generalized linear models (GLMs) implemented in the '*stats*' package (R Core Team, 2021) for the following morphological traits: tube length, flower gape, petal size, inflorescence height, length and width of the longest leaf. These traits were chosen as they represent functional traits directly linked to the biological variation associated with their biotic and abiotic niches (e.g., tube length is associated with pollinator proboscis length). In the models, each trait was set as the response variable while the explanatory variables were ecotype, and site nested within ecotype. The nested term was included to account for sampling at multiple sites per ecotype. All traits were fitted with either a Gaussian or Gamma error distribution, depending on the normality of the dataset. Significance of model terms were obtained using the *Anova* function from the '*car*' package (Fox and Weisberg, 2019) while the *emmeans* function from the '*emmeans*' package (Lenth, 2022) was used for pairwise comparisons.

Colour differences between putative Gladiolus carneus *ecotypes*

To test if there were differences in the colour traits between putative ecotypes of *G. carneus* within bee and fly colour vision, we sampled 1266 spectral measurements from 300 individuals across 24 populations in 2020, 2022, and 2023. Within each population, we took spectral measurements from between three and 28 individuals (*see sample sizes in Table S2.3*). All spectral data was collected within the same years as all morphological data. For each individual of the *macowanianus*, *blandus, prismatosiphon, high-altitude* and *langeberg* putative ecotypes, on a single flower we measured the spectral reflectance of the dorsal tepal, the outline and centre of the nectar guides (hereafter referred to as the 'guide' and 'centre') on the lower median tepal and lower lateral tepal (Figure S2.1D). Only the dorsal tepal and centre of the nectar guides were documented for *albidus* (Figure S2.1E), as the putative ecotype lacks well-developed outlines around the nectar guides. As *callistus* lacks any nectar guides, only the

dorsal tepal and the gullet for each individual was measured (Figure S2.1F). All spectra collected in 2020 were measured using an Ocean Optics S2000+ spectrometer with a DT-mini light source and fibre optic probe (UV/VIS 400 μm), while spectra collected in 2022 and 2023 were measured using an Ocean Insight FLAME Miniature spectrometer (Ostfildern, Germany) with a PX-2 Pulsed Xenon Light Source and a Premium 400 μm fibre optic probe. All putative ecotypes' spectra were processed, and negative values were corrected using the *procspec* function. Mislabelled, or spectra with incomplete information were removed. Aggregation plots showing the mean and standard error of the putative ecotypes for each trait were generated using the *aggplot* function to visualise the curvature of the reflectance spectra for each species (Figure S2.2A-F).

Colour vision models were used to determine how pollinators perceive the colours of each putative ecotype. Reflectance spectra of each putative ecotype were plotted in the trichromatic colour hexagon (Chittka, 1992) for the *Apis mellifera* visual system and the colour-opponent coding vision model for flies (Troje, 1993). Bees have a conserved trichromatic visual system with UV, blue and green photoreceptors (Briscoe and Chittka, 2001), which are represented as vertices in the Chittka (1992) trichromatic colour hexagon. Bees have continuous colour discrimination, which can be quantified by calculating the Euclidean distances between loci within the trichromatic colour hexagon. These Euclidean distances are a proxy for colour contrasts, with larger distances being more perceptible than smaller distances. As achromatic vision is suggested to be important for object detection in bees (van der Kooi and Kelber, 2022), we calculated the achromatic contrast between loci using the green photoreceptor (Giurfa *et al.*, 1996).

Fly colour vision was modelled using the colour-opponent coding (COC) model (Troje, 1993). The COC model is based on behavioural experiments with *Lucilia* blowflies that showed their colour vision was based on an opponency mechanism involving pairs of photoreceptors, namely R7p with R8p and R7y with R8y. *Lucilia* flies distinguish colour categories that depend on the relative excitation of the paired receptors. The COC model uses the relative quantum catches of the four fly photoreceptors to plot spectra into quadrants in a Cartesian plane. Loci plotted within a quadrant are too similar to be perceived, while loci in different quadrants are considered perceptible colour differences. However, Hannah *et al.* (2019) found that the hoverfly, *Eristalis tenax*, can discriminate between colours within the COC quadrants, and based on these experiments, Garcia *et al.* (2022) proposed four behaviourally relevant colour discrimination thresholds for *E. tenax*. As the spectral sensitivities of fly pollinators of *G. carneus* are currently unknown, we used the spectral sensitivities of *E. tenax*, a widespread nectar-feeding fly. We did not calculate the achromatic contrast between loci of *E. tenax* as there is little behavioural evidence of the relative importance of achromatic vision compared to chromatic vision (*but see* An *et al.*, 2018).

Using the spectra from each part of the flower, quantum catches for both the bee and fly models were calculated with the following formula:

$$P = R \int_{300}^{700} S_i(\lambda) I(\lambda) D(\lambda) d\lambda$$

where S_i is the sensitivity of each photoreceptor, $I(\lambda)$ is the spectral reflectance and $D(\lambda)$ is the daylight illuminant. Quantum catches were hyperbolically transformed using:

$$E = \frac{P}{P+1}$$

and plotted into hexagonal space using:

$$\chi = Sin60° \times (E_G - E_{UV})$$

$$\gamma = E_B - \frac{E_G - E_{UV}}{2}$$

to find the x and y coordinates. While the formulas:

$$\chi = E_{UV} - E_B$$

$$\gamma = E_V - E_G$$

were used to find the coordinates of the relative quantum catches in categorical fly space. All visual modelling used D65 daylight illuminant and green foliage background.

We used a MANOVA on the Cartesian coordinates within the colour vision models to test for statistical differences between the putative ecotypes for each colour trait. This approach accounts for the multivariate nature of the data (Maia and White, 2018). We used the *mvpaircomp* function with a bonferroni correction from the *'biotools'* package (da Silva *et al.*, 2017) for pairwise comparisons between the putative ecotypes for each colour trait. In cases where there were statistical differences between the putative ecotypes within bee and fly colour vision, we then calculated the Euclidean distances to test whether there were relative perceptual differences between the putative ecotypes (Maia and White, 2018). Empirical means and bootstrapped confidence intervals of colour distances between putative ecotypes were generated using the *bootcoldis* function (Maia and White, 2018). We considered larger distances to be more perceptible than smaller distances. All spectral processing, visualisation and colour vision modelling were completed using the R package '*pavo'* (Maia *et al.*, 2019)

Do putative ecotypes of *Gladiolus carneus* occupy distinct biotic and abiotic niches?

Point locality sampling from iNaturalist

We extracted flowering and point locality data for all putative *G. carneus* ecotypes from iNaturalist observations, which had over 1500 observations as of September 2024. The flowering data were used to test for differences in the phenological niche between putative

ecotypes, and the point localities were used to extract abiotic data from environmental layers that test for differences in the realized and fundamental abiotic niche between putative ecotypes. The observations include images of the flowers allowing for reliable identification of the putative ecotypes, and the associated locality and accuracy data provides reliable occurrence data across its geographic range. Additionally, *G. carneus* is documented yearly on iNaturalist allowing for multi-year observation dates that can be used to capture temporal variation in flowering times between years and localities. We classified iNaturalist observations into the seven putative ecotypes based on their floral morphology and location. Furthermore, we excluded any (1) observations that did not have clear photos of the flowers, (2) observations of closely related taxa that had been misidentified as *G. carneus,* (3) observations that did not fit the descriptions of previously identified putative ecotypes or were likely hybrids, (4) observations that occurred outside of the natural range of the species within the Cape Floristic Region (e.g., Australia), and (5) observations that were not research grade.

Do putative ecotypes of Gladiolus carneus *occupy distinct abiotic niches?*

To test whether the putative ecotypes of *G. carneus* occupy distinct abiotic niches, we modelled the predicted distribution of each putative ecotype using MaxEnt (Phillips *et al.*, 2006, Elith *et al.*, 2010). All iNaturalist observations were filtered to include coordinates with an open geoprivacy and an accuracy under 100 m to ensure that the niches of each putative ecotype were accurately represented at fine spatial scales. In addition to iNaturalist data, we provided point localities for putative ecotypes that were not well documented from observations in the field (K. Khoury, unpublished data). Overall, we documented 209 *albidus*, 33 *blandus*, 67 *callistus*, 34 *high-altitude*, 37 *langeberg*, 379 *macowanianus* and 27 *prismatosiphon* point localities to be used in subsequent analyses. We mined 19 bioclimatic layers and an elevation layer at the 30 arc second (~1km) resolution from WorldClim

(https://www.worldclim.org/data/worldclim21.html), while seven soil layers were taken from Cramer *et al.* (2019). The soil layers from Cramer *et al.* (2019) were modelled specifically in the Cape Floristic Region and allow for more reliable predictions of vegetation type in the CFR than the comparable SoilGrids layers. All stacking, resampling, and processing of abiotic layers was done using the '*raster*' package (Hijmans, 2024). The *res* function was used to ensure resolution of all WorldClim and soil variables matched. All abiotic layers were resampled to match the distribution of the soil layers using the *resample* function. The resampled abiotic layers covered the entire native range of *G. carneus*. The collinearity of all abiotic variables was tested using a Pearson correlation and any abiotic variables with a correlation coefficient >|0.69| were excluded from further analysis. In total, we were left with nine biologically relevant, uncorrelated abiotic variables that were used in the final models. These abiotic variables included isothermality (%), annual range in temperature (°C), annual precipitation (mm), precipitation seasonality, electrical conductivity (mS/m), total Nitrogen (%), extractable Phosphorus (mg/kg), extractable Sodium ($cmol^{+}kg^{-1}$), and elevation (metres above sea level) (*see Table S2.4 for descriptions of all layers*). We constructed maximum entropy species distribution models for each putative ecotype using the *maxent* function in the package '*dismo'* (Hijmans *et al.*, 2023). The models were implemented using 75% of the occurrence data for model training and 25% was used for model testing, with 10 000 background points (Elith *et al.*, 2010). The *evaluate* function was used to calculate AUC scores to assess model performance. AUC scores range from 0 to 1, with scores closer to 1 indicating better model performance. The equal sensitivity and specificity threshold was used to create binary maps from the probability predictions of the MaxEnt output using the *threshold* and *reclassify* functions. Values above the threshold were counted as present, while values below were counted as absent. A jackknife test was used to determine the most important environmental variable in each model.

We extracted abiotic layers for each point locality to test whether the putative ecotypes occupied distinct realised abiotic niches. We used a PCA to test for niche differentiation, which included the uncorrelated variables used in the niche modelling. We used a permutation MANOVA to test if the putative ecotypes cluster separately based on their abiotic niche and then a pairwise permutation MANOVA with a Bonferroni correction for pairwise comparisons between the putative ecotypes. The PCA, permutation MANOVA and pairwise permutation MANOVA were implemented using the same procedure described under the morphological analysis.

Do putative ecotypes of Gladiolus carneus *flower at different times?*

iNaturalist observations were used to document differences in flowering times across all putative ecotypes. As iNaturalist records have an observation date, we documented the total number of observations of flowering plants per day of the year as a proxy for the flowering times of each putative ecotype. We pooled observation data across years and associated each observation date with a day of the year (1 to 365) which provided a multi-year data set showing the time of year when each putative ecotype was commonly documented, and therefore flowering. In total, we used 307 *albidus*, 59 *blandus*, 129 *callistus*, 51 *high-altitude*, 38 *langeberg*, 612 *macowanianus*, and 33 *prismatosiphon* observations from iNaturalist in the temporal analysis.

As flowering data is a seasonal event, best represented as circular data, we used circular statistics to test for differences in flowering times between the *G. carneus* putative ecotypes (Pewsey *et al.*, 2013). To facilitate the analysis, each day of the year (1 to 365) was converted into radians, the standard unit of angular measurement. The number of observations against

each radian was then used in the analysis. A Mardia-Watson-Wheeler test, a non-parametric test of the homogeneity of two or more samples of circular data, was used to test for significant differences in the flowering times between putative ecotypes. We used a series of Mardia-Watson-Wheeler tests to conduct pairwise comparisons between the putative ecotypes' flowering times. A Bonferroni correction was applied to the resulting p-values to reduce the likelihood of Type I errors. All analysis was conducted using the *watson.wheeler.test* function in the '*circular'* package (Agostinelli and Lund, 2024).

Do putative ecotypes of Gladiolus carneus *occupy distinct pollination niches?*

Pollinator observations were conducted across 16 sites of *G. carneus* in 2020, 2022 and 2023 to identify the main pollinators of each putative ecotype. A total of 723 flowers were observed over more than 69 hours (*see breakdown of observations per site in Table S2.5*). Observations were conducted between 8.30am and 2.30pm on days above 20° Celsius. At each site, a maximum of two observers recorded all pollinator visits, the total observed flowers, and the total observation time. All visits recorded on focal plants within the observation time were used to the calculate visitation rates (visits.flower^{-1}.hour^{-1}) of pollinators at each population. In addition to recording visits, pollinators were caught using an insect net and euthanized using ethyl acetate fumes. These insects were used for species level identification, the measurements of pollinator functional traits, as well as counting conspecific pollen loads. On each insect we measured extended proboscis length and thorax depth as they are likely correlated with the tube length and flower gape. The head, thorax, and abdomen of each pollinator were swabbed for pollen using fuchsin gel, in which the number of pollen grains was counted using a compound microscope and identified as either *G. carneus* or heterospecific pollen, which was determined from pollen controls taken from each population. Pollen loads larger than 1 000 grains on each part of the pollinator were not counted any further. Insects recorded visiting and making contact

with the reproductive parts of the flowers or found with *G. carneus* pollen on the head, thorax, or abdomen were considered to be legitimate pollinators and used in the subsequent analyses. Once pollinators were identified, they were classified into functional pollinator groups based on similarities in body size, proboscis length, and foraging behaviours. The functional pollinator groups identified were solitary bees, carpenter bees, long-tongued flies (LTFs), medium-tongued flies (MTFs), honey bees (*Apis mellifera*) and Lycaenid butterflies, which were used for all subsequent analyses.

A series of networks were used to associate the main functional pollinators for each population and putative ecotype. We calculated the visitation rate (visits.flower^{-1}.hour^{-1}), mean pollen loads and pollinator importance (visitation rate * pollen loads) per functional pollinator for each site (*see Table S2.5 for sample sizes*). The visitation rates, pollen loads, and pollinator importance were then visualised in a network using the *plotweb* function. For all three networks, H_2' was used to assess the overall level of specialisation for the entire network. The H_2' values range between 0 (indicating no specialisation) and 1 (indicating complete specialisation) (Bluthgen *et al.*, 2006). We used a modularity test on the pollinator importance network to identify different pollinator niches for the *G. carneus* populations. The modularity test was conducted using the *computeModules* and *plotModuleWeb* functions (Beckett, 2016). All of these analyses used the *'bipartite'* package (Dormann *et al.*, 2008).

We further tested whether there were relationships between floral and pollinator morphology using ordinary least squares regressions, specifically between tube length and proboscis length, as well as flower gape and thorax depth. As many sites had more than one functional pollinator, pollinator importance values were used to calculate a 'weighted' proboscis length and thorax depth for each site. In the models, the focal floral measurement

(either tube length or flower gape) was set as the response, while the pollinator morphology (weighted proboscis length or thorax depth) was set as the explanatory variable. All models were implemented using the *lm* function in the '*stats*' package (R Core Team, 2021).

Are differences in the ecological niches of the putative *Gladiolus carneus* ecotypes resulting in premating reproductive isolation?

Calculation of premating barriers

As all the barriers documented affect the co-occurrence of the putative ecotypes, we used the first of Sobel and Chen (2014)'s equations to calculate ecogeographic, phenological, and pollinator-mediated isolation.

The equation:

$$RI = 1 - (\frac{S}{S + U})$$

where S is the shared and U is the unshared portion of occurrence is used to calculate reproductive isolation for prezygotic barriers that affect co-occurrence. The resulting reproductive isolation values range from 0 to 1, where a value of 0 represents complete overlap and absent reproductive isolation, and 1 represents no overlap and complete reproductive isolation.

For ecogeographic isolation, we used the binary niche model predictions of each putative ecotype to estimate the shared and unshared predicted niche occupancy for each pair of putative ecotypes. Areas where both putative ecotypes were present were counted as the 'shared' area while areas where only one putative ecotype was present was counted as 'unshared'. When measuring phenological isolation, we were unable to take into account the relative abundances of each flowering putative ecotype as suggested by Sobel and Chen (2014)

due to differences in sampling efforts on iNaturalist. As putative ecotypes such as *macowanianus, albidus, blandus* and *callistus* largely occur in residential areas and on easily accessible hiking routes, they are very well documented. Other putative ecotypes such as *high-altitude, langeberg* and *prismatosiphon* largely occur in remote or inaccessible areas, resulting in fewer occurrence points, making it difficult to estimate the number of individuals that are flowering in any area. Therefore, instead of using the relative abundance of each flowering putative ecotype, we documented binary flowering occurrences on each day of the year to calculate phenological isolation. We used the number of shared and unshared functional pollinators to calculate pollinator-mediated isolation. All legitimate functional pollinators (i.e., insects recorded visiting a putative ecotype and making contact with the reproductive parts of the flower, or found with *G. carneus* pollen on their head, thorax, or abdomen) were used to calculate pollinator-mediated isolation. As *blandus* lacked any pollinator data, pollinator-mediated isolation was not calculated for any gene flow direction including that putative ecotype.

Total reproductive isolation was calculated using equation 4E from Sobel and Chen (2014). The equation calculates total reproductive isolation sequentially from prezygotic barriers that affect co-occurrence, to prezygotic barriers not affecting co-occurrence and finally post-zygotic barriers. As only premating barriers have been included in the calculation, the resulting value represents total premating reproductive isolation. Total premating isolation for gene flow directions involving *blandus* only included ecogeographic and phenological isolation. Total premating isolation for all other gene flow directions were calculated using ecogeographic, phenological, and pollinator-mediated isolation. For each premating barrier, we calculated 95% confidence intervals from 10 000 bootstrapped samples of our raw data sets (Ostevik *et al.*, 2016). We further resampled each of the premating barrier distributions 10 000

times to calculate the 95% confidence intervals for total premating reproductive isolation (Ostevik *et al.*, 2016).

RESULTS

Are putative ecotypes of *Gladiolus carneus* morphologically distinct?

Morphological differences between ecotypes of Gladiolus carneus

The permutation MANOVAs of all morphological traits ($F = 14.36$, $df = 6$, $P = 0.001$, Figure 2.2), floral traits ($F = 9.38$, $df = 6$, $P = 0.001$, Figure S2.3A), and vegetative traits ($F = 17.29$, $df = 6$, $P = 0.001$, Figure S2.3B) showed that the putative ecotypes clustered separately, providing morphological evidence for ecotype status in the species complex. The pairwise MANOVA on all morphological traits found that all pairwise comparisons for the ecotypes were significant ($P < 0.05$). The pairwise comparisons on the floral traits showed that all pairings were significant ($P < 0.05$), except for *callistus* and *high-altitude* ($P = 1.00$). The pairwise comparisons between ecotypes based on their vegetative traits showed all pairings were significant ($P < 0.05$), except between *albidus* and *blandus* ($P = 0.13$); and also, *macowanianus* and *callistus* ($P = 0.19$).

We found that both ecotype and site nested within ecotype were significant predictors of tube length ($P < 0.0001$, $P < 0.0001$, Table S2.6, Figure S2.4A), flower gape ($P < 0.0001$, $P < 0.0001$, Table S2.6, Figure S2.4B), petal size ($P < 0.0001$, $P < 0.0001$, Table S2.6, Figure S2.4C), inflorescence height ($P < 0.0001$, $P < 0.0001$, Table S2.6, Figure S2.4D), the leaf length ($P < 0.0001$, $P < 0.0001$, Table S2.6, Figure S2.4E), and leaf width ($P < 0.0001$, $P < 0.0001$, Table S2.6, Figure S2.4F). Furthermore, pairwise comparisons showed that there were significant differences between the morphological traits of the ecotypes (Table S2.7).

Colour differences between putative ecotypes of Gladiolus carneus

There were statistical differences between the ecotypes for all colour traits modelled in bee and fly colour vision. Specifically, there were significant differences between the ecotypes' tepals (Bee: *Approx F* = 39.73, *df* = 6, *P* < 0.0001; Fly: *Approx F* = 38.84, *df* = 6, *P* < 0.0001; Figure 2.3A, 2.4A), centre of the median tepals (Bee: *Approx F* = 45.21, *df* = 5, *P* < 0.0001; Fly: *Approx F* = 39.74, *df* = 5, *P* < 0.0001; Figure 2.3B, 2.4B), guide of the median tepals (Bee: *Approx F* = 8.57, *df* = 4, *P* < 0.0001; Fly: *Approx F* = 7.68, *df* = 4, *P* < 0.0001; Figure 2.3C, 2.4C), centre of the lateral tepals (Bee: *Approx F* = 43.78, *df* = 5, *P* < 0.0001; Fly: *Approx F* = 51.14, *df* = 5, *P* < 0.0001; Figure 2.3D, 2.4D), and guide of the lateral tepals (Bee: *Approx F* = 4.54, *df* = 4, *P* < 0.0001; Fly: *Approx F* = 3.58, *df* = 4, *P* = 0.0005; Figure 2.3E, 2.4E). Pairwise comparisons showed there were significant differences between the ecotypes, for all of the colour traits within bee and fly colour vision (*see pairwise comparisons in Table S2.8*). As there were statistical differences between the ecotypes for all colour traits, it was necessary to test whether those differences are perceptible within bee and fly colour vision.

The Euclidean distances between the ecotypes' tepals were relatively small in both bee and fly colour vision (Figure S2.5A, S2.6A) suggesting that bees and flies were unlikely to be able to perceive the differences between the ecotypes' tepals. In contrast, the Euclidean distances between the ecotypes' centre of the median tepal and between lateral tepals were frequently large (Figure S2.5B, S2.6B, S2.5D, S2.6D) suggesting that both bees and flies were able to perceive the differences between the ecotypes. The Euclidean distances between the ecotypes' median guides and between the lateral guides were comparatively less perceptible than between the centre of the guides in both bee and fly colour vision (Figure S2.5C, S2.6C, S2.5E, S2.6E). These results suggest that most of the variation in the colour contrasts between the ecotypes occurs between the centre of the guides.

The achromatic contrasts between the ecotypes' tepal and between the centre of the median tepals was relatively imperceptible in bee vision (Figure S2.7A, S2.7B). However, many of the achromatic contrasts between the ecotypes' centre of the lateral tepal, guides of the median and guides of the lateral tepals were relatively large, suggesting these contrasts may be important in allowing bees to distinguish between these flowers (Figure S2.7C, S2.7D, S2.7E).

Do putative ecotypes of *Gladiolus carneus* occupy distinct biotic and abiotic niches?

Do putative ecotypes of Gladiolus carneus *occupy distinct abiotic niches?*

The MaxEnt models for all ecotypes performed well (AUC > 0.95), providing reliable predicted abiotic niches. All species distribution models closely matched the documented distributions of each ecotype (Figure 2.5, S2.8). Specifically, the *albidus* and *callistus* ecotypes had similar distributions around the lowlands of the Boland (Figure S2.8A, S2.8C). *Blandus* had the smallest distribution and was largely restricted to the Southern Cape coast between Rooi-Els and Hermanus (Figure S2.8B). The *high-altitude* ecotype was restricted to the Drakenstein, Hottentots-holland and Riviersonderend mountain ranges (Figure S2.8D). The *langeberg* ecotype was predicted to occur throughout the Langeberg Mountain range (Figure S2.8E). *Macowanianus* had a predicted range covering the peninsula and Southern Cape coast (Figure S2.8F), whilst *prismatosiphon* was largely restricted to the Southern Overberg (Figure S2.8G). The jackknife tests indicated that annual precipitation (mm) was the most important variable in the *albidus, callistus,* and *high-altitude* models, the annual temperature range (°C) was most important for the *blandus* and *macowaninaus* models, precipitation seasonality was the most important for the *langeberg* model and extractable phosphorus (mg/kg) was the most important for the *prismatosiphon* model. The permutation MANOVA showed that there were

significant differences in the realised abiotic niches of the ecotypes (***F*** = 100.29, ***df*** = 6, ***P*** = 0.001, Figure 2.5B). Furthermore, the pairwise permutation MANOVA indicated that all ecotypes occupied realised abiotic niches that were significantly different from each other (***P*** < 0.05).

Do putative ecotypes of Gladiolus carneus *flower at different times?*

There were significant differences in the flowering times between *G. carneus* ecotypes (*W* = 389.23, *df* = 12, *P* < 0.0001; Figure 2.6), suggesting that different ecotypes occupy distinct phenological niches. The pairwise comparisons between the flowering times of the ecotypes showed all pairings were significant (*P* < 0.01) except between *blandus* and *langeberg* (*P* = 0.10), and *callistus* and *prismatosiphon* (*P* = 1.00).

Do putative ecotypes of Gladiolus carneus *occupy distinct pollinator niches?*

Across all sampled *G. carneus* populations, a diverse range of pollinators were found which were subsequently classified into the following functional groups: solitary bees, carpenter bees, long-tongued flies (LTFs), medium-tongued flies (MTFs), honey bees (*Apis mellifera*) and Lycaenid butterflies. Solitary bees included *Amegilla spilostoma, Amegilla obscuritarsis* (Apidae), and *Anthophora diversipes* (Apidae); carpenter bees included species belonging to the genus *Xylocopa* (Apidae subfamily Xylocopinae); LTFs included *Philoliche rostrata* and *Moegistorhynchus manningi* (Nemestrinidae) which had proboscis between 28 and 39 mm; MTFs included *Prosoeca nitidula*, *Prosoeca westermanii* (Nemestrinidae), and *Philoliche lateralis* (Tabanidae) which had proboscis lengths between 4 and 16mm.

The networks of visitation rates (*H*2' = 0.76, Figure 2.7A), pollen loads (*H*2' = 0.71, Figure 2.7B) and pollinator importance (*H*2' = 0.99, Figure 2.7C) all showed high levels of

specialisation. In particular, the pollinator importance network showed near complete specialisation, with each population having a single highly effective functional pollinator. Across all *G. carneus* populations, there were only three important functional pollinator groups: solitary bees, MTFs and LTFs. The modularity analysis on the pollinator importance network showed that *G. carneus* populations were associated with the same pollinator niches: solitary bees, MTFs and LTFs (Figure S2.9). Although the network and modularity analysis showed high levels of specialisation to a specific functional pollinator at the population level, at the ecotypic level, the most important functional pollinator was not consistent. Across populations, *callistus*, *high-altitude*, and *macowanianus* were all pollinated by MTFs, LTFs and solitary bees; *prismatosiphon* was pollinated by LTFs and solitary bees; *langeberg* was pollinated by solitary bees, honey bees and Lycaenid butterflies; and *albidus* was pollinated by solitary bees and carpenter bees.

Gladiolus carneus populations show high levels of specialisation towards a single functional pollinator, and we further found a significant positive relationship between the tube length and weighted proboscis length ($R^2 = 0.46$, $\boldsymbol{F} = 8.622$, $df = 8$, $P = 0.02$; Figure S2.10A); however, there was no significant relationship between flower gape and weighted thorax depth ($R^2 = 0.01$, $F = 1.10$, $df = 8$, $P = 0.33$; Figure S2.10B).

Are differences in the ecological niches of the putative ecotypes of *Gladiolus carneus* resulting in premating reproductive isolation?

Ecogeographic isolation was the strongest gene flow barrier across the *G. carneus* species complex ($RI_{ecogeo} = 0.83$, Figure 2.8A). There was weak ecogeographic isolation from *albidus* to *callistus* and the *high-altitude* ecotype (Ecogeo: $RI_{al \rightarrow cl} = 0.35$, $RI_{al \rightarrow ha} = 0.52$), and from *callistus* to *albidus* and *macowanianus* (Ecogeo: $RI_{cl \rightarrow al} = 0.52$, $RI_{cl \rightarrow mc} = 0.52$). There was

also weak ecogeographic isolation from *albidus, callistus,* and *macowanianus* to *blandus* (Ecogeo: $RI_{al \rightarrow bl} = 0.30$, $RI_{cl \rightarrow bl} = 0.21$, $RI_{mc \rightarrow bl} = 0.41$). The small range of *blandus* is largely encased within the larger ranges of *albidus*, *callistus* and *macowanianus,* resulting in asymmetric ecogeographic isolation. All other gene flow directions between the ecotypes were above 0.6 indicating strong ecogeographic isolation, with many gene flow directions being near complete (Figure 2.8A).

Phenological isolation was a relatively strong gene flow barrier across the species complex ($RI_{phenology} = 0.67$, Figure 2.8B). There was weak phenological isolation from *albidus* to *callistus* (Phenology: $RI_{al \rightarrow cl} = 0.27$) and from *callistus* to *prismatosiphon* (Phenology: $RI_{cl \rightarrow pr} = 0.21$) due to overlapping flowering times. There was also weak phenological isolation from *macowanianus* to *albidus, blandus, callistus* and *prismatosiphon* (Phenology: $RI_{mc \rightarrow al} = 0.02$, $RI_{mc \rightarrow bl} = 0.12$, $RI_{mc \rightarrow cl} = 0.06$, $RI_{mc \rightarrow pr} = 0.11$). *Macowanianus* has the longest flowering time (stretching from September to early January) resulting in a large overlap in the flowering times of other ecotypes. However, other ecotypes have flowering times that are largely encased within the longer flowering time of *macowanianus*. This overlap only occurs for a short period of *macowanianus'* total flowering time. This provides a larger opportunity for gene flow from *macowanianus* to other ecotypes than from other ecotypes back to *macowanianus*, resulting in highly asymmetric gene flow.

Pollinator-mediated isolation was a relatively weak gene flow barrier between the ecotypes ($RI_{pollinator} = 0.39$, Figure 2.8C). As the sample of shared and unshared pollinators for each ecotype was small, the 95% confidence intervals for pollinator-mediated isolation were very large, indicating a high degree of uncertainty. Pollinator-mediated isolation was weakest from *callistus* to *albidus, high-altitude, macowanianus* and *prismatosiphon* (Pollinator: $RI_{cl \rightarrow}$

$_{al}$ = 0.00, $RI_{cl \rightarrow ha}$ = 0.00, $RI_{cl \rightarrow mc}$ = 0.00, $RI_{cl \rightarrow pr}$ = 0.00); from *high-altitude* to *prismatosiphon* and *macowanianus* (Pollinator: $RI_{ha \rightarrow pr}$ = 0.00, $RI_{ha \rightarrow mc}$ = 0.25); and from *macowanianus* to *prismatosiphon*, *high-altitude* and *callistus* (Pollinator: $RI_{mc \rightarrow pr}$ = 0.20, $RI_{mc \rightarrow ha}$ = 0.00, $RI_{mc \rightarrow cl}$ = 0.00). *Callistus, macowanianus* and *high-altitude* ecotypes have broad pollinator niches resulting in more opportunities for gene flow to other ecotypes.

The combined effects of ecogeographic, phenological and pollinator-mediated isolation has resulted in near complete premating isolation across the species complex (RI = 0.95, Figure 2.8D). The only weak gene flow direction for total premating reproductive isolation was from *macowanianus* and *albidus* to *blandus* ($RI_{mc \rightarrow bl}$ = 0.48, $RI_{al \rightarrow bl}$ = 0.49).

DISCUSSION

We provided evidence that morphologically distinct ecotypes of *G. carneus* occupied distinct realized and fundamental abiotic niches resulting in strong ecogeographic isolation across the species complex. The ecotypes additionally had different flowering times that caused moderate phenological isolation. Although individual populations of *G. carneus* were pollinated by a single, highly effective functional pollinator, at the ecotypic level plants had multiple highly effective functional pollinators resulting in relatively weak pollinator-mediated isolation. The strength of these premating barriers, and in particular ecogeographic isolation, caused near complete reproductive isolation between the ecotypes. These results suggested that niche differentiation, and particularly abiotic factors, may be playing a role in driving incipient speciation within the species complex.

Are Gladiolus carneus *ecotypes morphologically distinct*?

All ecotypes showed evidence of being morphologically distinct in both floral and vegetative traits lending support to the ecotypes initially included by Delpierre and du Plessis (1974) and for the two previously undescribed ecotypes (*langeberg* and the *high-altitude*). The ecotypes also differed significantly in their colour traits. *Albidus* only had a large central UV absorbent nectar guide (Figure S2.1E, S2.2C, S2.2E) and *callistus* had no nectar guides and instead had a dark purple gullet (Figure S2.1F, S2.2B). All other ecotypes had distinctly coloured centres and guides on their lower tepals (Figure S2.1D, Figure S2.2C-F). The bee and fly colour vision models indicated that most of the perceptible differences between the ecotypes were in the centres of the median and lateral tepals. In particular, *langeberg* and *albidus* had distinct centres on their median tepals, while *albidus*, *high-altitude* and *prismatosiphon* had distinct centres on their lateral tepals. These divergent colour properties are likely associated with adaptations to distinct functional pollinators (Demarche *et al.*, 2015). In particular, the UV absorbent centres of *albidus* likely evolved to attract their pollinators, solitary bees (Chittka, 1992, Demarche *et al.*, 2015, de Camargo *et al.*, 2019, Finnell and Koski, 2021, Newman *et al.*, 2022). The purple and red nectar guides found on all other ecotypes, except for *callistus,* is consistent with nectar guides documented in long proboscid Nemestrinid and Philoliche fly systems, and may represent a unique adaptation to the long-proboscid fly pollination syndrome (Goldblatt *et al.*, 2001, Newman *et al.*, 2014). However, since the ecotypes were not associated with a single highly effective functional pollinator, direct associations between nectar guide properties and functional pollinators should be assessed at the population level with reference to the most important pollinator (Moir *et al.*, 2025).

Abiotic niche differentiation causing ecogeographic isolation

Gladiolus carneus ecotypes occupied distinct realised and fundamental niches (Figure 2.5, S2.9) leading to strong ecogeographic isolation across the species complex. There were a

number of cases of asymmetric ecogeographic isolation, which occur when there are unequal opportunities for directional gene flow between taxa (Christie *et al.*, 2022), often caused by one taxon having a range largely encased within the other. These cases were firstly caused by the large *albidus* range overlapping with the *callistus* and *high-altitude* ecotypes, and secondly from the small *blandus* range being largely encased within the ranges of *albidus, callistus* and *macowaniaus.* Across plant taxa, ecogeographic isolation is relatively symmetrical, however individual cases can vary substantially, which largely corroborates the results found in the *G. carneus* complex (Christie *et al.*, 2022). These results, along with the differences in vegetative morphology documented between the ecotypes (Figure S2.3B), suggest that abiotic niche differentiation plays a potential role in the diversification of the species complex. The importance of abiotic niche differentiation driving diversification is largely congruent with previous experimental evidence in the CFR (e.g., Latimer *et al.*, 2009, Carlson *et al.*, 2011, Mitchell *et al.*, 2015, Carlson *et al.*, 2016). For example, Carlson *et al.* (2011) found that white *Protea* populations differ in functional traits across environmental gradients, some of which are likely maintained by divergent selection imposed by ecological differences. Macroevolutionary evidence supporting abiotic niche differentiation in the CFR is somewhat mixed. van der Niet and Johnson (2009) tested for ecological shifts in 188 Cape sister species and found evidence that habitat, pollinator and fire-frequency shifts were more frequent than soil type shifts, while Schnitzler *et al.* (2011) analysed 470 species from the phylogenies of four Cape clades and found that soil type had the highest variability between sister species in three of the clades. Outside of the CFR, abiotic niche differentiation is a major driver of diversification (Grossenbacher *et al.*, 2014, Fernandez-Mazuecos and Glover, 2024) and the resulting gene flow barrier, ecogeographic isolation, has been found to be one of the strongest gene flow barriers between recently diverged taxa (Christie *et al.*, 2022).

Flowering time differences causing phenological isolation

There were differences in the flowering times of the *G. carneus* ecotypes leading to varying strengths of phenological isolation (Figure 2.6). In a few cases, phenological isolation was asymmetric which was largely due to *macowanianus* having a long flowering time that overlapped with *albidus, blandus, callistus* and *prismatosiphon*. These shifts in phenology may also be driving diversification within the species complex. Phenological shifts have been well documented within the CFR, with van der Niet and Johnson (2009) showing that over 30% of 188 species pairs from eight Cape clades had phenological differences. Similarly, Linder (2020) found that 47% of 112 sister species pairs in the Restionaceae had non-overlapping flowering times. These findings indicate that phenological shifts seem to be a relatively frequent isolating barrier between taxa in the CFR (Ellis *et al.*, 2014). However, this seems to contradict the results from a global comparison showing phenological isolation seems to play a lesser role in speciation events between recently diverged taxa ($RI_{phenology} = 0.38$) (Christie *et al.*, 2022).

Differing functional pollinators causing pollinator-mediated isolation

Although each population of *G. carneus* had a single highly effective functional pollinator, each ecotype was not associated a single functional pollinator. This suggests that the ecotypes do not occupy distinct pollination niches and that pollinators are unlikely to be driving the diversification at the ecotypic level. These results are similar to Schnitzler *et al.* (2011) which found that in four highly diverse Cape Clades, pollinator shifts were relatively infrequent compared to shifts in soil type and fire survival strategy. However, these results contrast with both phylogenetic and experimental evidence showing that pollinator-driven speciation is common in both the CFR (van der Niet and Johnson, 2009, Johnson, 2010, Anderson *et al.*, 2014, Forest *et al.*, 2014, Newman *et al.*, 2015, Newman and Johnson, 2021) and in the genus

Gladiolus (Anderson *et al.*, 2010, Valente *et al.*, 2012). Furthermore, Christie *et al.* (2022) found that pollinator-mediated isolation, along with ecogeographic isolation, was one of the strongest reproductive isolation barriers documented across 89 taxa pairs of seed plants. However, as populations of *G. carneus* only had one highly effective functional pollinator and there were associations between floral and pollinator morphology across sites, pollinators may be driving population level shifts and causing reproductive isolation between populations rather than between ecotypes. This is further supported by the significant correlations between the weighted proboscis lengths and floral tube lengths across sites (Figure S2.10A) suggesting that there is population level divergence in some floral traits. Alternatively, the estimates of pollinator-mediated isolation may be inaccurate. Taking into account only the shared and unshared functional pollinators does not account for differential efficiency of functional pollinators to alternative ecotypes (Ostevik *et al.*, 2016, Moir *et al.*, 2025). The strength of pollinator-mediated isolation could be more accurately estimated between ecotypes with sympatric populations (e.g., *macowanianus* and *callistus*) where pollinator transitions (Sobel and Streisfeld, 2015) and pollen flow (Kay, 2006) could be used to estimate behavioural and mechanical isolation.

Should Gladiolus carneus *ecotypes be treated as separate taxa?*

The biological species concept posits that taxa should be treated as separate species when they are reproductively isolated from one another (Coyne and Orr, 2004). Ecotypes of *G. carneus* showed evidence of distinct vegetative and floral morphology (Figure 2.1, 2.2) and are strongly reproductively isolated from one another (RI_{total} = 0.95 SE). The only exception, *blandus*, does not differ from *macowanianus* in morphology and is encased within *macowanianus'* range and flowering time, potentially leading to weak reproductive isolation. As premating reproductive isolation is near complete between the ecotypes, they can likely be treated as separate taxa

regardless of the strength of postpollination isolation. In the CFR, there are examples of interfertile orchids being treated as separate taxa (Newman and Johnson, 2024). However, whether these taxa should be treated as separate species depends on whether species are defined as being reproductively isolated or when reproductive isolation is irreversible (Lowry, 2012). If species are defined by whether they are reproductively isolated from one another, premating barriers alone can be used to delineate species. However, divergent selection on traits that mediate reproductive isolation can allow for introgression and result in the collapse of species boundaries in the future (Lowry, 2012). If species are instead defined by whether reproductive isolation is irreversible, separate species would only be delineated when intrinsic postzygotic isolation is complete which would be tested using a series of controlled crosses. The *G. carneus* ecotypes, apart from *blandus*, meet the criteria of being reproductively isolated from one another, but it remains to be seen if it is reversable. Although we have provided ecological evidence that quantifies the potential gene flow between these ecotypes, population genetic data would provide insights into the extent of ongoing gene flow and 'genetic distinctness' between ecotypes (Westram *et al.*, 2022). This should be further paired with genetic and ecological evidence of whether these ecotypes can exist stably in sympatry (Coyne and Orr, 2004, Mallet and Mullen, 2022).

CONCLUSION

Overall, we provided evidence of seven morphologically distinct ecotypes within the *G. carneus* species complex that occupied contrasting abiotic and biotic niches resulting in near complete premating reproductive isolation. These results suggested niche differentiation likely played a key role in driving the diversification both within this species complex and within the CFR. Future research should test for local adaptation using reciprocal translocations and common gardens, which would provide further evidence of ecological divergence. These field

studies should be paired with greenhouse experiments that identify the ecological factors that cause the morphological and niche differentiation between the ecotypes. Additionally, postpollination isolation, specifically a series of controlled crosses, should be quantified between these ecotypes to determine both its relative contribution to maintaining reproductive isolation, and whether reproductive isolation is reversable. These experimental approaches should be paired with phylogenomic and population genetic data to provide evidence of the evolutionary relationships and gene flow patterns within the species complex. This integrated approach would provide insights into the ongoing divergence within this species complex and the wider CFR.

LITERATURE CITED

Agostinelli C, Lund U. 2024. R package 'circular': circular statistics. version 0.5-1. https://CRAN.R-project.org/package=circular.

An L, Neimann A, Eberling E, Algora H, Brings S, Lunau K. 2018. The yellow specialist: dronefly *Eristalis tenax* prefers different yellow colours for landing and proboscis extension. *Journal of Experimental Botany*, **221**: jeb184788.

Anderson B, Alexandersson R, Johnson SD. 2010. Evolution and coexistence of pollination ecotypes in an African *Gladiolus* (Iridaceae). *Evolution*, **64**: 960-972.

Anderson B, Ros P, Wiese TJ, Ellis AG. 2014. Intraspecific divergence and convergence of floral tube length in specialized pollination interactions. *Proceedings of the Royal Society B: Biological Sciences*, **281**: 20141420.

Beckett SJ. 2016. Improved community detection in weighted bipartite networks. *Royal Society Open Science*, **3**: 140536.

Bluthgen N, Menzel F, Bluthgen N. 2006. Measuring specialization in species interaction networks. *BMC Ecology*, **6**: 9.

Boucher FC, Verboom GA, Gallien L, Ellis AG. 2023. Multiple reproductive barriers maintain species boundaries in stone plants of the genus *Argyroderma*. *Botanical Journal of the Linnean Society*, **204**: 187–197.

Briscoe AD, Chittka L. 2001. The evolution of colour vision in insects. *Annual Review of Entomology*, **46**: 471–510.

Carlson JE, Adams CA, Holsinger KE. 2016. Intraspecific variation in stomatal traits, leaf traits and physiology reflects adaptation along aridity gradients in a South African shrub. *Annals of Botany*, **117**: 195-207.

Carlson JE, Holsinger KE, Prunier R. 2011. Plant responses to climate in the Cape Floristic Region of South Africa: evidence for adaptive differentiation in the Proteaceae. *Evolution*, **65**: 108-124.

Chittka L. 1992. The colour hexagon: a chromaticity diagram based on photoreceptor excitations as a generalized representation of colour opponency. *Journal of Comparative Physiology A*, **170**: 533-543.

Christie K, Fraser LS, Lowry DB. 2022. The strength of reproductive isolating barriers in seed plants: insights from studies quantifying premating and postmating reproductive barriers over the past 15 years. *Evolution*, **76**: 2228-2243.

Christie K, Strauss SY. 2019. Reproductive isolation and the maintenance of species boundaries in two serpentine endemic Jewelflowers. *Evolution*, **73**: 1375-1391.

Coyne JA, Orr HA. 2004. *Speciation.* Sunderland, MA: Sinauer Associates.

Cramer MD, West AG, Power SC, Skelton R, Stock WD. 2014. Plant ecophysiological diversity. In: Allsopp N, Colville JF, Verboom GA, eds. *Fynbos: ecology, evolution and conservation of a megadiverse region*. Oxford: Oxford University Press.

Cramer MD, Wootton LM, Mazijk R, Verboom GA. 2019. New regionally modelled soil layers improve prediction of vegetation type relative to that based on global soil models. *Diversity and Distributions,* **25**: 1736-1750.

da Silva AR, Malafaia G, Menezes IPP. 2017. Biotools: an R function to predict spatial gene diversity via an individual-based approach. *Genetics and Molecular Research* **16**: 1-6.

de Camargo MGG, Lunau K, Batalha MA, Brings S, de Brito VLG, Morellato LPC. 2019. How flower colour signals allure bees and hummingbirds: a community-level test of the bee avoidance hypothesis. *New Phytologist*, **222**: 1112-1122.

Dellinger AS, Lagomarsino L, Michelangeli F, Dullinger S, Smith SD. 2024. The sequential direct and indirect effects of mountain uplift, climatic niche, and floral trait evolution on diversification dynamics in an Andean plant clade. *Systematic Biology,* **73**: 594-612.

Delpierre GR, du Plessis NM. 1974. *The winter-growing Gladioli of South Africa.* London: Nasionale Bokhandel Ltd.

Demarche ML, Miller TJ, Kay KM. 2015. An ultraviolet floral polymorphism associated with life history drives pollinator discrimination in *Mimulus guttatus*. *American Journal of Botany,* **102**: 396-406.

Dormann CF, B. G, Fruend J. 2008. Introducing the bipartite package: analysing ecological networks. *R news,* **8**.

Elith J, Phillips SJ, Hastie T, Dudík M, Chee YE, Yates CJ. 2010. A statistical explanation of MaxEnt for ecologists. *Diversity and Distributions,* **17**: 43-57.

Ellis AG, Verboom GA, van der Niet T, Johnson SD, Linder HP. 2014. Speciation and extinction in the greater Cape Floristic Region. In: Allsopp N, Colville JF, Verboom

GA, eds. *Fynbos: ecology, evolution and conservation of a megadiverse region*. Oxford: Oxford University Press.

Elzinga JA, Atlan A, Biere A, Gigord L, Weis AE, Bernasconi G. 2007. Time after time: flowering phenology and biotic interactions. *Trends in Ecology & Evolution,* **22**: 432-439.

Farnitano MC, Sweigart AL. 2023. Strong postmating reproductive isolation in *Mimulus* section Eunanus. *Journal of Evolutionary Biology,* **36**: 1393-1410.

Fernandez-Mazuecos M, Glover BJ. 2024. Climatic and edaphic niche shifts during plant radiation in the Mediterranean biodiversity hotspot. *Annals of Botany,* **135**: 717–734.

Finnell LM, Koski MH. 2021. A test of Sensory Drive in plant-pollinator interactions: heterogeneity in the signalling environment shapes pollinator preference for a floral visual signal. *New Phytologist,* **232**: 1436-1448.

Forest F, Goldblatt P, Manning JC, *et al.* 2014. Pollinator shifts as triggers of speciation in painted petal irises (*Lapeirousia*: Iridaceae). *Annals of Botany,* **113**: 357-371.

Fox J, Weisberg S. 2019. *An {R} Companion to applied regression.* Thousand Oaks CA: Sage.

Garcia JE, Hannah L, Shrestha M, Burd M, Dyer AG. 2022. Fly pollination drives convergence of flower coloration. *New Phytologist,* **233**: 52 - 61.

Giurfa M, Vorobyev M, Kevan P, Menzel R. 1996. Detection of coloured stimuli by honeybees: minimum visual angles and receptor specific contrasts. *Journal of Comparative Physiology A,* **178**: 699-709.

Goldblatt P, Manning J. 1998. *Gladiolus in Southern Africa.* Vlaeberg: Fernwood Press.

Goldblatt P, Manning JC. 1999. The long-proboscid fly pollination system in *Gladiolus* (Iridaceae). *Annals of the Missouri Botanical Garden,* **86**: 758-774.

Goldblatt P, Manning JC, Bernhardt P. 2001. Radiation of pollination systems in *Gladiolus* (Iridaceae: Crocoideae) in southern Africa. *Annals of the Missouri Botanical Garden,* **88**: 713-734.

Grant V. 1994. Modes and origins of mechanical and ethological isolation in angiosperms. *Proceedings of the National Academy of Sciences,* **91**: 3-10.

Grossenbacher DL, Veloz SD, Sexton JP. 2014. Niche and range size patterns suggest that speciation begins in small, ecologically diverged populations in North American monkeyflowers (*Mimulus* spp.). *Evolution,* **68**: 1270-1280.

Hannah L, Dyer AG, Garcia JE, Dorin A, Burd M. 2019. Psychophysics of the hoverfly: categorical or continuous color discrimination? *Current Zoology,* **65**: 483-492.

Herve M. 2023. RVAideMemoire: testing and plotting procedures for biostatistics. R package version 0.9-83-7. https://CRAN.R-project.org/package=RVAideMemoire.

Hijmans RJ. 2024. raster: geographic data analysis and modeling. R package version 3.6-30. https://rspatial.org/raster.

Hijmans RJ, Phillips S, Leathwick J. 2023. dismo: species distribution modeling. R package version 1.3-15. https://github.com/rspatial/dismo.

Ivey CT, Habecker NM, Bergmann JP, Ewald J, Frayer ME, Coughlan JM. 2023. Weak reproductive isolation and extensive gene flow between *Mimulus glaucescens* and *M. guttatus* in northern California. *Evolution,* **77**: 1245-1261.

Johnson SD. 2010. The pollination niche and its role in the diversification and maintenance of the southern African flora. *Philosophical Transactions of the Royal Society B,* **365**: 499-516.

Kay KM. 2006. Reproductive isolation between two closely related hummingbird-pollinated neotropical gingers. *Evolution,* **60**: 538-552.

Latimer AM, Silander Jr. JA, Rebelo AG, Midgley GF. 2009. Experimental biogeography: the role of environmental gradients in high geographic diversity in Cape Proteaceae. *Oecologia,* **160**: 151-162.

Lenth RV. 2022. emmeans: estimated marginal means, aka least-squares means. R package version 1.7.2. https://CRAN.R-project.org/package=emmeans.

Lewis GJ, Obermeyer AA, Barnard TT. 1972. *Gladiolus a revision of the South African species.* Cape Town: Purnell & Sons.

Linder HP. 2003. The radiation of the Cape flora, southern Africa. *Biological Reviews,* **78**: 597–638.

Linder HP. 2020. The evolution of flowering phenology: an example from the wind-pollinated African Restionaceae. *Annals of Botany*, **126**: 1141-1153.

Lowry DB. 2012. Ecotypes and the controversy of stages in the formation of new species. *Biological Journal of the Linnean Society*, **106**: 241–257.

Lunau K, Papiorek S, Eltz T, Sazima M. 2011. Avoidance of achromatic colours by bees provides a private niche for hummingbirds. *Journal of Experimental Biology*, **214**: 1607-1612.

Maia R, Gruson H, Endler JA, White TE, O'Hara RB. 2019. pavo 2: new tools for the spectral and spatial analysis of colour in R. *Methods in Ecology and Evolution,* **10**: 1097-1107.

Maia R, White TE. 2018. Comparing colors using visual models. *Behavioral Ecology,* **29**: 649-659.

Mallet J, Mullen SP. 2022. Reproductive isolation is a heuristic, not a measure: a commentary on Westram et al., 2022. *Journal of Evolutionary Biology,* **35**: 1175-1182.

Manning J, Goldblatt P. 2012. *Plants of the Greater Cape Floristic Region 1: the core Cape flora.* Pretoria: Strelitzia 29.

Minnaar C, de Jager ML, Anderson B. 2019. Intraspecific divergence in floral-tube length promotes asymmetric pollen movement and reproductive isolation. *New Phytologist,* **224**: 1160-1170.

Mitchell N, Moore TE, Mollmann HK, *et al.* 2015. Functional traits in parallel evolutionary radiations and trait-environment associations in the Cape Floristic Region of South Africa. *The American Naturalist,* **185**: 525-537.

Moir M, Butler H, Peter C, Dold T, Newman E. 2025. A test of the Grant-Stebbins pollinator-shift model of floral evolution. *New Phytologist,* **245**: 2322–2335.

Munguia-Rosas MA, Ollerton J, Parra-Tabla V, De-Nova JA. 2011. Meta-analysis of phenotypic selection on flowering phenology suggests that early flowering plants are favoured. *Ecology Letters,* **14**: 511-521.

Newman E, Anderson B. 2020. Character displacement drives floral variation in *Pelargonium* (Geraniaceae) communities. *Evolution,* **74**: 283-296.

Newman E, Anderson B, Johnson SD. 2012. Flower colour adaptation in a mimetic orchid. *Proceedings of the Royal Society B,* **279**: 2309-2313.

Newman E, Johnson SD. 2021. A shift in long-proboscid fly pollinators and floral tube length among populations of *Erica junonia* (Ericaceae). *South African Journal of Botany,* **142**: 451-458.

Newman E, Johnson SD. 2024. Pollinator-mediated isolation promotes coexistence of closely related food-deceptive orchids. *Journal of Evolutionary Biology,* **38**: 190-201.

Newman E, Manning J, Anderson B. 2014. Matching floral and pollinator traits through guild convergence and pollinator ecotype formation. *Annals of Botany,* **113**: 373-384.

Newman E, Manning J, Anderson B. 2015. Local adaptation: mechanical fit between floral ecotypes of *Nerine humilis* (Amaryllidaceae) and pollinator communities. *Evolution*, **69**: 2262-2275.

Newman EL, Khoury KL, Niekerk SEV, Peter CI. 2022. Structural anther mimics improve reproductive success through dishonest signaling that enhances both attraction and the morphological fit of pollinators with flowers. *Evolution*, **76**: 1749-1761.

Oksanen J, Blanchet FG, Friendly M, *et al.* 2020. vegan: community ecology package. R package version 2.5-7. https://CRAN.R-project.org/package=vegan.

Ostevik KL, Andrew RL, Otto SP, Rieseberg LH. 2016. Multiple reproductive barriers separate recently diverged sunflower ecotypes. *Evolution*, **70**: 2322-2335.

Paudel BR, Burd M, Shrestha M, Dyer AG, Li QJ. 2018. Reproductive isolation in alpine gingers: how do coexisting *Roscoea* (*R. purpurea* and *R. tumjensis*) conserve species integrity? *Evolution*, **72**: 1840-1850.

Pewsey A, Neuhäuser M, G.D. R. 2013. *Circular statistics in R.* Oxford: Oxford University Press.

Phillips SJ, Anderson RP, Schapire RE. 2006. Maximum entropy modeling of species geographic distributions. *Ecological Modelling*, **190**: 231-259.

R Core Team. 2021. R: A language and environment for statistical computing. Vienna, Austria: R Foundation for Statistical Computing.

Ramirez-Aguirre E, Marten-Rodriguez S, Quesada-Avila G, *et al.* 2019. Reproductive isolation among three sympatric *Achimenes* species: pre- and post-pollination components. *American Journal of Botany*, **106**: 1021-1031.

Ramsey J, Bradshaw HD, Schemske DW. 2003. Components of reproductive isolation between the monkeyflowers *Mimulus lewisii* and *M. cardinalis* (Phrymaceae). *Evolution,* **57**: 1520-1534.

Rundle HD, Nosil P. 2005. Ecological speciation. *Ecology Letters,* **8**: 336-352.

Sandstedt GD, Wu CA, Sweigart AL. 2021. Evolution of multiple postzygotic barriers between species of the *Mimulus tilingii* complex. *Evolution,* **75**: 600-613.

Schluter D. 2000. *The ecology of adaptive radiation.* New York: OUP Oxford.

Schluter D. 2001. Ecology and the origin of species. *Trends in Ecology & Evolution,* **16**: 372-380.

Schnitzler J, Barraclough TG, Boatwright JS, *et al.* 2011. Causes of plant diversification in the Cape biodiversity hotspot of South Africa. *Systematic Biology,* **60**: 343-357.

Sobel JM. 2014. Ecogeographic isolation and speciation in the genus *Mimulus*. *The American Naturalist,* **184**: 565-579.

Sobel JM, Chen GF. 2014. Unification of methods for estimating the strength of reproductive isolation. *Evolution,* **68**: 1511-1522.

Sobel JM, Streisfeld MA. 2015. Strong premating reproductive isolation drives incipient speciation in *Mimulus aurantiacus*. *Evolution,* **69**: 447-461.

Troje N. 1993. Spectral categories in the learning behaviour of blowflies. *Zeitschrift für Naturforschung C,* **48**: 96-104.

Turesson G. 1922. The species and the variety as ecological units. *Hereditas,* **3**: 100-113.

Valente LM, Manning JC, Goldblatt P, Vargas P. 2012. Did pollination shifts drive diversification in southern African *Gladiolus*? Evaluating the model of pollinator-driven speciation. *The American Naturalist,* **180**: 83-98.

van der Kooi CJ, Kelber A. 2022. Achromatic cues are important for flower visibility to hawkmoths and other insects. *Frontiers in Ecology and Evolution,* **10**: 819436.

van der Niet T, Johnson SD. 2009. Patterns of plant speciation in the Cape Floristic Region. *Molecular Phylogenetics and Evolution*, **51**: 85-93.

Westram AM, Stankowski S, Surendranadh P, Barton N. 2022. What is reproductive isolation? *Journal of Evolutionary Biology*, **35**: 1143-1164.

FIGURES

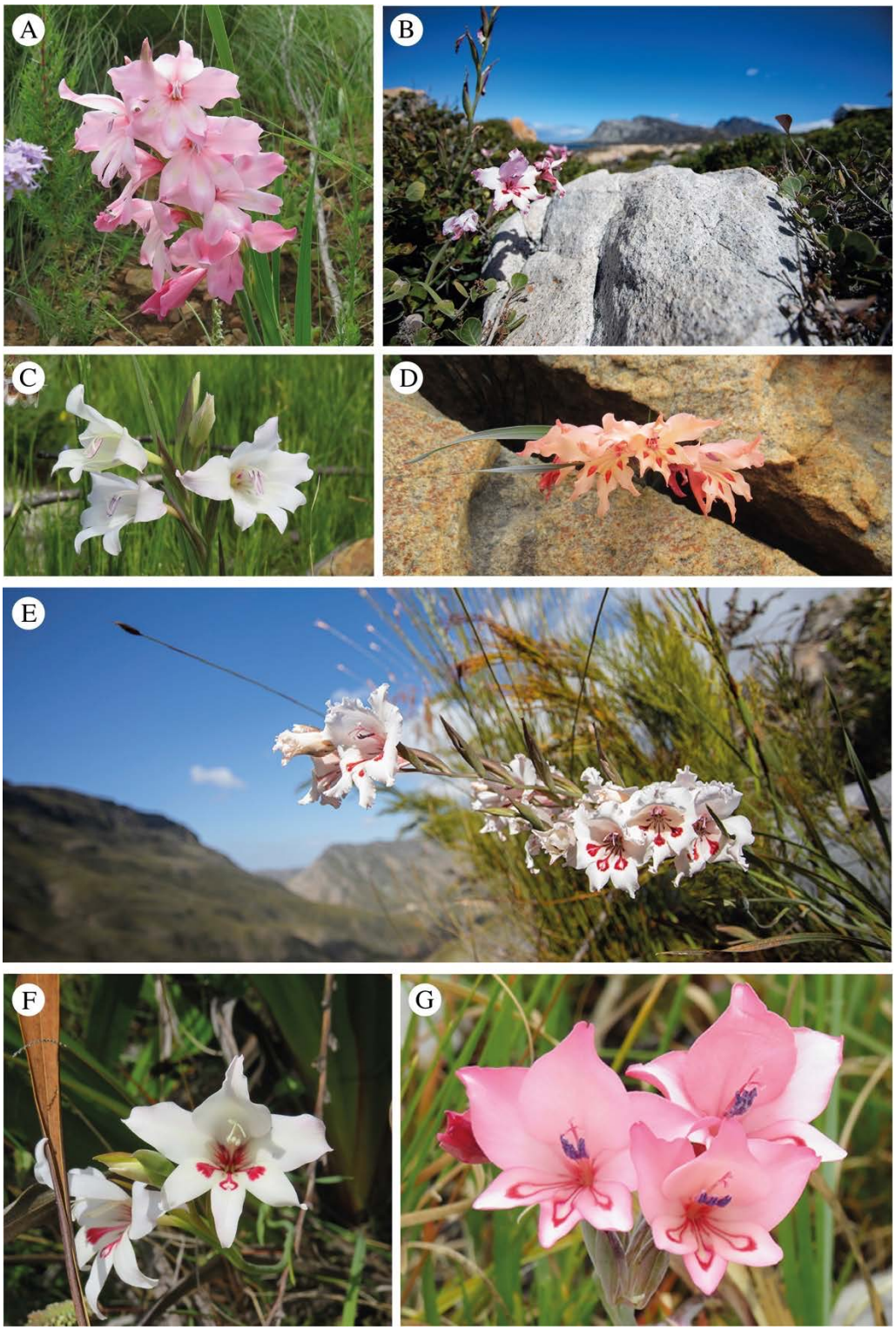

Figure 2.1. Colour plate of all *Gladiolus carneus* ecotypes. These include (A) *albidus*, (B) *blandus*, (C) *callistus*, (D) *high-altitude*, (E) *langeberg*, (F) *macowanianus*, and (G) *prismatosiphon*. Photos: A, C, D, F, G: Katharine Khoury; B, E: Ethan Newman.

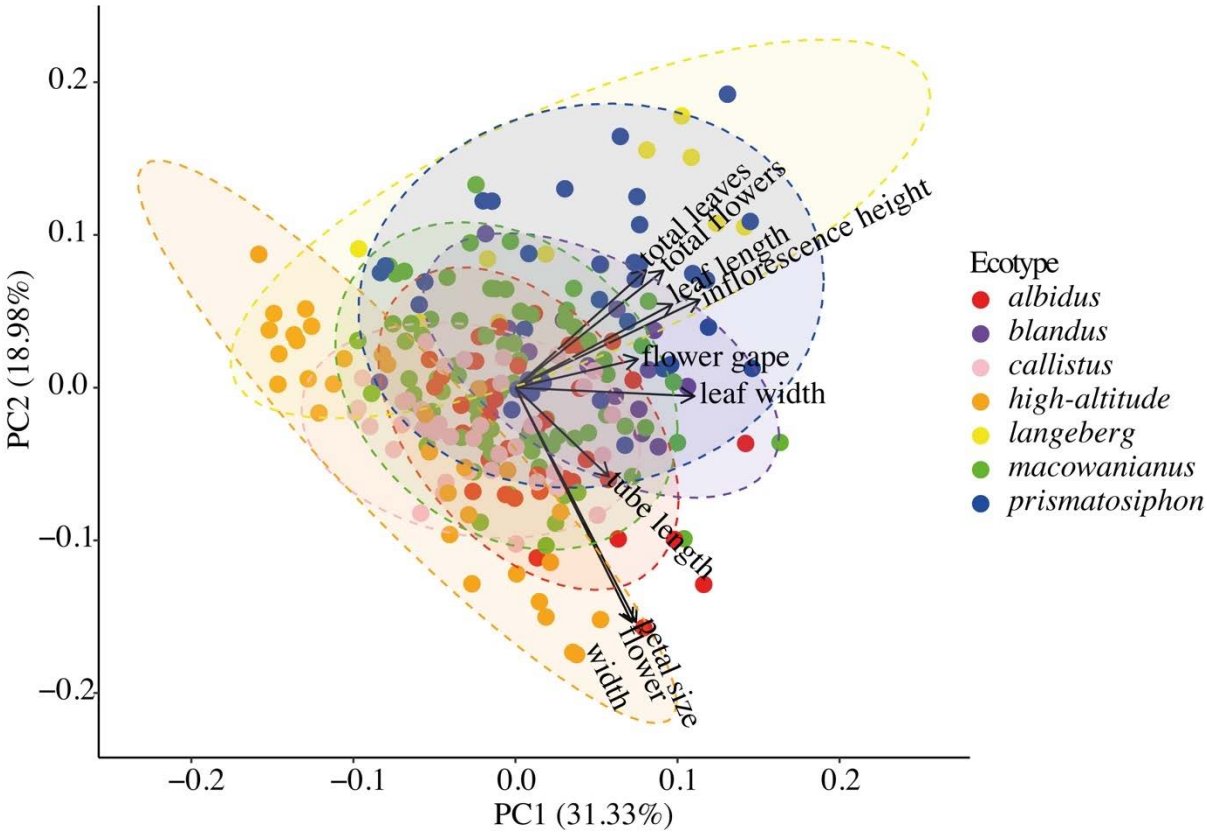

Figure 2.2. PCA of floral and vegetative traits of *Gladiolus carneus* ecotypes. The PCA includes ellipses showing 95% confidence intervals and a biplot of trait loadings. The variables included in the PCA are: tube length, flower gape, flower width, petal size, inflorescence height, leaf length, leaf width, total flowers and total leaves.

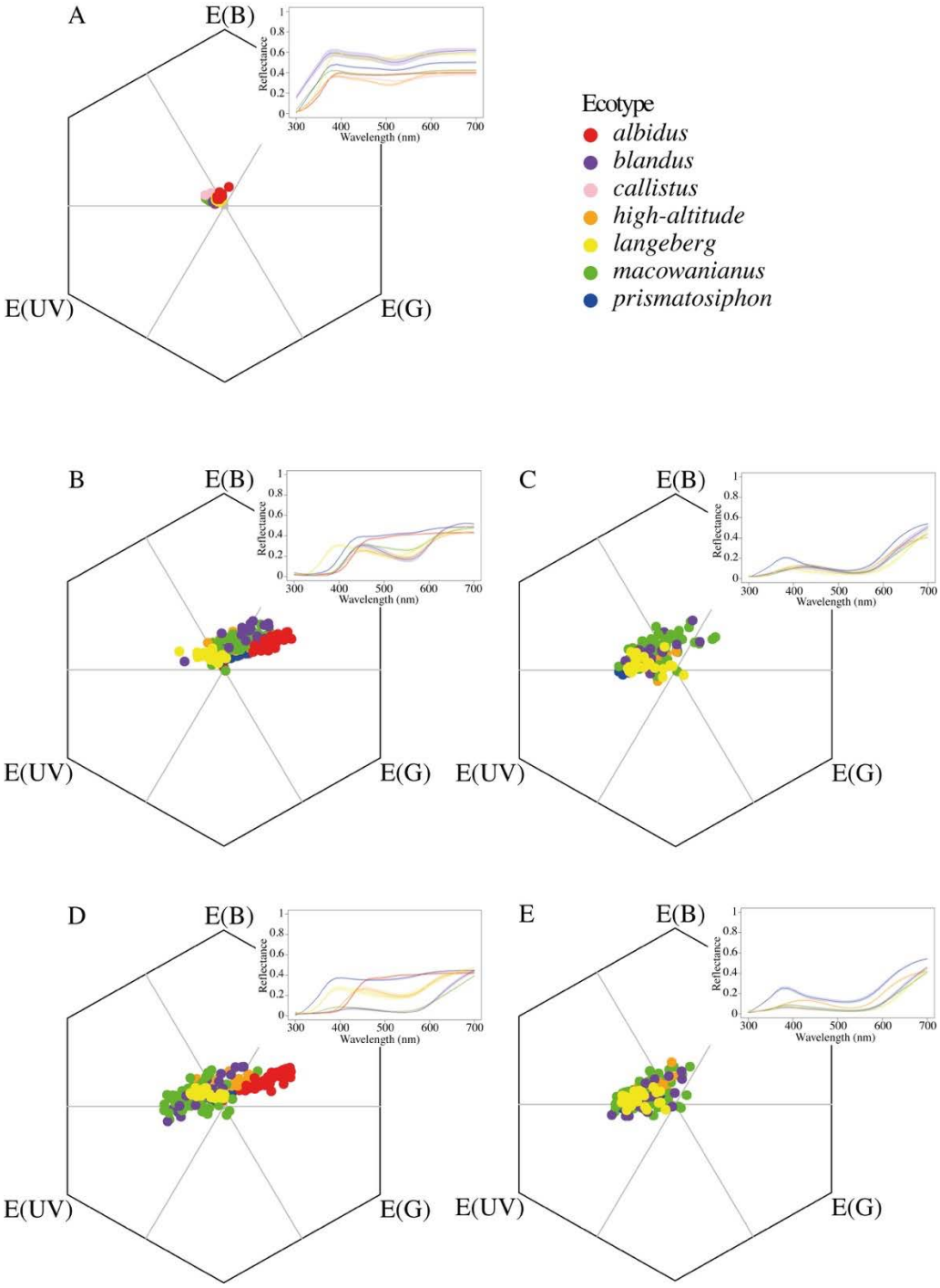

Figure 2.3. Spectra of *Gladiolus carneus* ecotypes' (A) tepal, (B) centre of the median tepal, (C) guide of median tepal, (D) centre of lateral tepal, and (E) guide of lateral tepal plotted in bee colour vision with *Apis mellifera* spectral sensitivities. Top right of each colour vision model shows the associated spectral reflectance curves for each *G. carneus* ecotype. Mean spectral reflectance curve is depicted by the dark line in the centre with lighter shading representing the standard error.

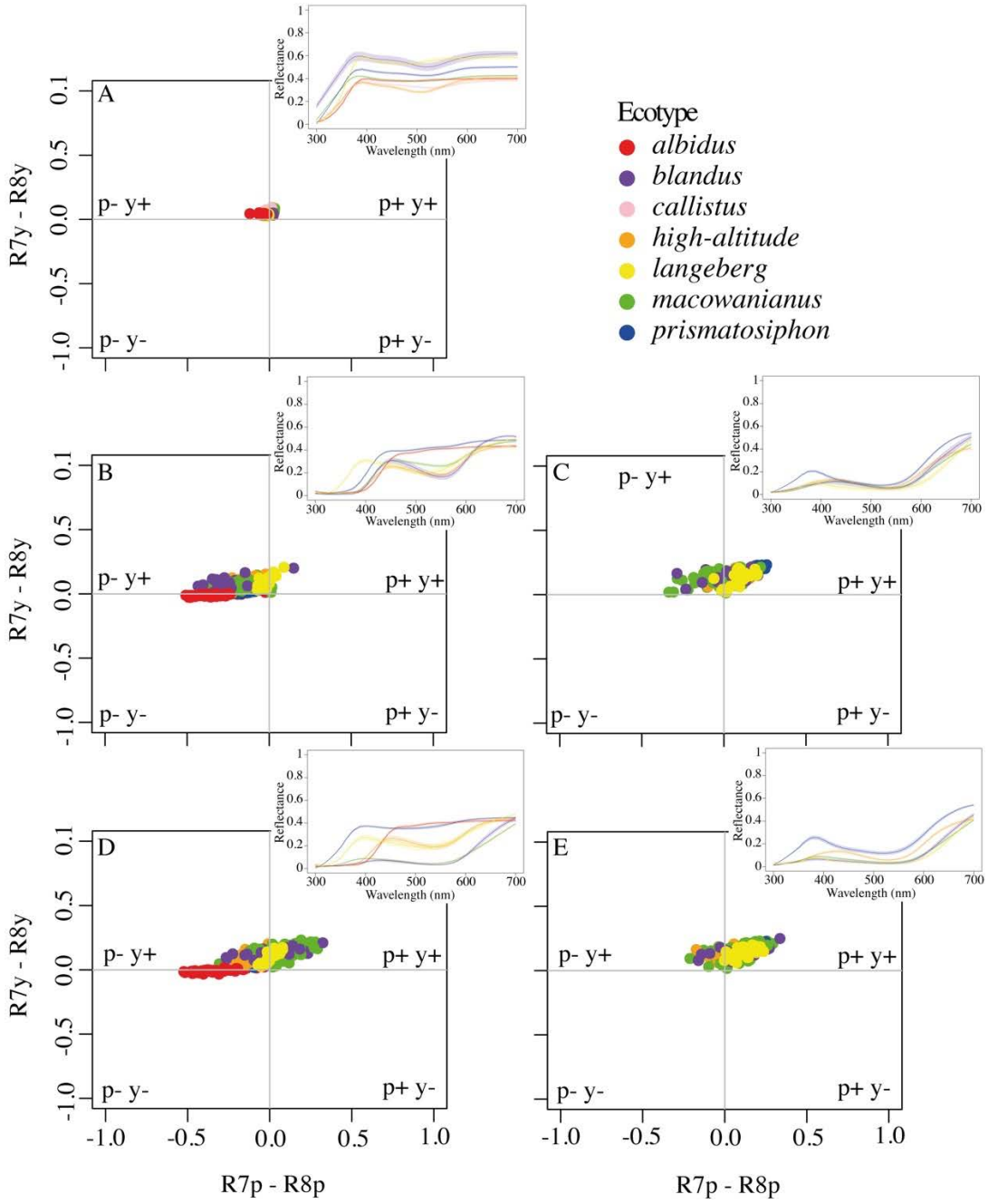

Figure 2.4. Spectra of *Gladiolus carneus* ecotypes' (A) tepal, (B) centre of the median tepal, (C) guide of median tepal, (D) centre of lateral tepal, and (E) guide of lateral tepal plotted in fly colour vision with *Eristalis tenax* spectral sensitivities. Top right of each colour vision model shows the associated spectral reflectance curves for each *G. carneus* ecotype. Mean spectral reflectance curve is depicted by the dark line in the centre with lighter shading representing the standard error.

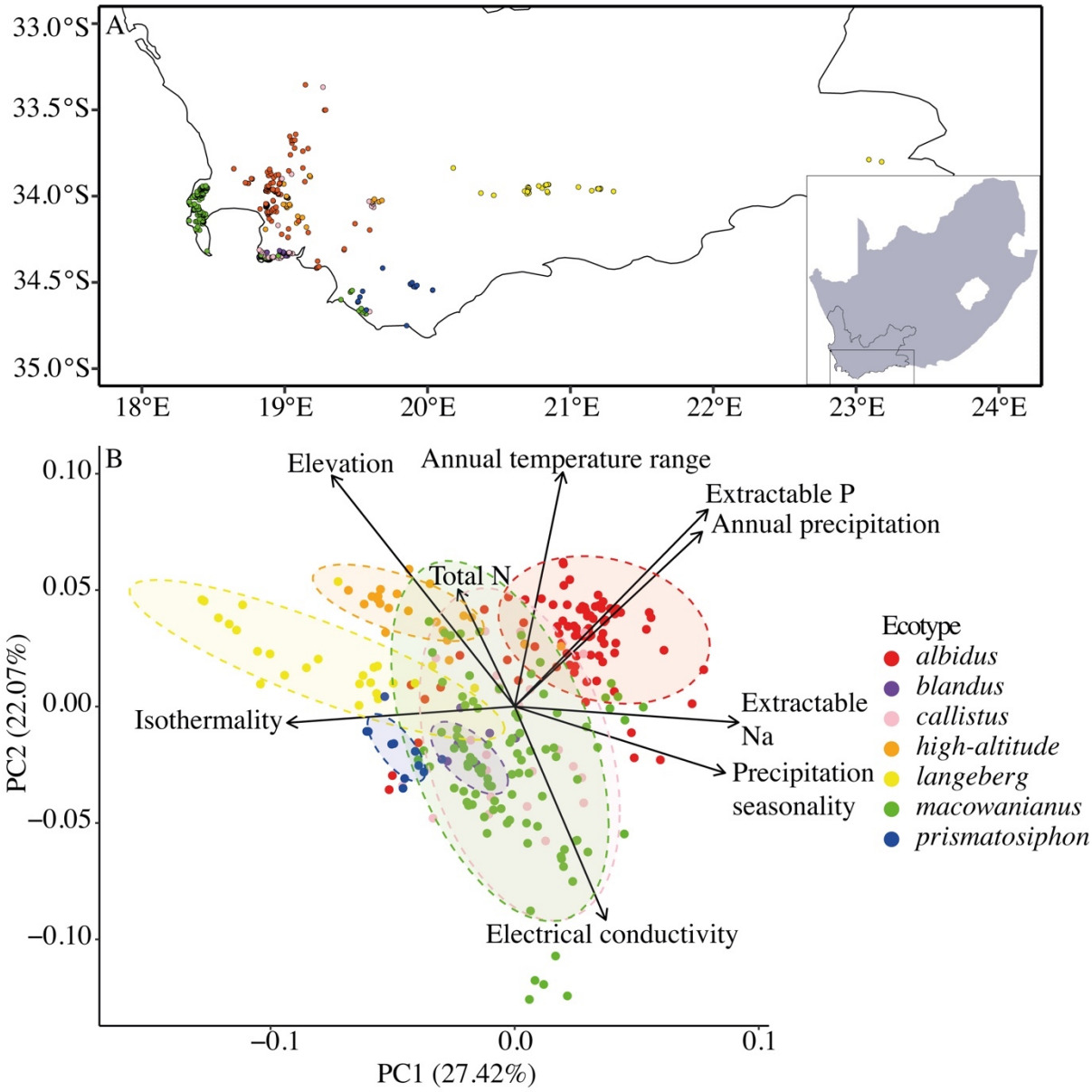

Figure 2.5. (A) Distribution map of *Gladiolus carneus* ecotypes in the Western Cape of South Africa. All circles on the map show the point localities of all iNaturalist observations used in the environmental niche modes for each *G. carneus* ecotype. (B) PCA of the abiotic niche of the *G. carneus* ecotypes. Abiotic layers include uncorrelated bioclimatic, elevation and soil variables. The variables include elevation, isothermality, annual temperature range, annual precipitation, precipitation seasonality, electrical conductivity, total nitrogen, extractable phosphorus, and extractable sodium.

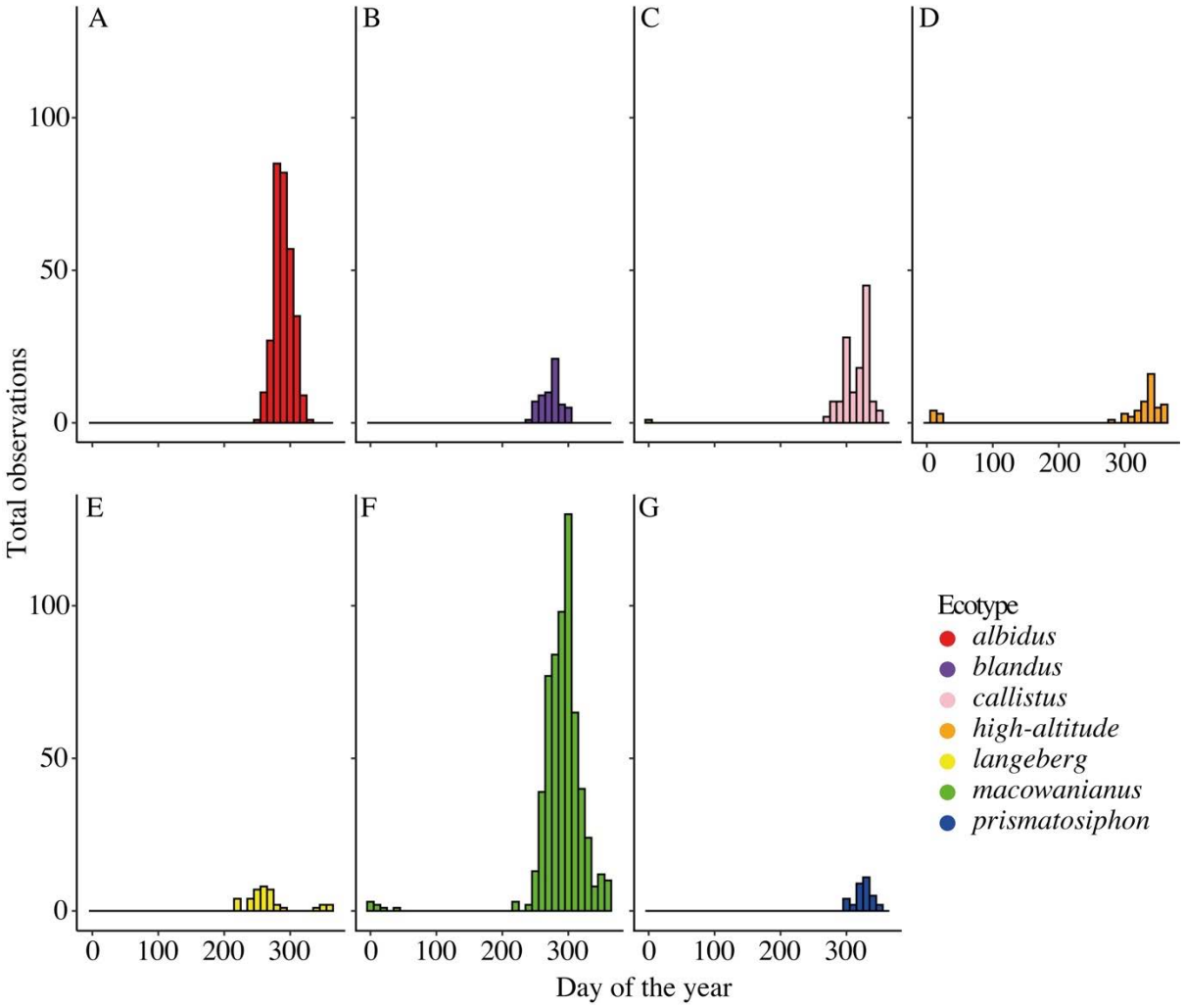

Figure 2.6. Flowering phenology of *Gladiolus carneus* ecotypes shown by the total iNaturalist observations on each day of the year. *G. carneus* ecotypes are (A) *albidus*, (B) *blandus*, (C) *callistus*, (D) *high-altitude*, (E) *langeberg*, (F) *macowanianus*, and (G) *prismatosiphon*.

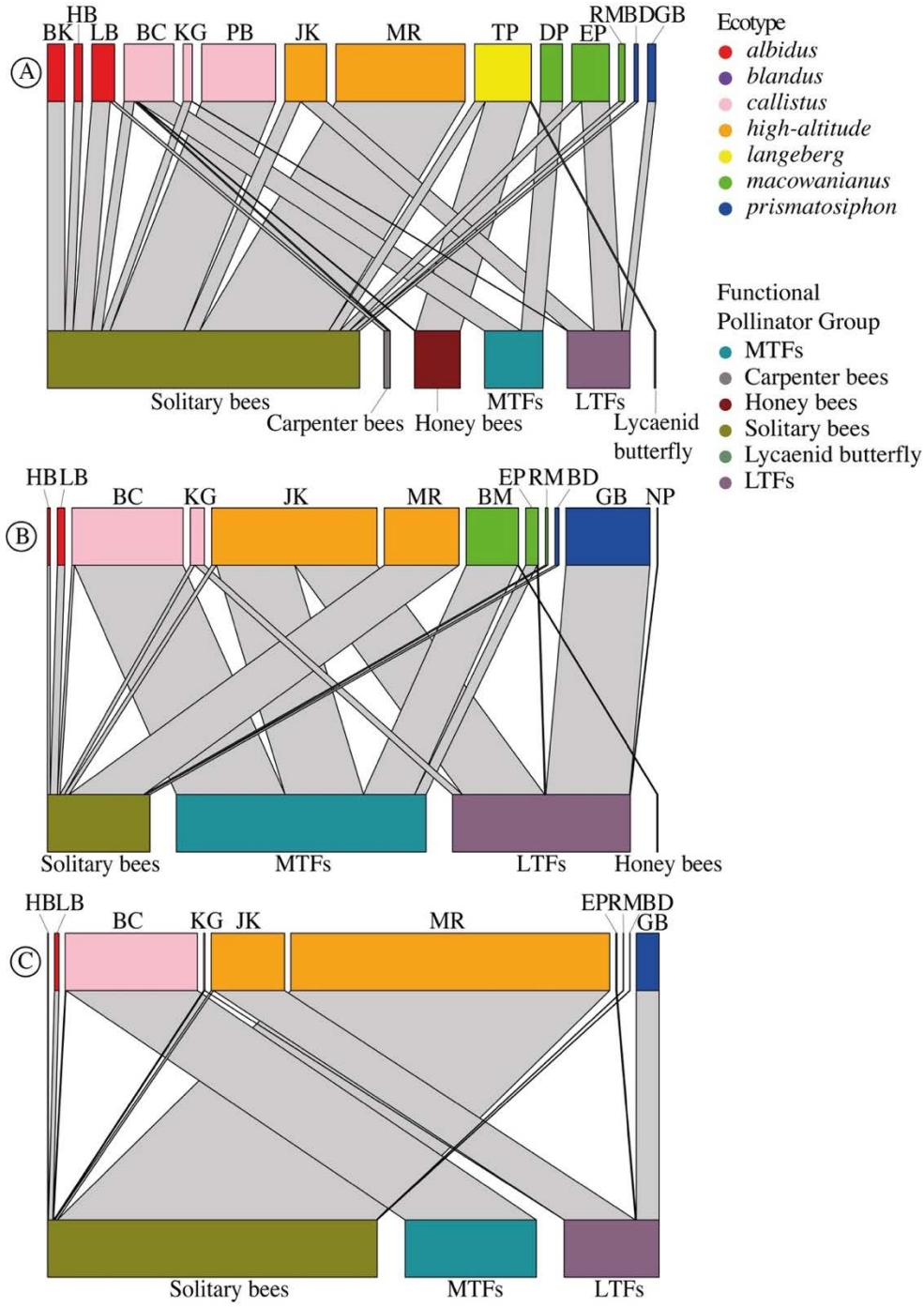

Figure 2.7. Networks of the (A) visitation rates, (B) pollen loads, and (C) pollinator importance of the functional pollinator groups: solitary bees, honeybees, carpenter bees, medium-tongued flies (MTFs), long-tongued flies (LTFs), and Lycaenid butterflies to different populations of *Gladiolus carneus* ecotypes. Abbreviations above each network refer to distinct populations of G. carneus with full site names and coordinates provided in Table S2.1.

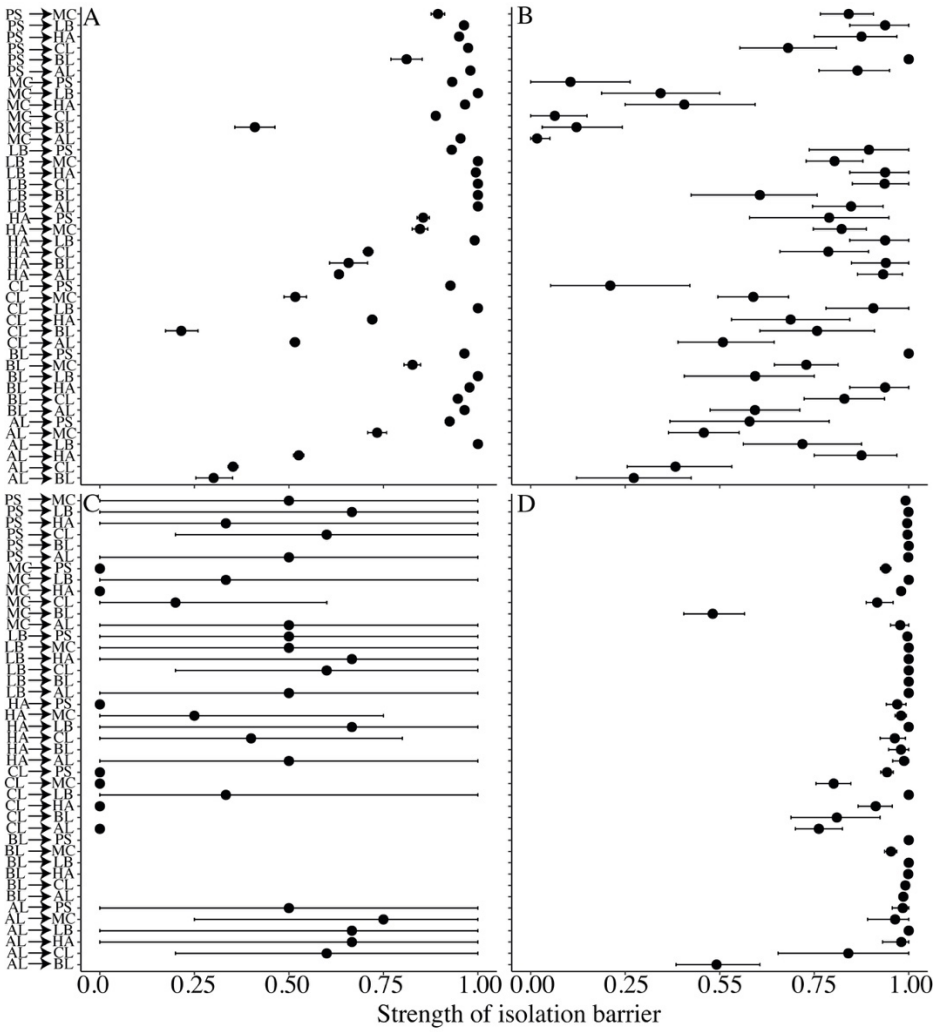

Figure 2.8. (A) Ecogeographic, (B) phenological, (C) pollinator-mediated isolation and (D) total premating isolation for all gene flow directions between the *Gladiolus carneus* ecotypes. Each figure includes all gene flow directions between ***albidus*** (AL), ***blandus*** (BL), ***callistus*** (CL), ***high-altitude*** (HA), ***langeberg*** (LB), ***macowanianus*** (MC) and ***prismatosiphon*** (PS) with arrows indicating directionality. Each point indicates the estimate of reproductive isolation with 95% confidence intervals based on 10 000 bootstrapped replicates. There are no estimates of pollinator-mediated isolation for gene flow directions including *blandus* due to a lack of pollinator data. Total premating isolation has been estimated using ecogeographic and phenological isolation for gene flow directions including *blandus*. Premating isolation has been calculated using ecogeographic, phenological and pollinator-mediated isolation for all other gene flow directions.

SUPPLEMENTARY MATERIALS

Table S2.1. Coordinates, and elevation (m) of all 29 *Gladiolus carneus* sites sampled for this manuscript. The codes for each site are used throughout the manuscript.

Ecotype	Site	Code	Latitude	Longitude	Elevation (m)	Voucher Specimen
albidus	Bainskloof A	BK	-33.641822	19.075238	337	
albidus	Bainskloof B	BL	-33.639557	19.080812	372	
albidus	Franschhoek Pass	FP	-33.921289	19.141642	510	
albidus	Helderberg	HB	-34.054097	18.874192	216	
albidus	Hermanus	HM	-34.416530	19.227500	48	
albidus	Limietberg	LB	-33.707683	19.053684	457	Khoury, K. 1 (GRA)
albidus	Stellenboschberg	SB	-33.943373	18.886395	210	
albidus	Shaw's Pass	SP	-34.305006	19.417495	339	
blandus	Kleinmond Coast	KC	-34.345452	19.008462	9	Khoury, K. 2 (GRA)
callistus	Brodie-link C	BC	-34.361673	18.865795	17	Khoury, K. 9 (GRA)
callistus	Kleinmond Golf Course	KG	-34.326530	19.030778	74	Khoury, K. 3 (GRA)
callistus	Pringle Bay C	PB	-34.343890	18.847427	19	
high-altitude	Jonkershoek	JH	-34.001640	19.012690	1235	Khoury, K. 6 (GRA)
high-altitude	Jonaskop	JK	-33.963432	19.510247	1403	Khoury, K. 5 (GRA)
high-altitude	Mont Rochelle	MR	-33.882298	19.173532	1303	Khoury, K. 7 (GRA)
langeberg	Garcia's Pass	GP	-33.957285	21.201655	749	
langeberg	Prince Alfred's Pass	PA	-33.801141	23.178886	366	
langeberg	Tradouw Pass	TP	-33.950402	20.702005	249	
macowanianus	Brodie-Link M/Betty's Bay	BM	-34.362433	18.866515	16	Khoury, K. 8 (GRA)
macowanianus	Devil's Peak	DP	-33.956420	18.425135	475	

macowanianus	Elsie's Peak	EP	-34.146345	18.430717	211	Khoury, K. 13 (GRA)
macowanianus	Franskraal/Gansbaai	FK	-34.600648	19.394002	17	Khoury, K. 10 (GRA)
macowanianus	Flower Valley Conservation	FV	-34.548015	19.472299	122	
macowanianus	Lomond Wine Farm	LW	-34.567372	19.481217	27	
macowanianus	Pringle Bay M	PM	-34.348830	18.832518	18	
macowanianus	Rhodes Memorial	RM	-33.950491	18.455636	231	Khoury, K. 14 (GRA)
prismatosiphon	Bredasdorp	BD	-34.544306	20.035664	225	Khoury, K. 15 (GRA)
prismatosiphon	Grootbos/Farm 215	GB	-34.553089	19.546951	262	Khoury, K. 11 (GRA)
prismatosiphon	Napier	NP	-34.509889	19.879167	404	Khoury, K. 12 (GRA)

Table S2.2. Sample sizes of the morphological trait measurements at each *Gladiolus carneus* study population. Ecotypes include those based on former descriptions by Delpierre and du Plessis (1974) and the two previously undescribed ecotypes of the species.

Population number	Ecotype	Site	tube length (mm)	flower gape (mm)	petal size (mm)	flower width (mm)	inflore scence height (cm)	total flowers	total leaves	leaf length (cm)	leaf width (cm)
1	*albidus*	Bainskloof A	5	5	0	5	0	5	0	0	0
2	*albidus*	Bainskloof B	7	6	0	7	0	7	0	0	0
3	*albidus*	Franschhoek pass	9	9	0	8	0	8	0	0	0
4	*albidus*	Helderberg	35	31	26	29	20	28	20	20	20
5	*albidus*	Hermanus	5	4	5	3	5	5	5	2	5
6	*albidus*	Limietberg	34	30	17	30	16	30	16	15	15
7	*albidus*	Shaw’s Pass	8	8	8	8	0	10	0	0	0
8	*albidus*	Stellenboschberg	11	8	11	11	11	11	11	9	10
9	*blandus*	Kleinmond Coast	38	37	21	38	22	31	22	22	22
10	*callistus*	Brodie-Link C	26	24	26	26	20	20	20	20	20
11	*callistus*	Kleinmond Golf Course	32	31	32	29	23	23	23	20	22
12	*callistus*	Pringle Bay C	9	10	0	10	0	10	0	0	0
13	*high-altitude*	Jonaskop	31	31	31	30	15	30	15	15	15
14	*high-altitude*	Jonkershoek	16	17	17	14	7	17	7	5	7
15	*high-altitude*	Mont Rochelle	40	35	38	29	32	40	15	15	15
16	*langeberg*	Garcias pass	16	14	0	17	0	17	0	0	0
17	*langeberg*	Tradouw pass	40	39	29	40	10	40	10	10	10
18	*macowanianus*	Betty's Bay	27	27	10	27	10	27	10	10	10
19	*macowanianus*	Brodie-Link M	15	12	15	12	10	10	10	10	9
20	*macowanianus*	Devil's Peak	28	25	25	25	20	25	20	20	19
21	*macowanianus*	Elsie’s Peak	35	34	24	33	20	30	20	20	20

22	*macowanianus*	Flower Valley Conservation Trust	26	26	26	0	0	0	0	0	0
23	*macowanianus*	Franskraal	34	30	18	31	14	30	14	8	13
24	*macowanianus*	Lomond Wine Farm	8	8	8	7	0	8	0	0	0
25	*macowanianus*	Rhodes Memorial	35	34	34	34	20	20	20	20	20
26	*prismatosiphon*	Bredasdorp	21	19	20	18	15	15	15	15	15
27	*prismatosiphon*	Grootbos	26	26	26	25	20	20	20	20	19
28	*prismatosiphon*	Napier	23	23	23	22	0	0	0	0	0
Total			**640**	**603**	**490**	**568**	**310**	**517**	**293**	**276**	**286**

Table S2.3. Sample sizes of individuals for which spectral reflectance were collected for each *Gladiolus carneus* study population and ecotype.

Site number	Ecotype	Site	Number of individuals	Year collected
1	*albidus*	Bainskloof A	5	2020
2	*albidus*	Franschhoek Pass	7	2020
3	*albidus*	Helderberg	18	2020, 2023
4	*albidus*	Hermanus	3	2023
5	*albidus*	Limietberg	14	2020
6	*albidus*	Stellenboschberg	6	2023
7	*blandus*	Kleinmond Coast	22	2020, 2023
8	*callistus*	Brodie-link C	12	2023
9	*callistus*	Kleinmond golf course	14	2023
10	*callistus*	Pringle Bay C	6	2020
11	*high-altitude*	Jonaskop	14	2022, 2023
12	*high-altitude*	Jonkershoek	10	2023
13	*high-altitude*	Mont Rochelle	8	2023
14	*langeberg*	Garcia's Pass	16	2020
15	*langeberg*	Tradouw Pass	10	2020
16	*macowanianus*	Betty's Bay	28	2020, 2023
17	*macowanianus*	Devil's Peak	11	2023
18	*macowanianus*	Elsie's Peak	19	2020, 2023
19	*macowanianus*	Franskraal/Gansbaai	16	2020
20	*macowanianus*	Pringle bay M	10	2020
21	*macowanianus*	Rhodes Memorial	12	2023
22	*prismatosiphon*	Bredasdorp	12	2023
23	*prismatosiphon*	Grootbos	12	2023
24	*prismatosiphon*	Napier	15	2022
Subtotals				
	albidus		53	
	blandus		22	
	callistus		32	
	high-altitude		32	
	langeberg		26	
	macowanianus		96	
	prismatosiphon		39	
Total			300	

Table S2.4. Bioclimatic and topography layers mined from Worldclim and the soil layers from Cramer *et al*. (2019) that were used in the abiotic niche analysis. Bioclimatic, soil, and elevational layers in bold were the uncorrelated variables used in the niche modelling and differentiation analysis.

Layer category	Abiotic layers	Description	Unit
Bioclimatic	Bio1	Annual Mean Temperature	°C
	Bio2	Mean Diurnal Range (Mean of monthly (max temp - min temp))	°C
	Bio3	**Isothermality (BIO2/BIO7) (×100)**	%
	Bio4	Temperature Seasonality (standard deviation ×100)	-
	Bio5	Max Temperature of Warmest Month	°C
	Bio6	Min Temperature of Coldest Month	°C
	Bio7	**Temperature Annual Range (BIO5-BIO6)**	°C
	Bio8	Mean Temperature of Wettest Quarter	°C
	Bio9	Mean Temperature of Driest Quarter	°C
	Bio10	Mean Temperature of Warmest Quarter	°C
	Bio11	Mean Temperature of Coldest Quarter	°C
	Bio12	**Annual Precipitation**	mm
	Bio13	Precipitation of Wettest Month	mm
	Bio14	Precipitation of Driest Month	mm
	Bio15	**Precipitation Seasonality (Coefficient of Variation)**	-
	Bio16	Precipitation of Wettest Quarter	mm
	Bio17	Precipitation of Driest Quarter	mm
	Bio18	Precipitation of Warmest Quarter	mm
	Bio19	Precipitation of Coldest Quarter	mm
Soil	pH	pH	-
	EC	**electrical conductivity**	mS/m
	total C	total Carbon	%, w/w
	total N	**total Nitrogen**	%, w/w
	extractable P	**extractable Phosphorus**	mg/kg
	extractable K	extractable Potassium	$cmol^{+}kg^{-1}$
	extractable NA	**extractable Sodium**	$cmol^{+}kg^{-1}$
Topography		**Elevation**	meters above sea level

Table S2.5. Mean and sample size of visitation rates and pollen loads for each functional pollinator collected across populations and ecotypes of *Gladiolus carneus.*

Ecotype	Site	Site Code	Functional pollinator	Visitation rate (visits.flower^{-1}.hour^{-1})				Pollen loads	Pollinators caught
				Mean	Sample size	Obs flowers	Obs time (hours)	Mean	Total
albidus	Bainskloof A	BK	Solitary bees	0.133	1	5	3.00	-	-
albidus	Helderberg	HB	Solitary bees	0.065	2	51	4.98	38	2
albidus	Limietberg	LB	Carpenter bees	0.035	1	52	1.10	-	-
albidus	Limietberg	LB	Solitary bees	0.142	3	190	10.45	104	4
callistus	Brodie-Link C	BC	Carpenter bees	0.014	1	66	3.27	-	-
callistus	Brodie-Link C	BC	Honey bees	0.009	1	66	3.27	-	-
callistus	Brodie-Link C	BC	MTFs	0.283	1	66	3.27	1549	5
callistus	Brodie-Link C	BC	Solitary bees	0.079	1	66	3.27	36	4
callistus	Kleinmond Golf Course	KG	LTFs	0.006	1	42	4.32	139	1
callistus	Kleinmond Golf Course	KG	Solitary bees	0.065	2	50	7.97	62	5
callistus	Pringle Bay	PB	Solitary bees	0.571	1	14	1.00	-	-
high-altitude	Jonaskop	JK	LTFs	0.202	1	23	3.23	1175	8
high-altitude	Jonaskop	JK	MTFs	-	-	-	-	1117	1
high-altitude	Jonaskop	JK	Solitary bees	0.121	1	23	3.23	68	2
high-altitude	Mont Rochelle	MR	Solitary bees	1.000	1	7	1.00	1065	1
langeberg	Tradouw Pass	TP	Honey bees	0.344	1	30	3.00	-	-
langeberg	Tradouw Pass	TP	Lycaenid butterfly	0.011	1	30	3.00	-	-
langeberg	Tradouw Pass	TP	Solitary bees	0.084	2	46	5.00	-	-
macowanianus	Brodie-Link M	BM	Honey bees	-	-	-	-	14	1
macowanianus	Brodie-Link M	BM	MTFs	-	-	-	-	731	7

macowanianus	Devils Peak	DP	MTFs	0.170	3	45	7.72	-	-
macowanianus	Elsies Peak	EP	LTFs	0.214	1	7	2.00	16	1
macowanianus	Elsies Peak	EP	MTFs	-	-	-	-	162	1
macowanianus	Elsies Peak	EP	Solitary bees	0.074	1	21	3.22	-	-
macowanianus	Rhodes Memorial	RM	Solitary bees	0.049	2	32	8.28	35	2
prismatosiphon	Bredasdorp	BD	Solitary bees	0.031	1	156	3.08	54	2
prismatosiphon	Grootbos	GB	LTFs	0.063	2	23	7.20	1197	2
prismatosiphon	Napier	NP	LTFs	-	-	-	-	10	1
Total						**729**	**69.40**		

Table S2.6. Generalised linear model outputs testing for differences between the *Gladiolus carneus* ecotypes' morphological traits. The models included two explanatory variables: ecotype and site nested within ecotypes.

	ecotype			ecotype:site		
Traits	χ^2	***df***	***P***	χ^2	***df***	***P***
tube length	749.82	6	**< 0.0001**	855.67	21	**< 0.0001**
flower gape	409.09	6	**< 0.0001**	161.64	21	**< 0.0001**
petal size	118.15	6	**< 0.0001**	345.85	21	**< 0.0001**
inflorescence height	44.11	6	**< 0.0001**	125.25	12	**< 0.0001**
leaf length	164.9	6	**< 0.0001**	222.57	12	**< 0.0001**
leaf width	359.23	6	**< 0.0001**	294.14	12	**< 0.0001**

Table S2.7. Pairwise comparisons between the morphological traits of *Gladiolus carneus* ecotypes. Significant differences between pairs of ecotypes are highlighted in bold.

Comparisons	Tube length	Flower gape	Petal size	Inflorescence height	Length longest leaf	Width of longest leaf
albidus - blandus	**< 0.0001**	**< 0.0001**	1.000	1.000	1.000	0.8449
albidus - callistus	**0.0384**	1.000	1.000	**0.0004**	**0.0003**	**< 0.0001**
albidus – high-altitude	1.000	1.000	1.000	**0.0059**	**< 0.0001**	**< 0.0001**
albidus - langeberg	**< 0.0001**	**< 0.0001**	0.2624	**0.0025**	**0.0010**	**0.0001**
albidus - macowanianus	0.3563	**< 0.0001**	**< 0.0001**	0.0773	1.000	**< 0.0001**
albidus - prismatosiphon	**< 0.0001**	**0.0002**	**< 0.0001**	0.0873	**0.0003**	**0.0032**
blandus - callistus	**< 0.0001**	**< 0.0001**	1.000	**0.0208**	**< 0.0001**	**< 0.0001**
blandus – high-altitude	**< 0.0001**	**< 0.0001**	1.000	0.1091	**< 0.0001**	**< 0.0001**
blandus - langeberg	**< 0.0001**	0.248	1.000	**0.0056**	**0.0032**	**< 0.0001**
blandus - macowanianus	**< 0.0001**	**< 0.0001**	0.4701	1.000	1.000	**< 0.0001**
blandus - prismatosiphon	**< 0.0001**	**< 0.0001**	**0.0003**	0.6848	**< 0.0001**	**< 0.0001**
callistus - high-altitude	**0.0165**	1.000	1.000	1.000	**0.0063**	**0.0002**
callistus - langeberg	**< 0.0001**	**< 0.0001**	**0.0168**	**< 0.0001**	**< 0.0001**	1.000
callistus - macowanianus	1.000	**< 0.0001**	**< 0.0001**	0.5866	**< 0.0001**	0.0774
callistus - prismatosiphon	0.0664	**0.0009**	**< 0.0001**	1.000	1.000	**< 0.0001**
high-altitude - langeberg	**< 0.0001**	**< 0.0001**	0.3949	**< 0.0001**	**< 0.0001**	**0.0002**
high-altitude - macowanianus	0.1434	**< 0.0001**	**< 0.0001**	1.000	**< 0.0001**	0.418
high-altitude - prismatosiphon	**< 0.0001**	**< 0.0001**	**< 0.0001**	1.000	0.0828	**< 0.0001**
langeberg - macowanianus	**< 0.0001**	**0.0055**	1.000	**< 0.0001**	**< 0.0001**	**0.0319**
langeberg - prismatosiphon	**< 0.0001**	**< 0.0001**	**0.009**	**< 0.0001**	**< 0.0001**	0.1527
macowanianus - prismatosiphon	**< 0.0001**	0.108	**0.0127**	1.000	**< 0.0001**	**< 0.0001**

Table S2.8. Pairwise comparisons between ecotypes of *Gladiolus carneus* plotted in bee and fly colour vision models. Significant differences are highlighted in bold.

	Bee colour vision model					Fly colour vision model				
Comparison	**Tepal**	**Median tepal centre**	**Median tepal guide**	**Lateral tepal centre**	**Lateral tepal guide**	**Tepal**	**Median tepal centre**	**Median tepal guide**	**Lateral tepal centre**	**Lateral tepal guide**
albidus – blandus	**< 0.001**	**< 0.001**	-	**< 0.001**	-	**< 0.001**	**< 0.001**	-	**< 0.001**	-
albidus – callistus	**< 0.001**	-	-	-	-	**< 0.001**	-	-	-	-
albidus – high-altitude	**< 0.001**	**< 0.001**	-	**< 0.001**	-	**< 0.001**	**< 0.001**	-	**< 0.001**	-
albidus - langeberg	**< 0.001**	**< 0.001**	-	**< 0.001**	-	**< 0.001**	**< 0.001**	-	**< 0.001**	-
albidus - macowanianus	**< 0.001**	**< 0.001**	-	**< 0.001**	-	**< 0.001**	**< 0.001**	-	**< 0.001**	-
albidus - prismatosiphon	**< 0.001**	**< 0.001**	-	**< 0.001**	-	**< 0.001**	**< 0.001**	-	**< 0.001**	-
blandus – callistus	**< 0.001**	-	-	-	-	**< 0.001**	-	-	-	-
blandus – high-altitude	**< 0.001**	**0.010**	1.000	**< 0.001**	**0.029**	**< 0.001**	**0.004**	1.000	**< 0.001**	0.052
blandus - langeberg	**< 0.001**	**< 0.001**	0.059	1.000	1.000	**< 0.001**	**< 0.001**	**0.023**	**0.035**	1.000
blandus - macowanianus	**< 0.001**	**< 0.001**	1.000	0.785	0.332	**0.024**	**< 0.001**	1.000	0.695	1.000
blandus - prismatosiphon	0.930	**< 0.001**	0.006	**< 0.001**	1.000	0.793	**< 0.001**	**0.032**	**< 0.001**	1.000
callistus – high-altitude	1.000	-	-	-	-	1.000	-	-	-	-
callistus - langeberg	**< 0.001**	-	-	-	-	**< 0.001**	-	-	-	-
callistus - macowanianus	**< 0.001**	-	-	-	-	**< 0.001**	-	-	-	-
callistus - prismatosiphon	**< 0.001**	-	-	-	-	**< 0.001**	-	-	-	-
high-altitude - langeberg	**< 0.001**	**< 0.001**	0.028	**< 0.001**	**< 0.001**	**< 0.001**	**< 0.001**	**0.03**	**< 0.001**	**< 0.001**
high-altitude - macowanianus	**< 0.001**	0.251	0.872	**< 0.001**	**0.002**	**< 0.001**	0.058	1.000	**< 0.001**	**0.001**
high-altitude - prismatosiphon	**< 0.001**	**< 0.001**	**< 0.001**	**< 0.001**	**< 0.001**	**< 0.001**	**< 0.001**	**0.002**	**< 0.001**	**< 0.001**
langeberg - macowanianus	**< 0.001**	**< 0.001**	**< 0.001**	0.051	1.000	**< 0.001**	**< 0.001**	**< 0.001**	**0.002**	1.000

langeberg - prismatosiphon	**< 0.001**	**< 0.001**	1.000	0.002	1.000	**< 0.001**	**< 0.001**	0.235	**< 0.001**	1.000
macowanianus - prismatosiphon	**0.002**	**< 0.001**	**< 0.001**	**< 0.001**	0.627	**0.018**	**< 0.001**	**< 0.001**	**< 0.001**	1.000

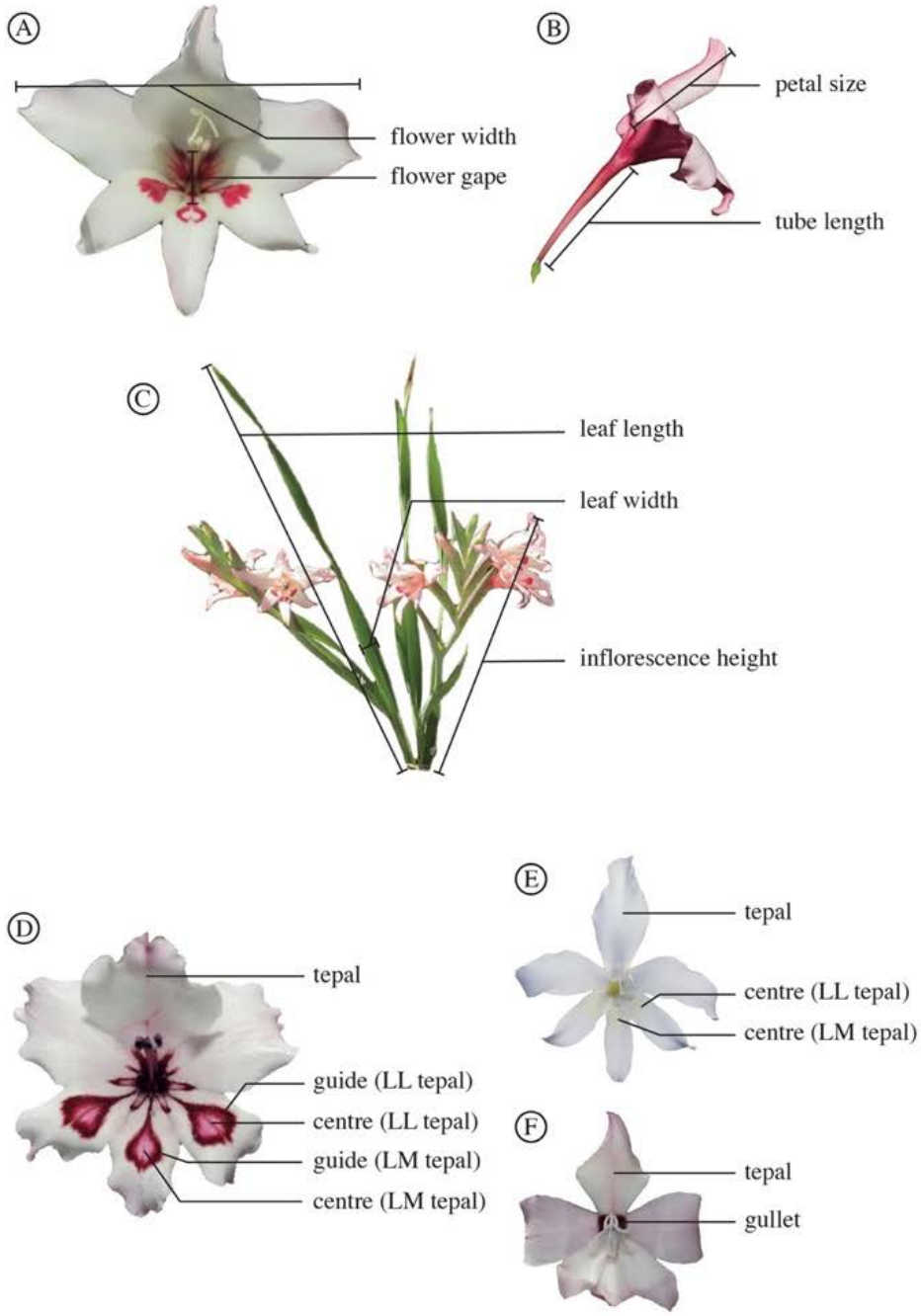

Figure S2.1. Morphological measurements of *Gladiolus carneus* ecotypes. The (A) front view of a *G. carneus* flower showing flower width and flower gape, (B) the side view showing petal size and tube length, (C) whole plant showing measurements of the leaf length, leaf width, and inflorescence height. Additionally, spectral measurements were taken for all ecotypes from the dorsal tepals, lower median tepal (LM tepal) and lower lateral tepal (LL tepal). Spectral measurements taken for (D) *blandus*, *high-altitude*, *langeberg*, *macowanianus*, *prismatosiphon*, (E) *albidus* and (F) *callistus*.

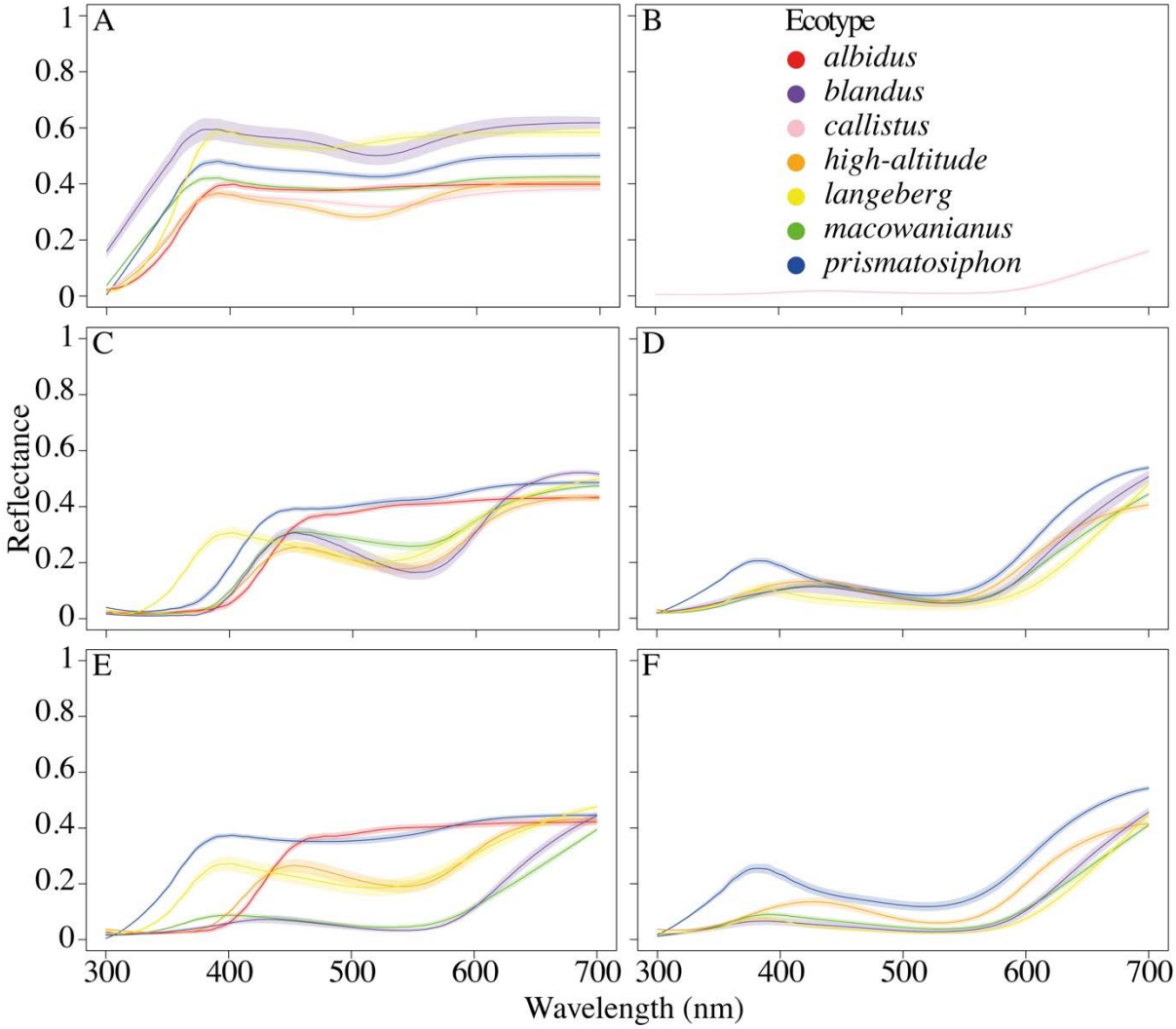

Figure S2.2. Spectral reflectance curves for the (A) tepal, (B) gullet, (C) centre of the median tepal, (D) guide of median tepal, (E) centre of lateral tepal, and (F) guide of lateral tepal for each of the *Gladiolus carneus* ecotypes. Mean spectral reflectance curve is depicted by the dark line in the centre with lighter shading representing the standard error.

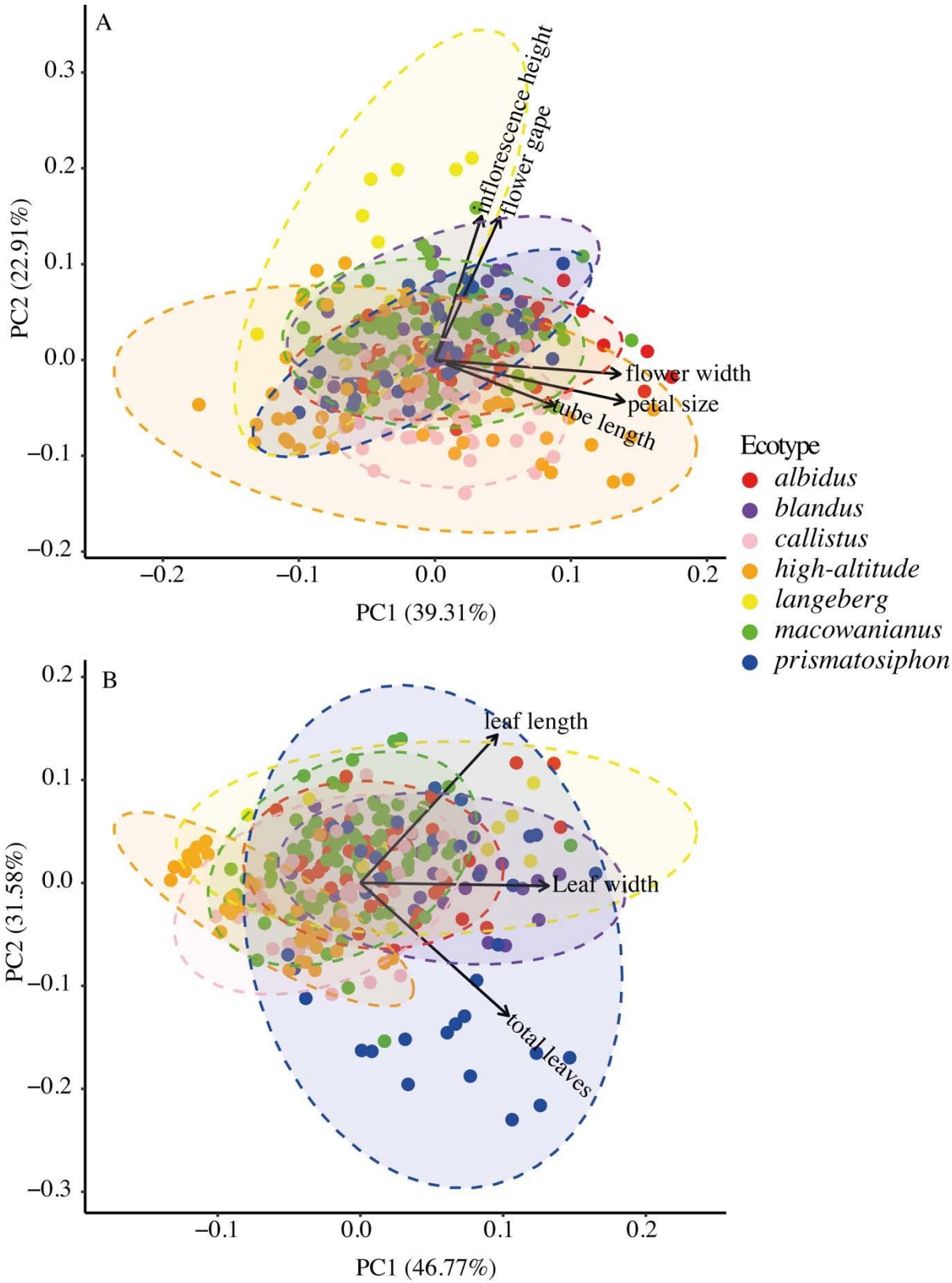

Figure S2.3. PCAs of (A) floral and (B) vegetative traits of the *Gladiolus carneus* ecotypes.

The PCA includes ellipses showing 95% confidence intervals and a biplot of trait loadings.

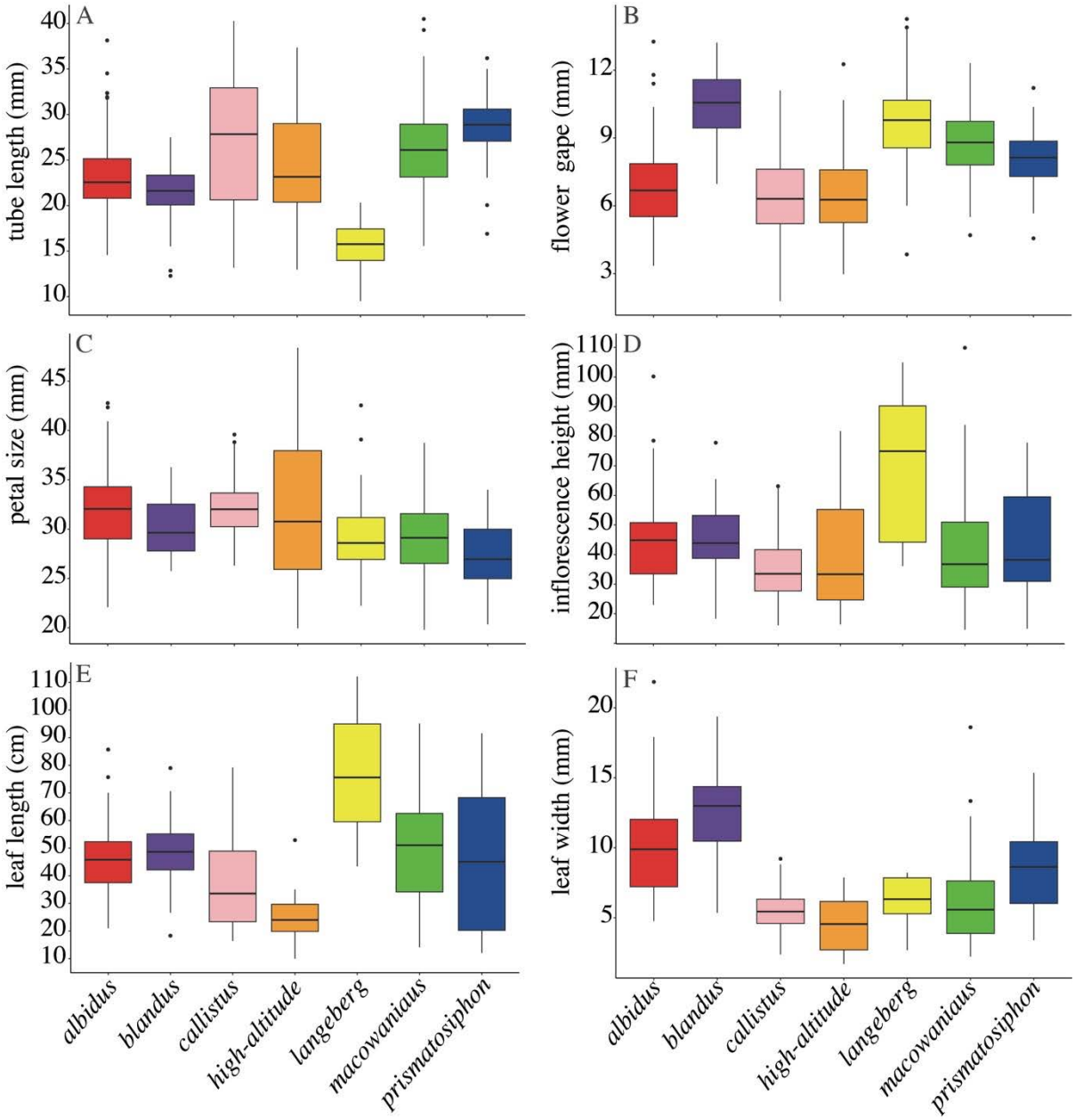

Figure S2.4. Comparisons of the functional traits (A) tube length, (B) flower gape, (C) petal size, (D) inflorescence height, (E) leaf length and (F) leaf width between *Gladiolus carneus* ecotypes.

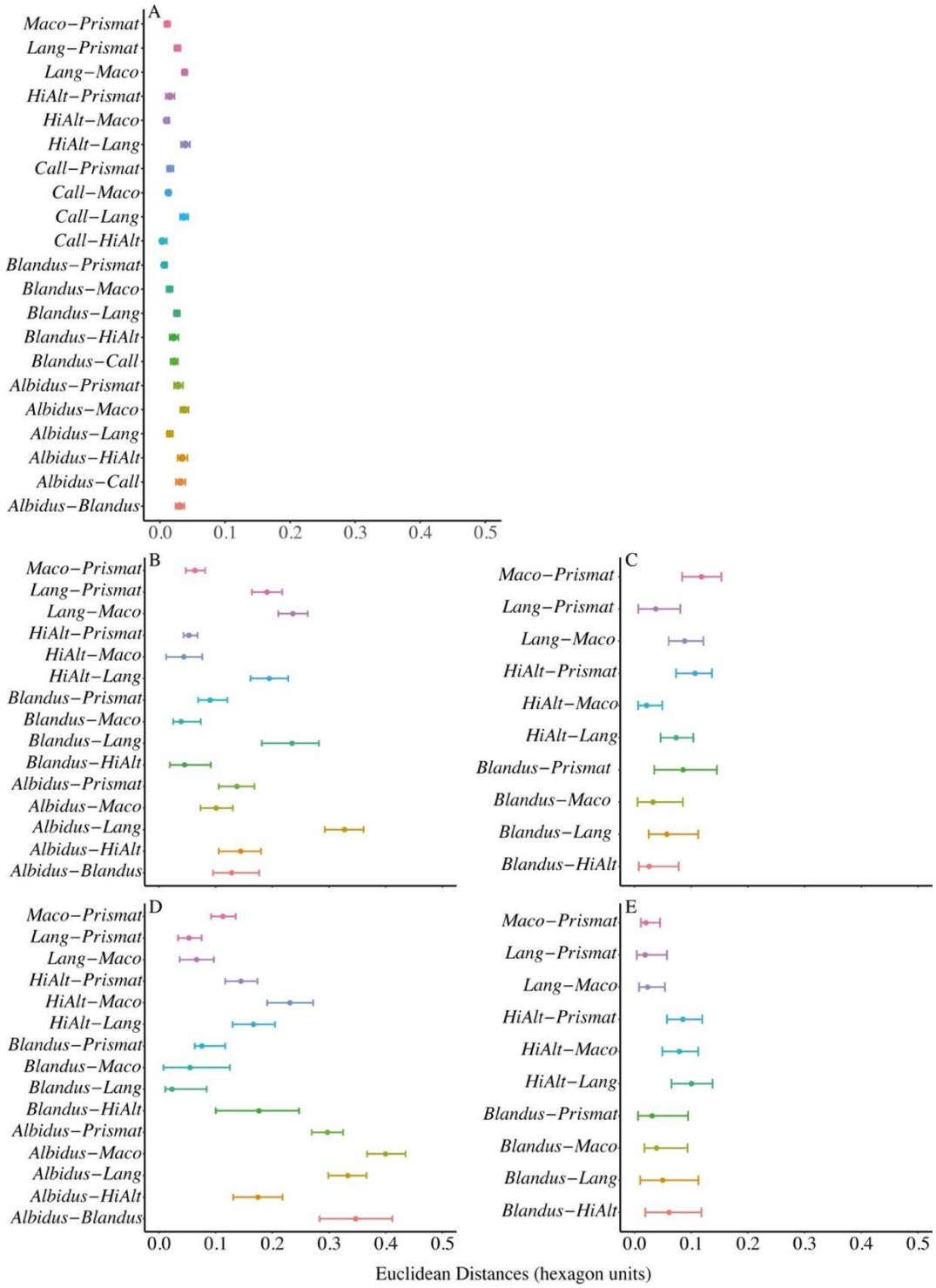

Figure S2.5. The Euclidean distances between each *Gladiolus carneus* ecotype for the (A) tepal, (B) centre of the median tepal, (C) guide of median tepal, (D) centre of lateral tepal, and (E) guide of lateral tepal modelled in bee colour vision with *Apis mellifera* spectral sensitivities. Euclidean distances have been used as a proxy for chromatic contrasts. Central point represents the mean with tails representing upper and lower bootstrapped confidence limits.

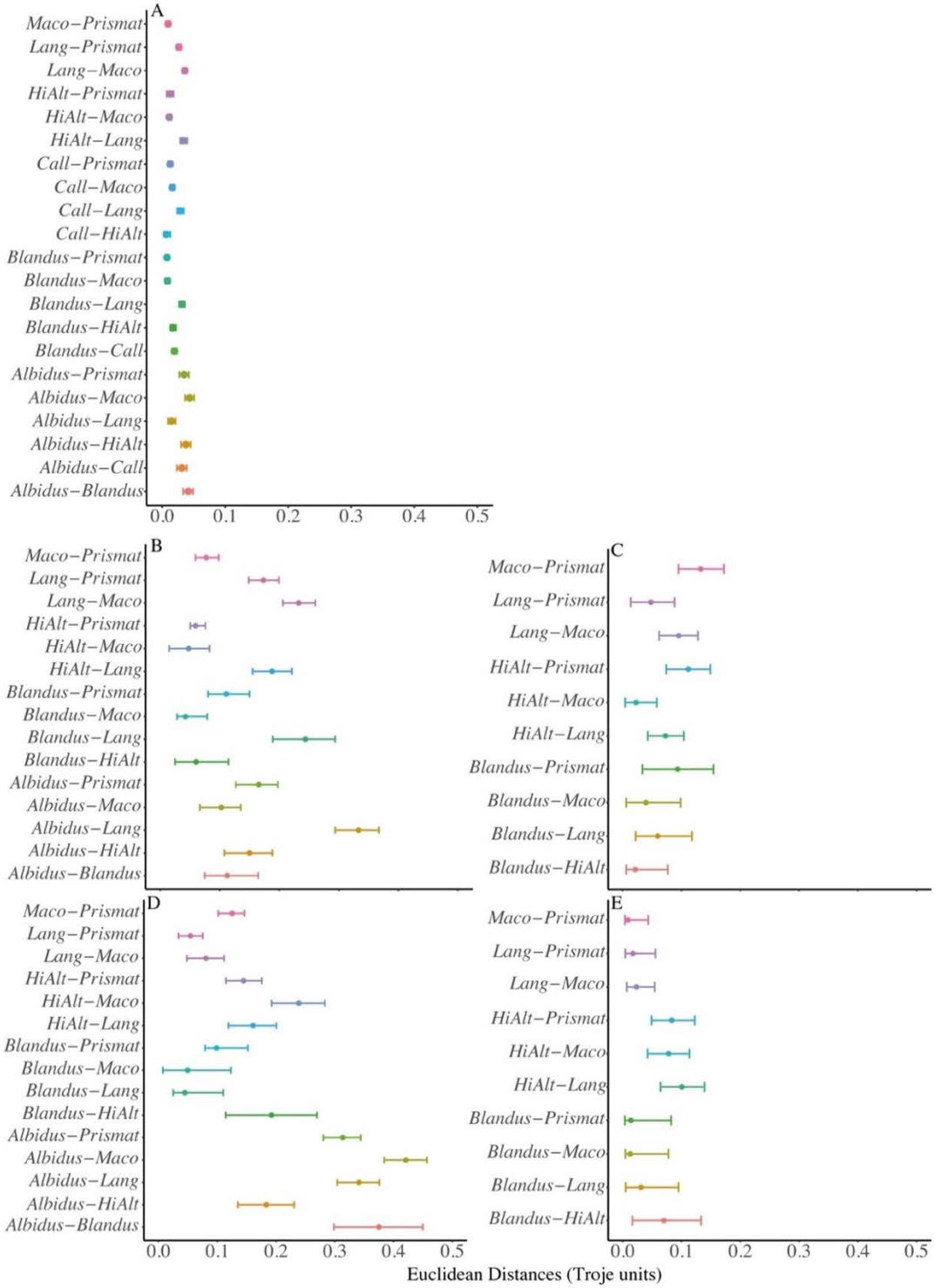

Figure S2.6. Euclidean distances between each *Gladiolus carneus* ecotype for (A) tepal, (B) centre of the median tepal, (C) guide of median tepal, (D) centre of lateral tepal, and (E) guide of lateral tepal modelled in fly colour vision with *Eristalis tenax* spectral sensitivities. Euclidean distances have been used as a proxy for chromatic contrasts. Central point represents the mean with tails representing upper and lower bootstrapped confidence limits.

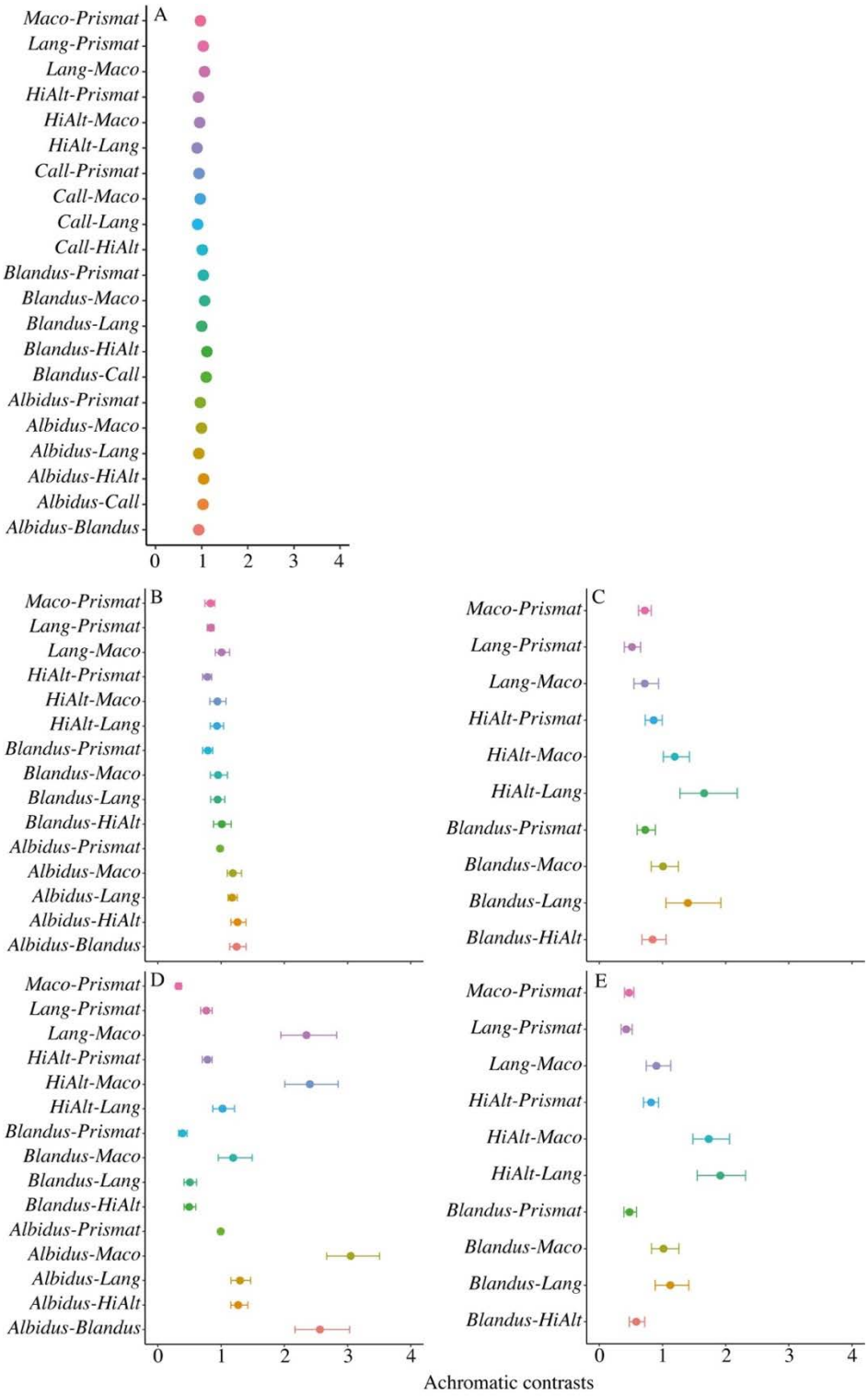

Figure S2.7: Achromatic contrasts between each *Gladiolus carneus* ecotype for the (A) tepal, (B) centre of the median tepal, (C) guide of median tepal, (D) centre of lateral tepal, and (E) guide of lateral tepal modelled in bee colour vision with *Apis mellifera* spectral sensitivities. Central point represents the mean with tails representing upper and lower bootstrapped confidence limits.

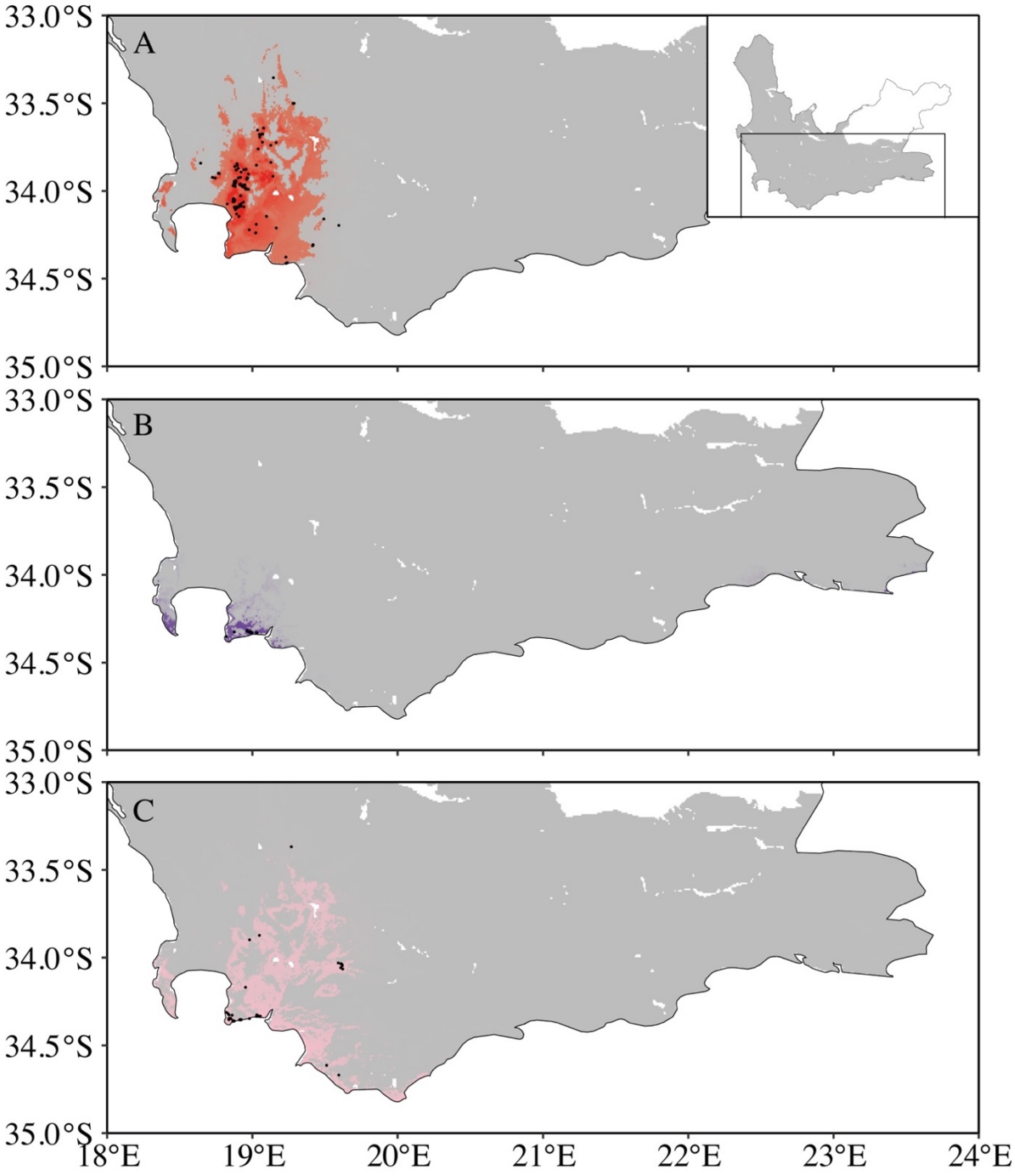

Figure S2.8. Niche model outputs for (A) *albidus*, (B) *blandus*, (C) *callistus*, (D) *high-altitude*, (E) *langeberg*, (F) *macowanianus*, and (G) *prismatosiphon* based on uncorrelated bioclimatic, elevation and soil layers. Top right shows the Western Cape of South Africa, with the black outline indicating the area displayed in all subsequent maps. The grey area is the extent of the modelled area, coloured areas show the model predictions, and black points show localities.

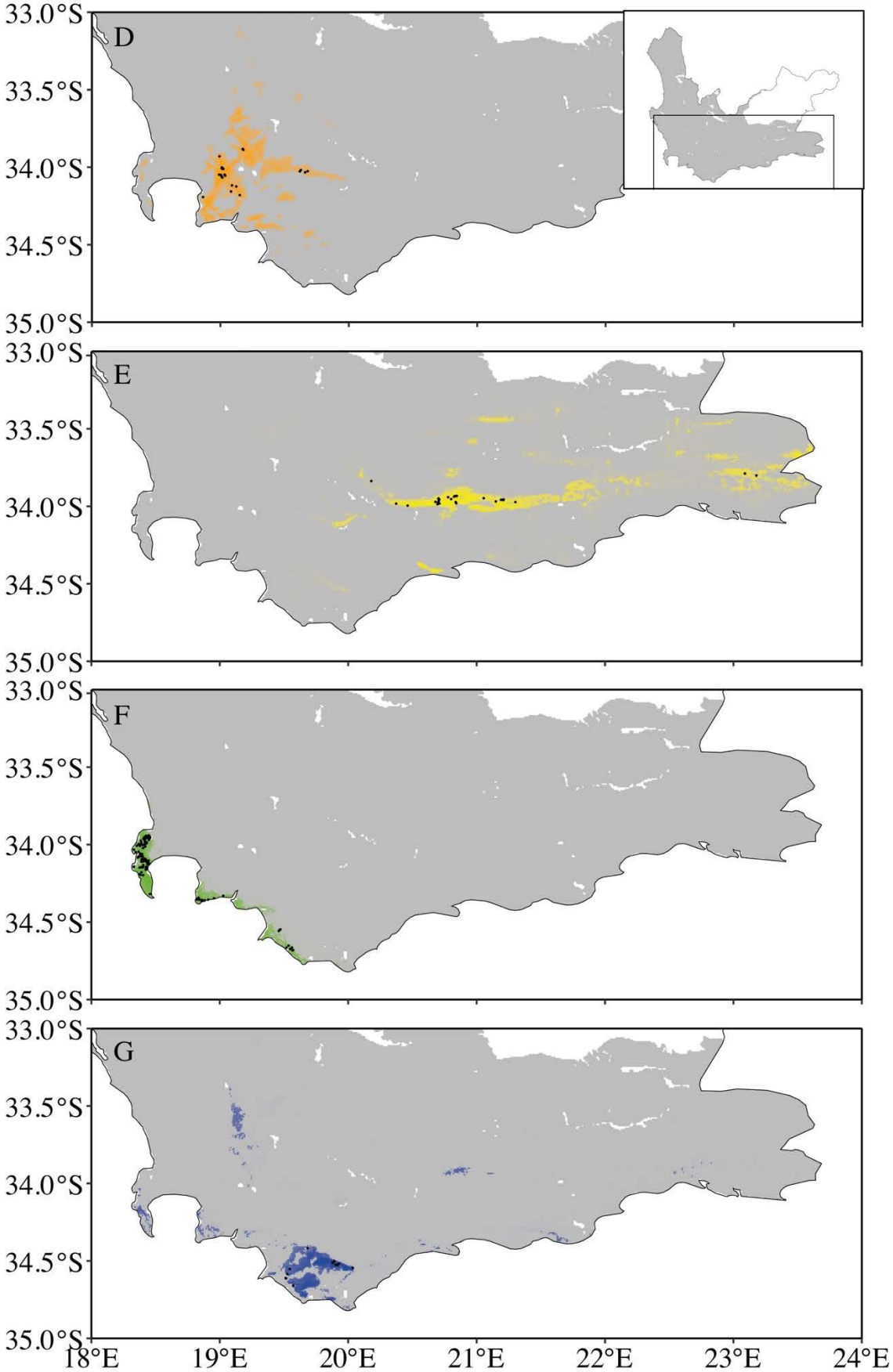

Figure S2.8. Continued

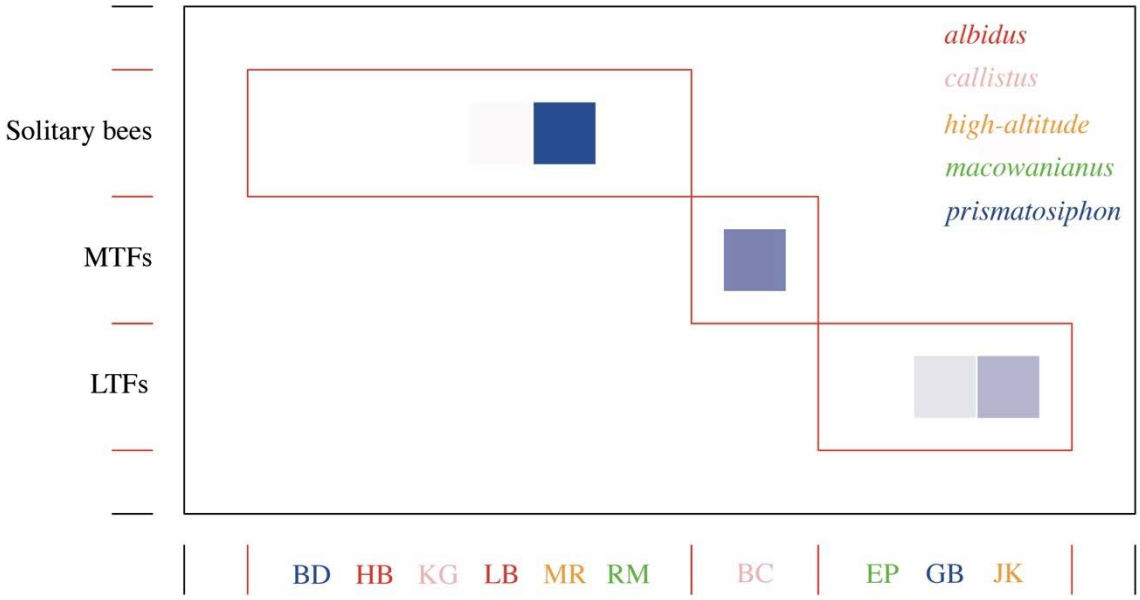

Figure S2.9. Modularity analysis of pollinator importance showing *Gladiolus carneus* sites associated with each functional pollinator group.

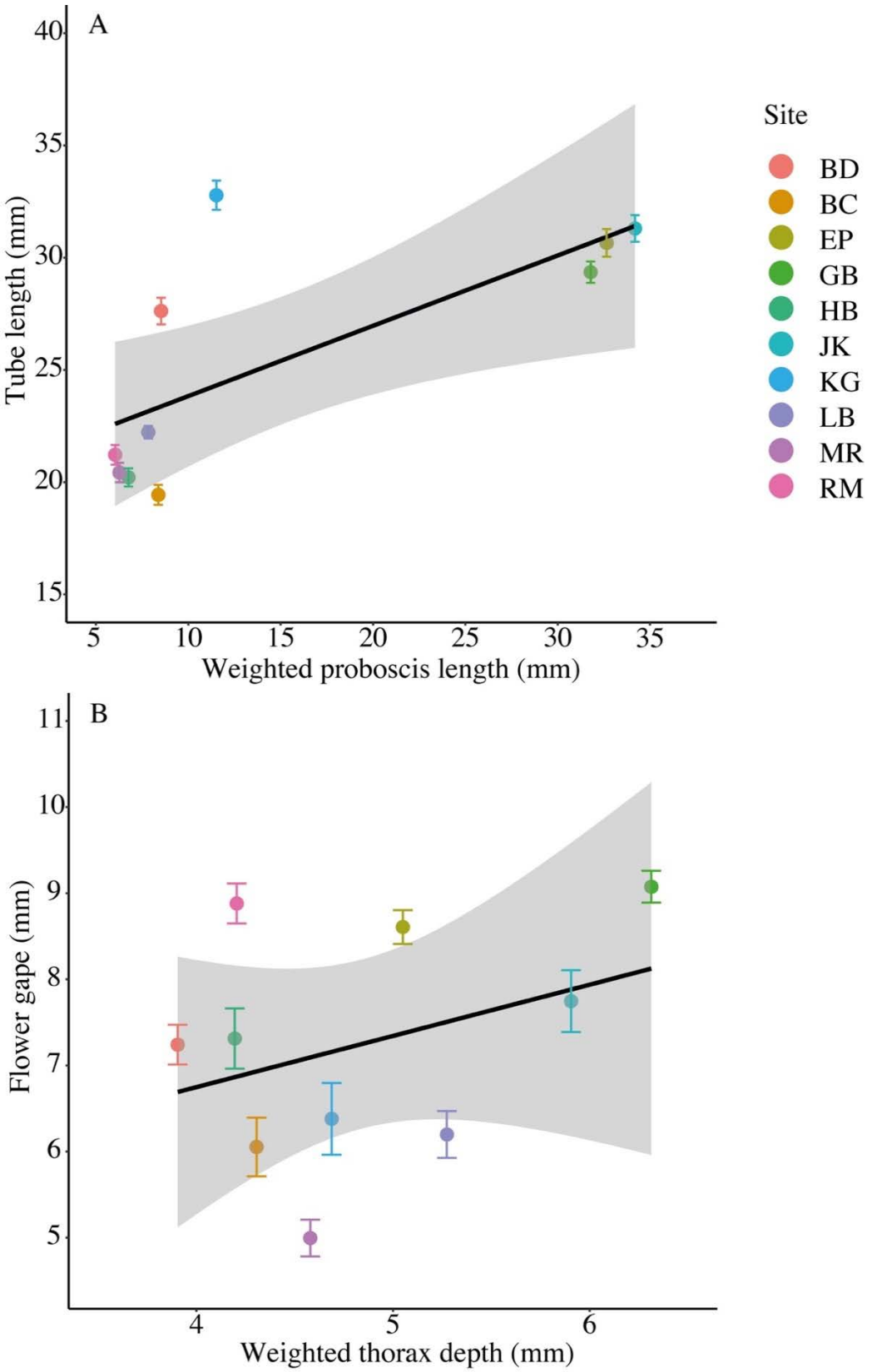

Figure S2.10. Correlations between the (A) weighted proboscis length (mm) of pollinators and *Gladiolus carneus* tube length (mean ± SE mm), and (B) weighted thorax depth (mm) of pollinators and *G. carneus* flower gape (mean ± SE mm) across populations of *G. carneus.*

CHAPTER 3:

Local adaptation of *Gladiolus carneus* to soil nutrient extremes in the Cape Floristic Region

Katharine L. Khoury* and Ethan Newman

Department of Botany, Rhodes University, Makhanda, South Africa

*For correspondence: E-mail katharinekhoury@gmail.com

ABSTRACT

Within the hyper-diverse Cape Floristic Region (CFR), divergent edaphic niches are hypothesised as an important driver of lineage diversification. However, the evidence for local adaptation on contrasting soils in this region remains limited. Using a reciprocal translocation and common garden approach, we use the polymorphic geophyte *Gladiolus carneus* to test for local adaptation to soil properties along an elevational gradient. We first quantified the edaphic niche of all ecotypes of *G. carneus* across its entire range and for three experimental populations used for reciprocal translocations. Next, under common garden conditions, we tested whether the three focal populations had a fitness advantage on their native soils relative to other populations. We then assessed whether those same populations showed evidence of and local adaptation. We found that *G. carneus* ecotypes occupied distinct edaphic niches and that our three experimental populations occurred in nutrient-poor, intermediate-nutrient and nutrient-rich soil conditions. The common garden showed that seedlings native to the nutrient-rich and nutrient-poor sites, experienced a fitness advantage over non-native seedlings. Additionally, we found evidence of local adaptation at all translocation sites. Together, the common garden and reciprocal translocation suggests that edaphic conditions are contributing to local adaptation at the nutrient-rich and nutrient-poor sites. We provide the first evidence of local adaptation to edaphic niches in the hyper-diverse Cape Floristic Region. These results suggest that edaphic conditions, along with other abiotic factors, may be important in driving incipient speciation in the CFR.

Keywords: aster models, Cape Floristic Region, edaphic niche, *Gladiolus carneus,* common garden, local adaptation, reciprocal translocation, soil nutrient extremes

INTRODUCTION

Local adaptation is commonly found in plants (Hereford, 2009), and is thought to play a key role mediating incipient speciation and lineage formation (Nosil *et al.*, 2005, Butlin and Faria, 2024). Local adaptation evolves when heterogenous environments cause divergent selection on functional traits, giving a population a fitness advantage in their local habitat relative to foreign populations [i.e., Kawecki and Ebert's (2004) "local versus foreign" criterion for local adaptation]. Some of the earliest studies documenting local adaptation used common garden experiments to showcase genetically based morphological differences, from different populations of the same species (*see* Turesson, 1922). Since then, local adaptation has been documented extensively between taxa occupying distinct climatic (Macel *et al.*, 2007, Ellis and Ågren, 2024), pollinator (Newman *et al.*, 2015, Gross *et al.*, 2023, Johnson, 2025), coastal (Lowry *et al.*, 2008, Popovic and Lowry, 2020), and edaphic niches (Ellis and Weis, 2006, Macel *et al.*, 2007, Thiergart *et al.*, 2020, Dittmar and Schemske, 2023).

As the edaphic environment can influence a plants' access to nutrients, microbiota, and water, local adaptation to contrasting edaphic conditions has been tested extensively (*see* Rajakaruna, 2017). In particular, local adaptation to extreme edaphic conditions have received much attention, and has been tested in geothermal soils (Lekberg *et al.*, 2012), serpentine soils (Sambatti and Rice, 2006, Yost *et al.*, 2012, Dittmar and Schemske, 2023), and soils containing heavy metals (Jimenez-Ambriz *et al.*, 2007). Reciprocal translocations between populations characterized by extreme and non-extreme soils, often show that both native and introduced genotypes have a higher fitness on the non-extreme, often resource-rich soils in comparison to the extreme soils (Dittmar and Schemske, 2023). Nevertheless, the increased fitness of both the native and introduced genotypes on the non-extreme soils may still fulfil the 'local vs foreign' criterion for local adaptation (Kawecki and Ebert, 2004), when the fitness of the native

individuals are higher, than those which are introduced. This is the pattern we would expect when comparing genotypes that are suspected to be adapted to nutrient-poor and nutrient-rich soils. For example, Dittmar and Schemske (2023) found that *Leptosiphon parviflorus* on sandstone soils exhibited a home-site advantage in two of the four years tested, whereas nutrient-extreme serpentine genotypes showed a home-site advantage in all four years, albeit with lower overall fitness. Although there is good evidence for local adaptation between extreme edaphic environments (Sambatti and Rice, 2006, Jimenez-Ambriz *et al.*, 2007, Dittmar and Schemske, 2023), the evidence on more moderate edaphic gradients is mixed (Yost *et al.*, 2012, Jimenez-Ramirez *et al.*, 2023, Ellis and Ågren, 2024). Neither Jimenez-Ramirez *et al.* (2023) or Ellis and Ågren (2024), who both tested for local adaptation between moderate edaphic environments, found any evidence of local adaptation to soil types. However, Yost *et al.* (2012), found local adaptation between cryptic *Lasthenia* species on a gradient of serpentine soils. These studies demonstrate heterogenous edaphic conditions do not always result in local adaptation, and a combination of multi-year reciprocal translocations and common garden experiments are needed to comprehensively test for local adaptation to soil types (Kawecki and Ebert, 2004).

Edaphic factors are hypothesised to be a major driver of diversification in the Cape Floristic Region (CFR), however the extent of its contribution has long been questioned (Linder, 2003, Ellis *et al.*, 2014). This is mainly due to the dearth of experimental evidence for divergent soil types driving diversification in the CFR (but see Verboom *et al.*, 2004, Verboom *et al.*, 2012), at least in comparison to phylogenetic evidence, of which the evidence is conflicting in its support (see van der Niet and Johnson, 2009, Schnitzler *et al.*, 2011, Forest *et al.*, 2014, Verboom *et al.*, 2017). To our knowledge, no study exists that isolates local adaptation to soil conditions in the CFR. Although most soils in the CFR are highly leached

and infertile, complex geological and geomorphic processes have created heterogenous soils ranging from young, relatively fertile soils, to old, extremely nutrient-poor soils (Cramer *et al.*, 2014). Specifically, the erosion-resistant sandstone of the Cape Fold Mountains has the most nutrient-poor soils recorded on earth (Cramer *et al.*, 2014), with particularly low phosphorus concentrations (Linder, 2003, Cramer *et al.*, 2014). However, the soils in the coastal planes and intermontane valleys are generally derived from shale and are moderately fertile (Cramer *et al.*, 2014). This has resulted in a diverse array of soil niches and selective regimes that may drive divergence between closely related taxa in the CFR.

Gladiolus carneus (Iridaceae) is a polymorphic geophyte endemic to the CFR (Goldblatt and Manning, 2020), consisting of seven morphologically distinct ecotypes (Khoury *et al.*, in press). These ecotypes occur along an elevational gradient and likely occupy distinct soil niches, allowing for comprehensive tests of local adaptation to divergent soil properties. Due to the heterogeneity of soil types in the CFR, and the wide geographic range of the species, we would expect *G. carneus* ecotypes to occupy a range of nutrient-rich to nutrient-poor edaphic niches. We further predict all tested ecotypes will experience increased fitness on nutrient-rich soils, and that ecotypes occupying any extreme edaphic environments (both nutrient-rich and nutrient-poor) will be locally adapted. However, ecotypes occupying less extreme edaphic niches are not expected to be locally adapted to soil type exclusively. Overall, we use environmental sampling, a single-year common garden and a multi-year reciprocal translocation between the *G. carneus* ecotypes, to test:

(1) Are there differences in the soil niche between the seven *Gladiolus carneus* ecotypes? and do three focal populations of *G. carneus* occupy distinct soil niches?

(2) Do *Gladiolus carneus* ecotypes have a fitness advantage on their native soil relative to other ecotypes within a common garden?

(3) Do *Gladiolus carneus* ecotypes show evidence of local adaptation in a reciprocal translocation across an elevational gradient?

MATERIALS AND METHODS

Study Species

Gladiolus carneus (Iridaceae) is a cormous geophyte native to the CFR (Figure 3.1A-C). The species can be divided into seven morphologically distinct ecotypes, with each occupying distinct geographic range and abiotic niche (Khoury *et al.*, in press). The CFR is characterised by a Mediterranean climate with winter rainfall and hot, dry summers (Manning and Goldblatt, 2012). *G. carneus* is winter growing, with individuals emerging from the dormant period in April or May and growing until they flower, from August to early January (Khoury *et al.*, in press). All individuals go dormant in the late summer and only emerge at the beginning of the wet growing season.

To test for local adaptation between different ecotypes, we focused on three sites (Figure 3.1D-F), namely Jonaskop (JK, -33.963432, 19.510247), Kleinmond Coast (KC, -34.345452, 19.008462), and Limietberg (LB, -33.707683, 19.053684), which represent large populations of three ecotypes: *high-altitude*, *blandus*, and *albidus*, respectively. These three focal populations occupy divergent abiotic niches along an elevational gradient (Khoury *et al.*, in press). JK, the *high-altitude* site, represents the highest elevational extreme (1403 m) while KC, the *blandus* site, represents the lowest elevation (9 m) in the *G. carneus* range. LB (457 m) represents a mid-elevation site.

Do different ecotypes of *Gladiolus carneus* occupy distinct soil niches?

Rangewide ecotypic differences in soil niche

We tested whether there were differences in the soil niche of the different *G. carneus* ecotypes using point localities and soil layers from Cramer *et al.* (2019). The soil layers from Cramer *et al.* (2019) were modelled specifically for the Greater Cape Floristic Region (GCFR) using georeferenced soil data mined from the literature. When compared to SoilGrids layers, which predicts soil layers at a global scale, Cramer *et al.* (2019)'s regionally specific soil layers more accurately represent the heterogeneity of soil properties and make more reliable predictions of the vegetation types (E.g., fynbos, renosterveld) in the GCFR. The soil layers include electrical conductivity (mS/m), extractable potassium ($cmol^+/kg$), extractable sodium ($cmol^+/kg$), extractable phosphorus (mg/kg), pH, total carbon (%) and total nitrogen (%).

We used iNaturalist observations to compile a database of point localities of all ecotypes of *G. carneus.* The observations were classified into seven distinct ecotypes identified in Khoury *et al.* (in press). We excluded any observations that (1) did not have clear photos of the flowers, (2) observations of closely related taxa that had been misidentified as *G. carneus,* (3) observations that did not fit the descriptions of previously described ecotypes or were likely hybrids, (4) observations that occurred outside of the natural range of the species within the CFR (E.g., Australia), and (5) observations that were not research grade. All observations were filtered to include coordinates with an open geoprivacy and an accuracy under 100m. In addition to iNaturalist data, we provided additional point localities for poorly documented ecotypes based on field observations. Overall, we included 789 localities in total, consisting of 209 *albidus*, 33 *blandus*, 67 *callistus*, 34 *high-altitude*, 37 *langeberg*, 379 *macowanianus* and 27 *prismatosiphon* point localities. These point localities were used to extract the soil properties from the seven soil layers in Cramer *et al.* (2019) using the '*raster*' package (Hijmans, 2024).

Population level differences in soil niche

To test if there were differences between the *G. carneus* populations' soil niche, we collected soil samples from three experimental sites, JK, KC, and LB which correspond to the populations used in the common garden and reciprocal translocation experiments. At each site, we collected five soil samples that were 200g each which were placed into Ziplock bags. All soil samples were taken within approximately one metre of a *G. carneus* individual. Samples were collected between the 20th and the 23rd of June 2024, the middle of the growing season of *G. carneus* and were then sent to Elsenburg, Western Cape Department of Agriculture for soil analyses. For each soil sample, potassium (mg/kg), sodium (mg/kg), phosphorus (mg/kg), pH, carbon (%), and NH_4 nitrogen (%) was measured.

Statistical Analyses

We used Principal Component Analyses (PCAs) to determine if the *G. carneus* ecotypes and populations cluster separately based on their soil niche. We implemented the PCAs using the *prcomp* function from the '*stats*' package (R Core Team, 2021) and tested whether the ecotypes cluster separately using a permutation MANOVA from the package '*vegan*' (Oksanen *et al.*, 2020). Depending on the normality and homoscedasticity of the soil properties, we used a series of Kruskal-Wallis tests and one-way ANOVAs to test for differences between the ecotypes' soil properties, both across the species range, and between the experimental populations. In each Kruskal-Wallis test or ANOVA, the soil variable was set as the response and ecotype or population as the fixed effect. Either a Dunn's test, implemented using the '*dunn.test'* package (Dinno, 2024), or a pairwise t-test, implemented using the *pairwise.t.test* function in the '*stats*' package (R Core Team, 2021), was used to determine the significance between ecotypes and populations. A Bonferroni correction was applied to all pairwise comparisons to reduce the likelihood of Type I errors.

Do different ecotypes of *Gladiolus carneus* have a fitness advantage on their native soil relative to other ecotypes within a common garden?

Common garden experiment

To test whether the *G. carneus* ecotypes have a fitness advantage on their native soil relative to other ecotypes, we set up a common garden to track seedling survival and height (mm) in 2024, at the Department of Botany, Rhodes University. As the common garden used soil from each of the ecotypes' native sites, we were testing whether there were fitness differences due to differences in the entire edaphic niche and not exclusively nutrient composition. In November and December 2023 and January 2024, we collected seeds from *G. carneus* populations from JK, KC, and LB. Each site was visited between four and six weeks after the peak flowering period where seeds were collected from dried-out, mature fruits of *G. carneus*. At JK, mesh organza bags were placed over flowering individuals that showed signs of early fruit development and were left to mature. Seeds were then collected roughly eight weeks after peak flowering from the bagged individuals. At each population, between 200 and 1 000 seeds were collected from 10 or more individuals. In the lab, the seeds were thoroughly mixed and stored in glass jars. On 1 May 2024, at the start of the next growing season of plants in the wild, seeds from the three populations were sowed in a 50:50 mix of pool sand and filtered soil collected from Mountain Drive, Makhanda (-33.328830, 26.507832) on which fynbos vegetation grows, the same vegetation type shared amongst the three populations. The growing medium was filtered using a stainless steel, mesh riddle with 0.5 x 0.5 cm squares to remove rocks, organic matter and large clumps of soil. This soil mixture resembles the topmost layer of soil in which the grit creates an airy medium where the seeds can germinate (Rachel Saunders, personal communication). This soil mixture was placed in seed trays (27 x 30 x 11.5 cm). Between 200 to 300 seeds were sprinkled on top of the soil and lightly covered in the soil-pool sand mix. Each tray contained seeds from only a single population. The trays were placed

on a metal growing stand in a sunny courtyard of the Department of Botany where they were exposed to natural temperature fluctuations, often below 10°C in the evenings and above 20°C during the daytime, similar to the conditions in their native range. Seedlings experienced natural winter rainfall, as experienced in Makhanda. However, in periods without regular rainfall, the seeds were kept moist by watering the seedlings approximately every two days using stored rainwater. The seeds took approximately six weeks to germinate.

Between the 20th and the 23rd of June 2024, 20 litres of soil was collected from JK, KC and LB. Similarly, the soil from each site was filtered and placed into black seed trays. In addition to the trays containing soil from the *G. carneus* sites, we also filled separate trays with the medium in which the seeds were germinated to control for transplant shock. If the seedling did not experience transplant shock, survival rates after being transplanted from their germination medium into the control soil should be high. Any reduction in seedling survival in another soil medium would therefore be due to the differential soil properties and not due to being transplanted. In total, there were three trays of soil for each *G. carneus* site, and three trays of the control soil. On the 7th of July 2024, we transplanted 30 germinated *G. carneus* seedlings from a single site into each tray. The 30 seedlings were evenly spaced out in six rows by five columns. Seedlings from all three *G. carneus* populations were transplanted into the four different soil types. All trays were placed on a single table a courtyard and rotated monthly. They were exposed to the same temperature and watering conditions as the germination trays.

Under greenhouse conditions with limited competition, frequent watering and nutrient-rich soil, *G. carneus* takes three years to flower (K. Khoury, unpublished data). Therefore, fitness measures such as the number of flowers or the number of seeds would only be used in long-term experiments on *G. carneus*. Instead, we used fitness components relevant to the early

life stages, namely the seedling survival and height (see Wadgymar *et al.,* 2024 for defining fitness through life history stages). These fitness measures were recorded once every four weeks for each individual in the common garden. Seedling height was measured from the soil to the tip of each leaf using digital calipers (0-200mm, TA). The last survival and height measurement for the year, taken on the 23rd of September 2024, was used in all subsequent analyses as it represented survival and growth to the end of 2024. Measurements were not taken later in the year as *G. carneus* naturally dies back in late spring and summer.

Statistical Analyses

We used a series of generalized linear models (GLMs) to test if there were differences in fitness between the three ecotypes, JK, KC, and LB, on all soil types (*see Table S3.1 for sample sizes used in each analysis*). To test if there were differences in survival between the ecotypes, we used a binomial GLM with soil type, ecotype and their interaction as explanatory terms. In the model, survival was treated as a binary response variable (1 and 0). In the survival analysis, all four soil types were included (JK, KC, LB and the control soil) to test if there was any evidence of transplant shock. Thereafter, the control soil was excluded from analyses as there was no evidence of transplant shock (Figure 3.3A). To test if there were differences in the seedling's height at the end of 2024, we modelled height using both gamma and Gaussian distributions. In both models, soil type, ecotype and their interaction were specified as explanatory variables. Any height measurements of seedlings that did not survive at the end of 2024 was excluded from the data set. The model diagnostics were checked using the *simulateResiduals* and *testDispersion* functions in the '*DHARMa*' package (Hartig, 2022). The model with the gamma distribution was selected due to the lower AIC score. The *Anova* function from '*car*' package (Fox and Weisberg, 2019) was used determine model significance for both the survival and height analysis. Furthermore, the *emmeans* function from the '*emmeans*' package (Lenth,

2022) was used to conduct pairwise comparisons between the ecotypes on each soil type. A Bonferroni correction was applied to the pairwise comparisons to reduce the likelihood of Type 1 errors when making multiple comparisons. For the survival analysis, we also used the '*emmeans*' function to obtain the average probability of survival, plotted together with asymmetric confidence intervals.

In addition to investigating the effects of each fitness component using GLMs, we used aster models to test if there were differences in lifetime fitness. Aster models estimate lifetime fitness by taking into account multiple fitness measures, each with different distributions, that are dependent on the previous life stage (Geyer *et al.*, 2007, Shaw *et al.*, 2008). We used two fitness components in the aster model, survival at the end of 2024, modelled with a Bernoulli distribution (0 and 1), and height at the end of 2024, modelled using a normal distribution (Figure S3.1A). A normal distribution was used for height, as it is the only distribution available for continuous data within the aster framework. Any individuals that did not survive were given a height of 0 mm as the aster framework does not allow for missing data (Geyer *et al.*, 2007, Shaw *et al.*, 2008, Popovic and Lowry, 2020). The soil type, ecotype and their interaction were set as fixed factors within the aster models. The significance of fixed effects was determined by comparing a series of nested null models using likelihood ratio tests (Geyer *et al.*, 2007, Shaw *et al.*, 2008). The full aster model was used to predict the mean height of each ecotype on every soil type at the end of 2024, which takes into account survival. All analyses were conducted using the package, '*aster*' (Geyer *et al.*, 2007).

Do different ecotypes of *Gladiolus carneus* show evidence of local adaptation across an elevational gradient?

Reciprocal translocation

To test whether the *G. carneus* ecotypes have a fitness advantage at their home site relative to other ecotypes, we set up a reciprocal translocation between Jonaskop (JK), Kleinmond Coast (KC), and Limietberg (LB). As the reciprocal translocation encompassed both the climatic and soil conditions for each site, we tested whether each of these ecotypes are locally adapted to their entire abiotic niche.

In November and December 2022 and January 2023, *G. carneus* seeds were collected from the three sites. The seeds were germinated in May 2023, at the Department of Botany, Rhodes University. The seed collection and germination followed the same procedure described for the common garden experiments. Between the 2nd and 9th of July 2023, a reciprocal translocation was set up between the three sites. From each of these sites, 120 litres of soil was collected in order to fill 16 or 20 black seed trays (27 x 30 x 11.5 cm) that were used in the reciprocal translocations. Soil from KC and JK was used fill 20 seed trays, while soil from LB filled 16 trays. Each tray contained eight seedlings from each locality which were transplanted into eight rows and four columns. The position of the seedlings from each locality was rotated through the trays. The trays were transported to each of the sites and set up under cages made of wire mesh that were designed to prevent large herbivores and rock falls from damaging the experiments. Cages were 1.2 x 0.6 x 0.8 m with 4 cm wide square holes painted with green rubberised paint to prevent rust. Each cage contained four randomly arranged trays, with each tray having a distinct arrangement of the seedlings. The cages were held in place by a combination of metal pegs and large rocks. Five cages were set up at the two most elevationally extreme sites, JK and KC, and four cages were set up at LB. Overall, 480 seedlings, consisting of 160 seedlings from each locality, were placed at JK and KC, while 384 seedlings with 128 from each locality were set up at LB. The cages were nested within the *G. carneus* populations at each site.

Similar to the common garden, seedling survival and height were documented as the fitness measures. Both survival and height were documented twice in 2023 and 2024, once during the middle of the growing season and once towards the end. Seedling survival was scored as a binary variable (0 or 1). The height (mm) of each seedling was measured in a straight-line distance from the surface of the soil to the tip of the leaf using digital callipers. Height measurements were not taken for individuals with evidence of damage on the leaf tips. The survival and height at the end of 2023 and 2024 were used in all analyses as this represented fitness at the end of each year.

Statistical Analyses

A series of generalized linear mixed models (GLMMs) were used to test whether there were differences in survival and height in both years between JK, KC and LB seedlings at each of their native sites. Survival in 2023 and 2024 were both modelled using a binomial error distribution while height (mm) in 2023 and 2024 were modelled using a normal distribution. All models had site, ecotype and their interaction as fixed factors. The models also included a nested random factor, tray within cage. Due to low sample sizes in the height measurements in 2024 (*see Table S3.2*) only cage, and not tray within cage, was included as a random factor in the 2024 height model. All models were implemented using the '*glmmTMB*' package (Brooks *et al.*, 2017). The model diagnostics were checked using the same procedure described for the common garden experiment. A type III ANOVA from the '*car*' package (Fox and Weisberg, 2019) was used to determine the significance of fixed factors and pairwise contrasts between ecotypes at each site were conducted using the *emmeans* function from the '*emmeans*' package (Lenth, 2022).

Similar to the common garden experiments, aster models were used to test for differences in the lifetime fitness of the seedlings at each reciprocal translocation site. We used three sets of aster models to look at differences in fitness in 2023, 2024 and both years in a full model. In the 2023 and 2024 models the fitness components included survival and height in their respective years, while the full model incorporated all four fitness components (Figure S3.1B). Survival was modelled using a Bernoulli distribution (0 or 1), while height was modelled using a normal distribution. Height in both years were set as terminal nodes within the models. In cases where seedlings did not survive, the height was set to 0 mm. Within the models, site, ecotype and their interaction were set as fixed effects. The significance of fixed effects was determined using likelihood ratio tests described under the common garden experiment. The three sets of aster models were used to make predictions about the height of the ecotypes at each site by the end of each year and while taking into account the previous dependencies. All data analyses was conducted in R v.4.1.2 (R Core Team, 2021) and the package '*ggplot2*' (Wickham, 2016) was used for all data visualisation.

RESULTS

Do different ecotypes of *Gladiolus carneus* occupy distinct soil niches?

Rangewide ecotypic differences in soil niche

The permutation MANOVA showed that there were statistical differences between the *G. carneus* ecotypes' soil niche (F = 33.35, df = 6, P < 0.001, Figure 3.2A). There were also statistical differences between the *G. carneus* ecotypes' electrical conductivity ($\chi 2$ = 117.75, df = 6, P < 0.0001, Table S3.3), extractable potassium ($\chi 2$ = 298.80, df = 6, P < 0.0001, Table S3.3), extractable sodium ($\chi 2$ = 198.94, df = 6, P < 0.0001, Table S3.3), extractable phosphorus ($\chi 2$ = 281.98, df = 6, P < 0.0001, Table S3.3), pH ($\chi 2$ = 147.28, df = 6, P < 0.0001, Table S3.3), total carbon ($\chi 2$ = 189.06, df = 6, P < 0.0001, Table S3.3) and total nitrogen ($\chi 2$ = 89.38, df =

6, $P < 0.0001$, Table S3.1). Pairwise comparisons showed there were significant differences between the ecotypes for all soil properties (*see Table S3.4*). These results suggest that there are differences in the ecotypes' soil niche.

Population level differences in soil niche

The permutation MANOVA showed that there were statistical differences between the soil properties at JK, KC, and LB ($F = 494.90$, $df = 2$, $P < 0.001$, Figure 3.2B). In particular, there were differences in the potassium ($F = 251.70$, $df = 2$, $P = 0.0001$, Table S3.5), sodium ($\chi 2 = 12.59$, $df = 2$, $P = 0.0018$, Table S3.5), phosphorus ($\chi 2 = 12.39$, $df = 2$, $P = 0.0020$, Table S3.5), pH ($\chi 2 = 458.60$, $df = 2$, $P < 0.0001$, Table S3.5), carbon ($\chi 2 = 10.92$, $df = 2$, $P = 0.0043$, Table S3.5), and NH_4 nitrogen ($F = 603.50$, $df = 2$, $P < 0.0001$, Table S3.5) measured at those three sites. Pairwise comparisons further showed there were significant differences between the sites for all soil properties documented (*see Table S3.6*). KC had the highest sodium (283.60 ± 9.68 SE mg/kg), phosphorus (107.60 ± 5.07 SE mg/kg), carbon (7.19 ± 0.21 SE %), NH_4 nitrogen (0.41 ± 0.01 SE %) and pH (5.52 ± 0.04 SE) indicating that it is a 'nutrient-rich' site (Table S3.5). JK had the lowest potassium (28.00 ± 1.34 SE mg/kg), sodium (9.00 ± 0.63 SE mg/kg), phosphorus (13.60 ± 0.68 SE mg/kg) and NH_4 nitrogen (0.03 ± 0.01 SE %) indicating that it is a 'nutrient-poor' site (Table S3.5). Additionally, LB had the highest potassium (95.20 ± 2.35 SE mg/kg) but lowest pH (4.50 ± 0.00SE) and carbon (0.62 ± 0.01 SE %) but was otherwise considered as a site with intermediate nutrients (Table S3.5). Overall, there are differences between the soil properties of the three sites, which represent a gradient between nutrient-rich and poor sites within the *G. carneus* species complex.

Do different ecotypes of *Gladiolus carneus* have a fitness advantage on their native soil relative to other ecotypes within a common garden?

Common garden experiment

Overall, all seedlings in the common garden did not have a survival advantage, but did have a growth advantage on nutrient-rich KC compared to the other two soils (Figure 3.3). Both KC and JK seedlings, which occupy the most extreme soil niches, had a fitness advantage on their native soils, while LB seedlings did not have fitness advantage on their native soil compared to JK and KC seedlings (Figure 3.3C).

Seedlings experienced high survival rates across all ecotypes on all soil types at the end of 2024 (Figure 3.3A). This included seedlings on the control soil indicating that there was no evidence of transplant shock (Figure 3.3A). Soil type ($\chi 2$ = 13.30, *df* = 3, *P* = 0.0040, Figure 3.3A) and ecotype ($\chi 2$ = 12.13, *df* = 2, *P* = 0.0023, Figure 3.3A) were significant predictors of survival in 2024, whilst the interaction between soil type and ecotype was not ($\chi 2$ = 8.04, *df* = 6, *P* = 0.2355, Figure 3.3A). The pairwise comparisons between the ecotypes on each soil type were all non-significant (*P* = 1.00, Table S3.7), indicating that there were no differences in survival between seedlings.

Soil type ($\chi 2$ = 94.22, *df* = 2, *P* < 0.0001, Figure 3.3B), ecotype ($\chi 2$ = 25.72, *df* = 2, *P* < 0.0001, Figure 3.3B) and their interaction ($\chi 2$ = 10.88, *df* = 4, *P* = 0.03, Figure 3.3B) were all significant predictors of seedling height at the end of 2024. The pairwise comparisons showed that JK seedlings were significantly larger than the KC seedlings on JK soil (*P* < 0.05, Table S3.7) and LB seedlings were significantly larger than KC seedlings on LB soil (*P* = 0.0007, Table S3.7). These results indicate that JK and LB seedlings have an advantage over KC seedlings on their native soil. There were no other significant differences between the seedling heights.

The aster model showed that soil type ($P < 0.0001$, Table 3.1, Figure 3.3C) was a significant predictor of lifetime fitness, but ecotype ($P = 0.75$, Table 3.1, Figure 3.3C) and the interaction between soil type and ecotype ($P = 0.21$, Table 3.1, Figure 3.3C) were not. Seedlings from JK and KC had the highest predicted mean height on their native soil, however, LB seedlings did not show the same homesite fitness advantage (Figure 3.3C).

Do different ecotypes of *Gladiolus carneus* show evidence of local adaptation across an elevational gradient?

Reciprocal Translocation

Over the two years, three cages were removed from the data set (*see resulting sample sizes in Table S3.2*). At the KC site, two of the cages were placed approximately 50m from the shoreline representing the edge of the native population, and nearly all the seedlings in those cages died within the first year. A third cage showed signs of human tampering. All three cages were excluded from analyses. Additionally, any seedlings showing signs of damage were excluded.

There were relatively high survival rates (>70%) of all ecotypes at every site in 2023, however, this was not the case in 2024 (Table S3.8). In 2023, site ($\chi 2 = 11.97$, $df = 2$, $P = 0.0025$, Figure 3.4A), ecotype ($\chi 2 = 19.31$, $df = 2$, $P < 0.0001$, Figure 3.4A) and their interaction ($\chi 2 = 10.53$, $df = 4$, $P = 0.0324$, Figure 3.4A) were all significant predictors of seedling survival. Similarly, in 2024, site ($\chi 2 = 19.46$, $df = 2$, $P < 0.0001$, Figure 3.4B), ecotype ($\chi 2 = 16.90$, $df = 2$, $P = 0.0002$, Figure 3.4B) and their interaction ($\chi 2 = 12.64$, $df = 4$, $P = 0.0132$, Figure 3.4B) were all significant predictors of seedling survival. At JK in 2023 and 2024, the native JK seedlings had significantly higher probability of survival than KC seedlings ($P < 0.01$, Table S3.9). Additionally, JK, KC and LB seedlings all had the highest survival rates at their native sites in 2024 (Figure 3.4B, Table S3.8).

In 2023, site ($\chi 2$ = 197.68, *df* = 2, *P* < 0.0001, Figure 3.4C), ecotype ($\chi 2$ = 20.42, *df* = 2, *P* < 0.0001, Figure 3.4C) and their interaction ($\chi 2$ = 28.75, *df* = 4, *P* < 0.0001, Figure 3.4C) were all significant predictors of seedling height. JK and LB seedlings were significantly larger than KC at JK (P < 0.05, Table S3.9). LB seedlings were significantly larger than KC at LB (P < 0.05, Table S3.9). Both JK and LB seedlings were significantly larger than KC at KC (P < 0.0001, Table S3.9). These results indicate that JK and LB seedlings have a fitness advantage over KC at their native sites. Additionally, JK and LB seedlings were both significantly larger than KC seedlings at KC, indicating that two introduced localities had a fitness advantage over the native (P < 0.0001, Table S3.9).

In 2024, site ($\chi 2$ = 23.03, *df* = 2, *P* < 0.0001, Figure 3.4D) and the interaction between site and ecotype ($\chi 2$ = 20.38, *df* = 4, *P* < 0.0004, Figure 3.4D) were significant predictors of height, however, ecotype was non-significant ($\chi 2$ = 0.08, *df* = 2, *P* = 0.9594, Figure 3.4D). LB seedlings were significantly larger than KC seedlings at LB (P < 0.05, Table S3.9). There were no other comparisons of the ecotypes' heights that were significantly different. Overall, native seedlings were, on average, the largest seedlings at their native site in 2024 (Figure 3.4D).

We used aster models to test whether there were differences in the lifetime fitness of the seedlings and to make predictions about the seedlings' heights at each reciprocal translocation site. The first and second aster models took into account the survival and height data from 2023 and 2024, respectively. These models were then used to make predictions of the seedling heights using only data from those years. The third full aster model took into account the seedling survival and height from 2023 and 2024, and the associated height predicted for the end of 2024 takes into account both years' data. The 2023 aster model showed

that site ($P < 0.0001$) and ecotype ($P < 0.001$), but not their interaction ($P = 0.0998$), were significant predictors of lifetime fitness. Furthermore, only JK seedlings had a fitness advantage at their native site in 2023. The 2024 and the full aster models showed that site (2024: $P < 0.0001$, full: $P < 0.0001$), ecotype (2024: $P < 0.05$, full: $P < 0.01$) and their interaction (2024: $P < 0.05$, full: $P = 0.05$) were all significant predictors of lifetime fitness (Table 3.1, Figure 3.5). In the 2024 model, all native seedlings were predicted to have a home-site advantage, while the full model suggested that JK and LB plants had a fitness advantage in their native environment while KC plants did not have a fitness advantage at their native site (Figure 3.5C). These results suggest that there is evidence for local adaptation at all three sites, with the strongest evidence for local adaptation being at the JK, the nutrient-poor site, and LB, the intermediate nutrient site.

DISCUSSION

This study provides evidence that the *G. carneus* ecotypes occupy distinct soil niches and that they are in part, locally adapted to these soil niches at the seedling stage. This is the first study providing evidence for local adaptation of plants occupying different soil niches in the CFR using both a common garden experiment that isolates the effects of soil properties from climatic variables on seedling survival and height, and a reciprocal translocation to test for local adaptation. Interestingly, and in agreement with the broader literature (see Sambatti and Rice, 2006, Lekberg *et al.*, 2012, Ferris and Willis, 2018), we found local adaptation between localities with extreme soil properties, namely between extremely nutrient-poor soils and nutrient-rich soils. As predicted, all ecotypes had a growth advantage on the on the nutrient-rich soils. However, the reciprocal translocation also revealed evidence of local adaptation at a locality with intermediate soil nutrient composition. However, in this case, it is likely that other abiotic factors, rather than soil type, is contributing to local adaptation, as the results from

the reciprocal translocation experiment were not entirely supported by the common garden experiment. Below we discuss the results in the context of the broader literature with the implications for the diversification of the Cape Floristic Region, a biodiversity hotspot.

Do Gladiolus carneus *ecotypes occupy distinct soil niches?*

All seven of the *G. carneus* ecotypes, and the three experimental populations, all occupied distinct soil niches (Figure 3.2). The three experimental populations occupied a gradient of soil niches, which included a nutrient-poor site (JK), one intermediate site (LB) and one nutrient-rich site (KC) (Figure 3.2B). These results provide evidence that shifts in soil nutrient composition between both ecotypes and populations are common in the species complex and is potentially a driver of diversification. Similar shifts have been documented between populations of the same species, occupying distinct soil niches (Sambatti and Rice, 2006, Jimenez-Ambriz *et al.*, 2007, Macel *et al.*, 2007, Lekberg *et al.*, 2012, Dittmar and Schemske, 2023, Jimenez-Ramirez *et al.*, 2023) or between closely related species (Verboom *et al.*, 2004, Ellis *et al.*, 2006) and even between populations within a wider species complex (Verboom *et al.*, 2012). Within the CFR, shifts in soil type between sister species have commonly been shown using molecular phylogenies and frequently show that edaphic shifts between sister taxa are common (van der Niet and Johnson, 2009, Schnitzler *et al.*, 2011, Forest *et al.*, 2014). These shifts in soil type are then inferred as a major driver of speciation.

Are Gladiolus carneus *ecotypes locally adapted to their soil niches?*

Despite all the populations at the translocation sites occupying distinct edaphic niches, the common garden experiment indicated that only JK and KC, which occupied the extreme soil niches, showed any evidence of local adaptation to their edaphic niche. In contrast, LB, which occupied an intermediate edaphic niche, showed no evidence local adaptation to its edaphic

niche. Similarly, Jimenez-Ramirez *et al.* (2023) found no evidence of local adaptation to non-extreme soils over small spatial scales during the early life stages of *Pinus sylvestus*. These results indicate that shifts in soil niche, and particularly non-extreme soil shifts, do not necessarily result in local adaptation. Furthermore, edaphic shifts often co-occur with climatic shifts, which may result in local adaptation to exclusively to climate (Macel *et al.*, 2007, Ellis and Ågren, 2024). As soil shifts do not necessarily result in local adaptation, they should be used cautiously when inferring speciation.

Additionally, the two populations showing evidence of local adaptation to their soil niche (JK and KC) also occupy the two elevational extremes of the *G. carneus* range and are thus exposed to other abiotic factors that may be contributing to local adaptation. In particular, the JK population is exposed to freezing temperatures and snow during the winter growing season, and the KC population grows along the coast and is frequently exposed to salt spray. Both freezing temperatures (Agren and Schemske, 2012) and salt spray (Lowry *et al.*, 2008, Busoms *et al.*, 2015, Popovic and Lowry, 2020) have been shown to exert strong selection that can result in local adaptation, which may be contributing to the low survival rates at the JK and KC sites. The relative contribution of these ecological factors can be disentangled using factorial reciprocal translocations (see Macel *et al.*, 2007, Popovic and Lowry, 2020, Ellis and Ågren, 2024). For example, Ellis and Ågren (2024) reciprocally transplanted populations of *Arabidopsis thaliana* and their soils between Italy and Sweden to isolate the contribution of soil type verses climate to local adaptation. Using this method, they found soil type made little contribution to local adaptation. Similar factorial reciprocal translocations could be employed between *G. carneus* populations to isolate the contribution of specific ecological factors to local adaptation.

This approach would be particularly useful for the LB population, which showed evidence of local adaptation to factors other than its edaphic niche. Other ecotypes within *G. carneus* may be locally adapted to other ecological factors that have not been explicitly tested (E.g.: climate, fire-regime, rocky outcrops), or to an interaction between their edaphic niche and other ecological factors. Dittmar and Schemske (2023) demonstrated such an interaction when they conducted a multi-year reciprocal translocation between *Leptosiphon parviflorus* populations on sandstone and serpentine soil. They found that the population native to the serpentine soil consistently had a home-site advantage, while the population native to the sandstone soil only had a home-site advantage in two of the four years. Using a greenhouse experiment, they further demonstrated that the sandstone population's fitness advantage was dependent on water availability. Dittmar and Schemske (2023)'s results also highlight that the interactions causing local adaptation may vary temporally. Furthermore, the other *G. carneus* ecotypes may be locally adapted at a different life stage. Both the common garden and reciprocal translocations presented here only measured local adaptation from the seedling stage. However, early life stages (E.g.: germination) has been shown to strongly contribute to local adaptation (Postma and Agren, 2016). This underscores that multi-year reciprocal translocations, that include all life stages, are needed to understand the variability of selection over time and the extent of local adaptation (Wadgymar *et al.*, 2022).

Are edaphic shifts a driver of diversification in the Cape Floristic Region?

We have presented data on the first reciprocal translocation and common garden experiments explicitly testing for local adaptation to divergent soil types between closely related taxa in the CFR. Our results suggest that shifts in edaphic niches occur in the CFR and can result in local adaptation, especially in some extreme niches. The frequency of these edaphic shifts in the CFR is somewhat disputed with Schnitzler *et al.* (2011) showing edaphic shifts between 20 –

72% of sister species pairs from four Cape clades, and van der Niet and Johnson (2009) showing edaphic shifts in only 17% of sister species pairs from eight Cape clades. Furthermore, shifts in substrate type have also been documented in *Lapeirousia* (Forest *et al.*, 2014) and *Ehrharta* (Verboom *et al.*, 2004). Despite these shifts being documented on a macroevolutionary scale, there is limited experimental evidence demonstrating shifts and there are no examples of reciprocal translocations or common garden experiments within the CFR explicitly testing for local adaptation between contrasting edaphic niches. The strongest experimental evidence comes from Verboom ***et al.*** (2004) which showed that seedlings from eight ***Ehrharta*** species grown under controlled nutrient-rich conditions, differed in their relative growth rates and were associated both with different adult stage growth forms (slow, intermediate and fast growers) and with their native edaphic conditions. Verboom ***et al.*** (2004) further showed that the shifts from the slow to the fast growth form only occurred after a transition from nutrient-poor, sandstone derived soils to richer, shale and granite derived soils. Furthermore, the only reciprocal translocation testing for local adaptation along an ecological gradient in the CFR, Latimer ***et al.*** (2009), did not isolate the edaphic niche from other abiotic factors. The only example of a reciprocal translocation testing for local adaptation between contrasting edaphic environments in the GCFR is that of Ellis and Weis (2006). They conducted a reciprocal translocation between *Argyroderma* species occupying distinct soil microenvironments in the Succulent Karoo and found evidence for local adaptation. Overall, these results are the first in the CFR showing both frequent edaphic shifts and finding evidence for local adaptation in contrasting edaphic niches.

CONCLUSION

In this study, we present a single year of a common garden experiments testing for differential fitness on contrasting soil types, and two years of a reciprocal translocation testing for local

adaptation. We found that only two of the three populations, JK and KC were locally adapted to their soil niche, while the LB was locally adapted its abiotic niche. Further research should identify ecological shifts and use multi-year common garden and reciprocal translocations, that include all life stages, to comprehensively test for local adaptation (Wadgymar *et al.*, 2017). We should additionally be using factorial reciprocal translocations and common garden experiments to isolate the role of specific, or interacting abiotic (E.g. climatic, topographic, and edaphic) or biotic (E.g. pollinators and herbivores) factors driving causing local adaptation (Dittmar and Schemske, 2023, Ellis and Ågren, 2024). Furthermore, when ecological factors causing local adaptation are identified in the CFR, their contribution to pre and postzygotic reproductive isolation should be quantified to better understand their role in driving speciation in this hyper-diverse region (Baack *et al.*, 2015, Rajakaruna, 2017).

LITERATURE CITED

Agren J, Schemske DW. 2012. Reciprocal transplants demonstrate strong adaptive differentiation of the model organism *Arabidopsis thaliana* in its native range. *New Phytologist,* **194**: 1112-1122.

Baack E, Melo MC, Rieseberg LH, Ortiz-Barrientos D. 2015. The origins of reproductive isolation in plants. *New Phytologist,* **207**: 968-984.

Brooks ME, Kristensen K, van Benthem KJ, *et al.* 2017. glmmTMB balances speed and flexibility among packages for zero-inflated generalized linear mixed modeling. *The R Journal,* **9**: 378-400.

Busoms S, Teres J, Huang XY, *et al.* 2015. Salinity is an agent of divergent selection driving local adaptation of *Arabidopsis* to coastal habitats. *Plant Physiology,* **168**: 915-929.

Butlin RK, Faria R. 2024. Local adaptation and reproductive isolation: when does speciation start? *Evolutionary Journal of the Linnean Society*, **3**: kzae003.

Cramer MD, West AG, Power SC, Skelton R, Stock WD. 2014. Plant ecophysiological diversity. In: Allsopp N, Colville JF, Verboom GA, eds. *Fynbos: ecology, evolution and conservation of a megadiverse region*. Oxford: Oxford University Press.

Cramer MD, Wootton LM, Mazijk R, Verboom GA. 2019. New regionally modelled soil layers improve prediction of vegetation type relative to that based on global soil models. *Diversity and Distributions*, **25**: 1736-1750.

Dinno A. 2024. dunn.test: Dunn's test of multiple comparisons using rank sums. R package version 1.3.6. https://CRAN.R-project.org/package=dunn.test.

Dittmar EL, Schemske D. 2023. Temporal variation in selection influences microgeographic local adaptation. *The American Naturalist*, **202**: 471-485.

Ellis AG, Verboom GA, van der Niet T, Johnson SD, Linder HP. 2014. Speciation and extinction in the Greater Cape Floristic Region. In: Allsopp N, Colville JF, Verboom GA, eds. *Fynbos: ecology, evolution and conservation of a megadiverse region*. Oxford: Oxford University Press.

Ellis AG, Weis AE. 2006. Coexistence and differentiation of ‘flowering stones’: the role of local adaptation to soil microenvironment. *Journal of Ecology*, **94**: 322-335.

Ellis AG, Weis AE, Gaut BS. 2006. Evolutionary radiation of “stone plants" in the genus *Argyroderma* (Aizoaceae): unraveling the effects of landscape, habitat, and flowering time. *Evolution*, **60**: 39-55.

Ellis TJ, Ågren J. 2024. Adaptation to soil type contributes little to local adaptation in an Italian and a Swedish ecotype of *Arabidopsis thaliana* on contrasting soils. *Biology Letters*, **20**: 20240236.

Ferris KG, Willis JH. 2018. Differential adaptation to a harsh granite outcrop habitat between sympatric *Mimulus* species. *Evolution,* **72**: 1225-1241.

Forest F, Goldblatt P, Manning JC, *et al.* 2014. Pollinator shifts as triggers of speciation in painted petal irises (*Lapeirousia*: Iridaceae). *Annals of Botany,* **113**: 357-371.

Fox J, Weisberg S. 2019. *An {R} Companion to applied regression.* Thousand Oaks CA: Sage.

Geyer CJ, Wagenius S, Shaw RG. 2007. Aster models for life history analysis. *Biometrika,* **94**: 415-426.

Goldblatt P, Manning JC. 2020. *Iridaceae of southern Africa.* Pretoria: Strelitzia 42.

Gross K, Undin M, Thompson JN, Friberg M. 2023. Components of local adaptation and divergence in pollination efficacy in a coevolving species interaction. *Ecology,* **104**: e4043.

Hartig F. 2022. DHARMa: Residual diagnostics for hierarchical (multi-Level / mixed) regression Models. R package version 0.4.5. https://CRAN.R-project.org/package=DHARMa.

Hereford J. 2009. A quantitative survey of local adaptation and fitness trade-offs. *The American Naturalist,* **173**: 579-88.

Hijmans RJ. 2024. raster: geographic data analysis and modeling. R package version 3.6-30. https://rspatial.org/raster.

Jimenez-Ambriz G, Petit C, Bourrie I, Dubois S, Olivieri I, Ronce O. 2007. Life history variation in the heavy metal tolerant plant *Thlaspi caerulescens* growing in a network of contaminated and noncontaminated sites in southern France: role of gene flow, selection and phenotypic plasticity. *New Phytologist,* **173**: 199-215.

Jimenez-Ramirez A, Sole-Medina A, Ramirez-Valiente JA, Robledo-Arnuncio JJ. 2023. Microgeographic variation in early fitness traits of *Pinus sylvestris* from contrasting soils. *American Journal of Botany*, **110**: e16159.

Johnson SD. 2025. Pollination ecotypes and the origin of plant species. *Proceedings of the Royal Society B*, **292**: 20242787.

Kawecki TJ, Ebert D. 2004. Conceptual issues in local adaptation. *Ecology Letters*, **7**: 1225-1241.

Khoury KL, Edwards S, Newman E. in press. Ecological niche differentiation mediates near complete premating reproductive isolation within the *Gladiolus carneus* (Iridaceae) species complex. *Annals of Botany*.

Latimer AM, Silander Jr. JA, Rebelo AG, Midgley GF. 2009. Experimental biogeography: the role of environmental gradients in high geographic diversity in Cape Proteaceae. *Oecologia*, **160**: 151-162.

Lekberg Y, Roskilly B, Hendrick MF, Zabinski CA, Barr CM, Fishman L. 2012. Phenotypic and genetic differentiation among yellow monkeyflower populations from thermal and non-thermal soils in Yellowstone National Park. *Oecologia*, **170**: 111-122.

Lenth RV. 2022. emmeans: estimated marginal means, aka least-squares means. R package version 1.7.2. https://CRAN.R-project.org/package=emmeans.

Linder HP. 2003. The radiation of the Cape flora, southern Africa. *Biological Reviews*, **78**: 597–638.

Lowry DB, Rockwood RC, Willis JH. 2008. Ecological reproductive isolation of coast and inland races of *Mimulus guttatus*. *Evolution*, **62**: 2196-2214.

Macel M, Lawson CS, Mortimer SR, *et al.* 2007. Climate vs. soil factors in local adaptation of two common plant species. *Ecology*, **88**: 424-433.

Manning J, Goldblatt P. 2012. *Plants of the Greater Cape Floristic Region 1: the core Cape flora.* Pretoria: Strelitzia 29.

Newman E, Manning J, Anderson B. 2015. Local adaptation: mechanical fit between floral ecotypes of *Nerine humilis* (Amaryllidaceae) and pollinator communities. *Evolution,* **69**: 2262-2275.

Nosil P, Vines TH, Funk DJ. 2005. Reproductive isolation caused by natural selection against immigrants from divergent habitats. *Evolution,* **59**: 705-719.

Oksanen J, Blanchet FG, Friendly M, *et al.* 2020. vegan: community ecology package. R package version 2.5-7. https://CRAN.R-project.org/package=vegan.

Popovic D, Lowry DB. 2020. Contrasting environmental factors drive local adaptation at opposite ends of an environmental gradient in the yellow monkeyflower (*Mimulus guttatus*). *American Journal of Botany*, **107**: 298-307.

Postma FM, Agren J. 2016. Early life stages contribute strongly to local adaptation in *Arabidopsis thaliana*. *Proceedings of the National Academy of Sciences,* **113**: 7590-7595.

R Core Team. 2021. R: A language and environment for statistical computing. Vienna, Austria: R Foundation for Statistical Computing.

Rajakaruna N. 2017. Lessons on evolution from the study of edaphic specialization. *The Botanical Review*, **84**: 39-78.

Sambatti JBM, Rice KJ. 2006. Local adaptation, patterns of selection, and gene flow in the Californian sepentine sunflower (*Helianthus exilis*). *Evolution,* **60**: 696–710.

Schnitzler J, Barraclough TG, Boatwright JS, *et al.* 2011. Causes of plant diversification in the Cape biodiversity hotspot of South Africa. *Systematic Biology,* **60**: 343-357.

Shaw RG, Geyer CJ, Wagenius S, Hangelbroek HH, Etterson JR. 2008. Unifying life-history analyses for inference of fitness and population growth. *The American Naturalist,* **172**: E35–E47.

Thiergart T, Duran P, Ellis T, *et al.* 2020. Root microbiota assembly and adaptive differentiation among European *Arabidopsis populations*. *Nature ecology and evolution,* **4**: 122-131.

Turesson G. 1922. The genotypical response of the plant species to the habitat. *Hereditas,* **3**: 211-350.

van der Niet T, Johnson SD. 2009. Patterns of plant speciation in the Cape Floristic Region. *Molecular Phylogenetics and Evolution,* **51**: 85-93.

Verboom GA, Linder HP, Stock WD. 2004. Testing the adaptive nature of radiation: growth form and life history divergence in the African grass genus *Ehrharta* (Poaceae: Ehrhartoideae). *American Journal of Botany,* **91**: 1364-1370.

Verboom GA, Moore TE, Hoffmann V, Cramer MD. 2012. The roles of climate and soil nutrients in shaping the life histories of grasses native to the Cape Floristic Region. *Plant Soil,* **355**: 323–340.

Verboom GA, Stock WD, Cramer MD. 2017. Specialization to extremely low-nutrient soils limits the nutritional adaptability of plant lineages. *The American Naturalist,* **189**: 684-699.

Wadgymar SM, DeMarche ML, Josephs EB, Sheth SN, Anderson JT. 2022. Local adaptation: causal agents of selection and adaptive trait divergence. *Annual Review of Ecology, Evolution, and Systematics,* **53**: 87-111.

Wadgymar SM, Lowry DB, Gould BA, *et al.* 2017. Identifying targets and agents of selection: innovative methods to evaluate the processes that contribute to local adaptation. *Methods in Ecology and Evolution,* **8**: 738-749.

Wadgymar SM, Sheth S, Josephs E, DeMarche M, Anderson J. 2024. Defining fitness in evolutionary ecology. *International Journal of Plant Sciences,* **185**: 218-227.

Wickham H. 2016. *ggplot2: Elegant graphics for data analysis.* New York: Springer-Verlag.

Yost JM, Barry T, Kay KM, Rajakaruna N. 2012. Edaphic adaptation maintains the coexistence of two cryptic species on serpentine soils. *American Journal of Botany,* **99**: 890-897.

TABLES

Table 3.1: Aster model results from the common garden and reciprocal translocation experiments. The common garden experiment includes survival and height (mm) in 2024. Three aster model results are presented for the reciprocal translocation, the first includes the survival and height (mm) in 2023, the second includes survival and height (mm) in 2024, and the third includes data from both years.

Experiment	Model	Factor Tested	Null df	Alternative df	Null deviance	Alternative deviance	Test df	Test deviance	Test *P* value
Common garden	2024	Soil type	4	6	2195.50	2215.00	2	19.50	< **0.0001**
		Ecotype	4	6	2214.40	2215.00	2	0.59	0.7461
		Soil type x Ecotype	6	10	2215.00	2220.90	4	5.89	0.2073
Reciprocal translocation	2023	Site	4	6	1254.90	1302.10	2	47.20	< **0.0001**
		Ecotype	4	6	1287.70	1302.10	2	14.38	**0.0008**
		Site x Ecotype	6	10	1302.10	1309.90	4	7.79	0.0998
	2024	Site	4	6	-69.84	110.79	2	180.63	< **0.0001**
		Ecotype	4	6	104.66	110.79	2	6.13	**0.0467**
		Site x Ecotype	6	10	110.79	123.63	4	12.85	**0.0120**
	full	Site	6	8	1365.00	1513.50	2	148.42	< **0.0001**
		Ecotype	6	8	1502.00	1513.50	2	11.41	**0.0033**
		Site x Ecotype	8	12	1513.50	1522.80	4	9.30	**0.0540**

FIGURES

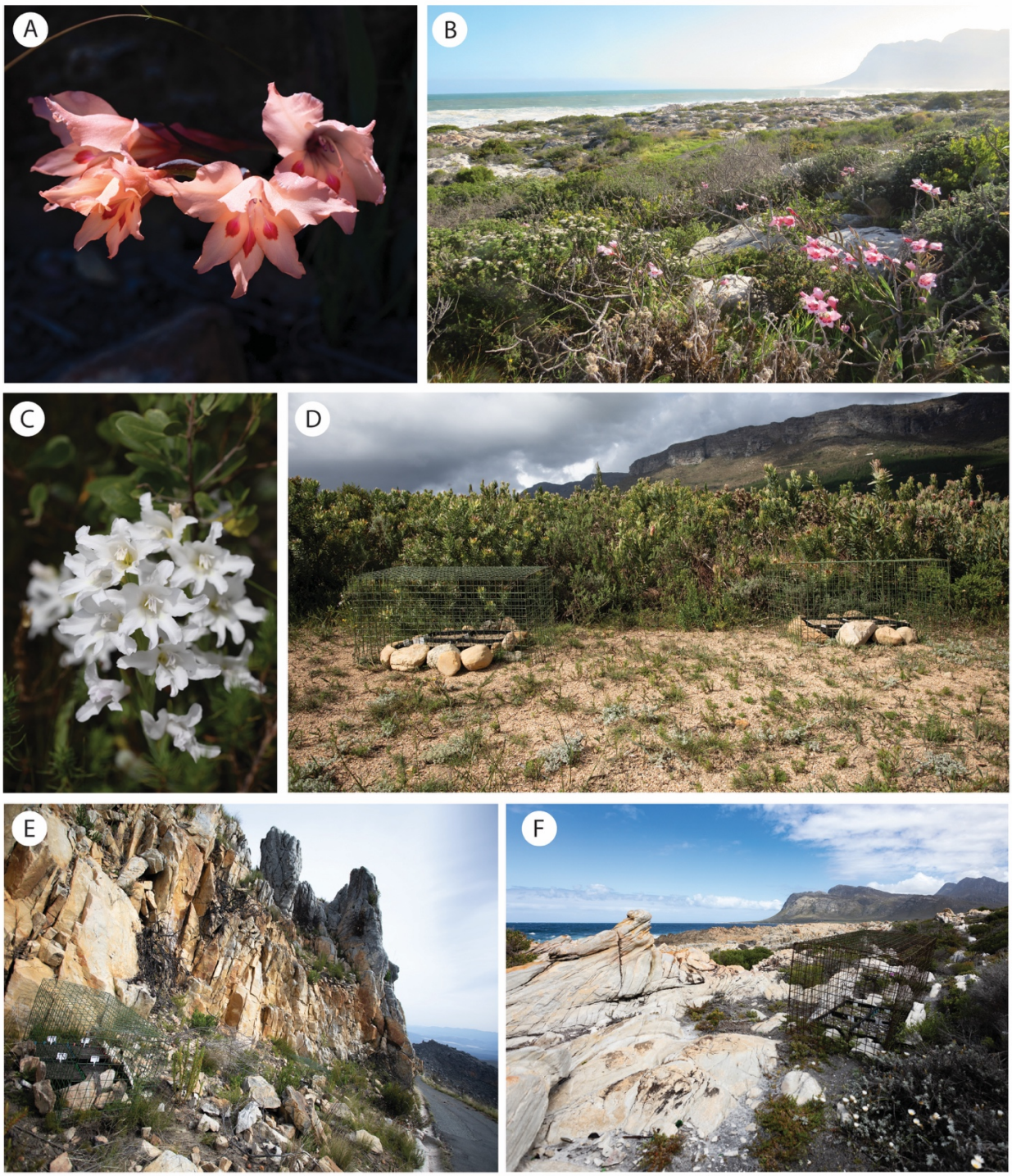

Figure 3.1. (A) Flowering *Gladiolus carneus* ecotypes from Jonaskop (JK), (B) Kleinmond Coast (KC), (C) and Limietberg (LB). Habitat images of reciprocal translocation sites (D) LB, (E) JK and (F) KC, with experimental plants in the foreground. Photos: A, C, D, E, F: Ethan Newman; B: Katharine Khoury.

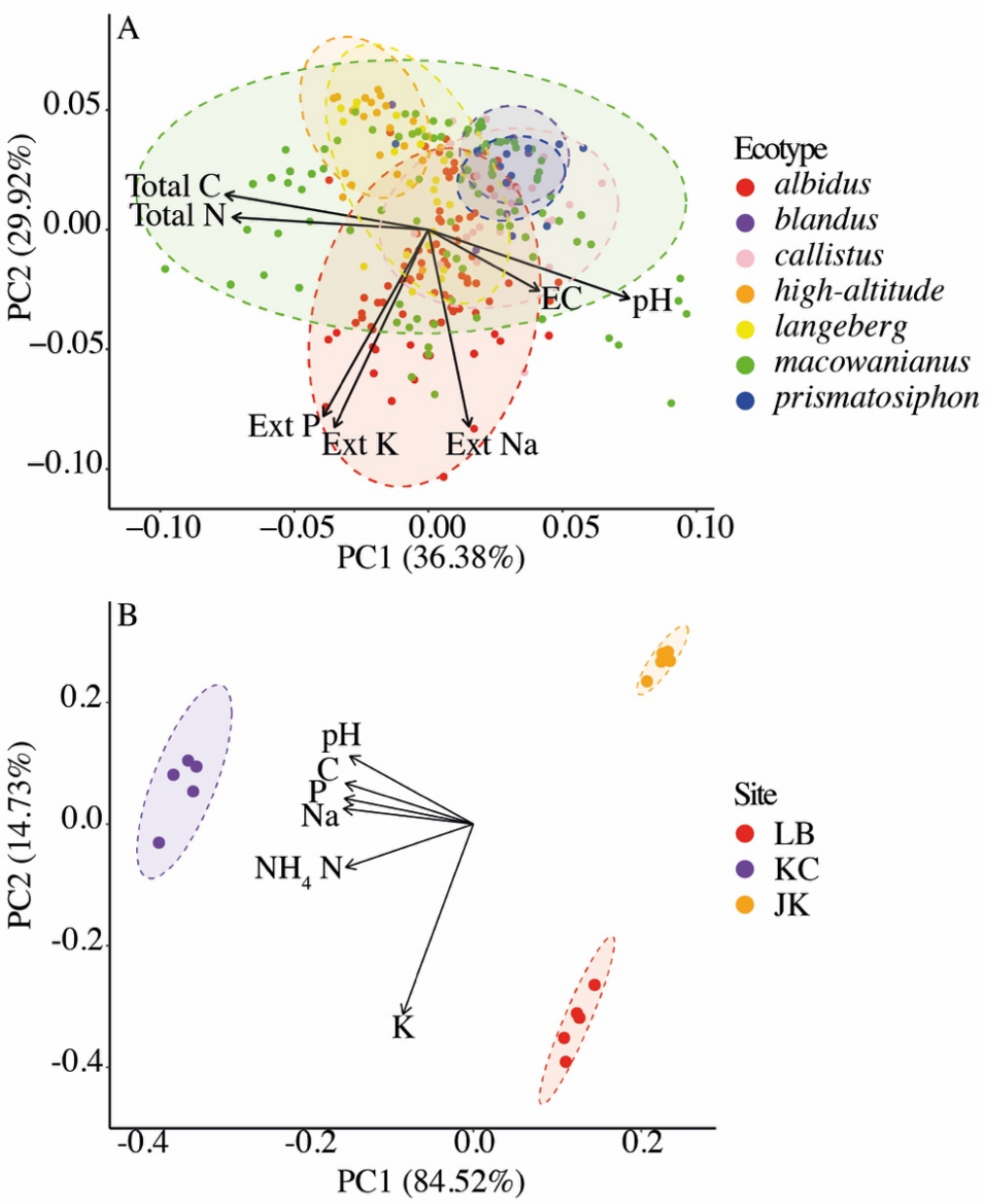

Figure 3.2. PCAs of the soil niches of the (A) *Gladiolus carneus* ecotypes, and (B) the three focal populations used in the common garden and reciprocal translocations. Both PCAs include 95% confidence ellipses and biplots of trait loadings. The variables included in the ecotypes' soil niche includes, electrical conductivity (mS/m), extractable potassium ($cmol^+/kg$), extractable sodium ($cmol^+/kg$), extractable phosphorus (mg/kg), pH, total carbon (%), and total nitrogen (%) extracted from Cramer *et al.* (2019). The variables used to test for differences between the populations' soil niche includes, potassium (mg/kg), sodium (mg/kg), phosphorus (mg/kg), pH, carbon (%), and NH_4 Nitrogen (%).

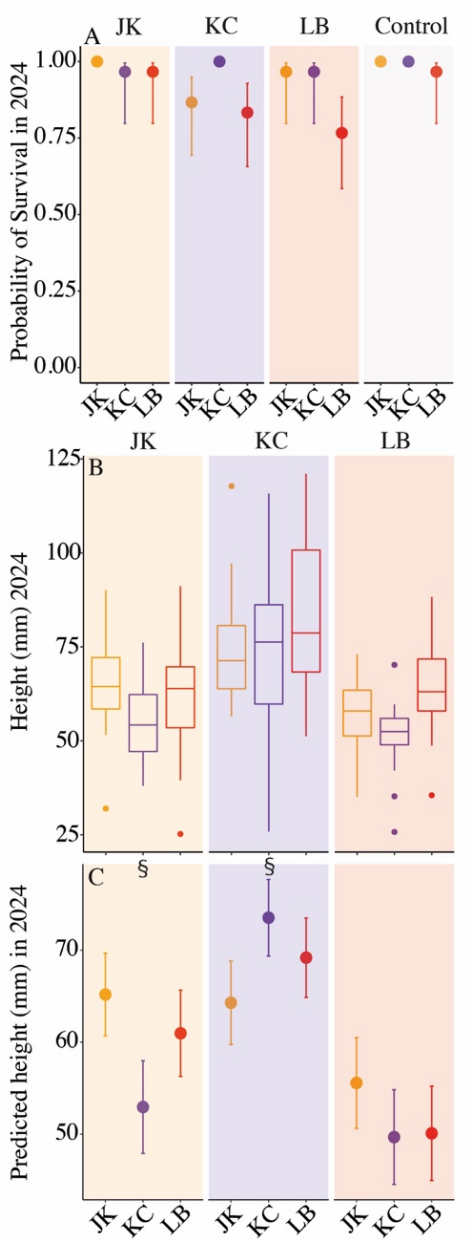

Figure 3.3. **Common garden:** (A) The probably of survival, (B) height (mm), and (C) the predicted height (mm) at the end of 2024 of the seedlings in the common garden. Jonaskop (JK), Kleinmond Coast (KC), and Limietberg (LB) seedlings were transplanted into JK, KC, LB, and control soil. The soil types are represented by the bands through the figure. In A, the round points represent the predicted probably of survival with asymmetric confidence intervals. In C, the round points represent the mean height and standard error as predicted by the aster analysis. The '§' indicates the native ecotype has a fitness advantage based on foreign vs local criteria for local adaptation.

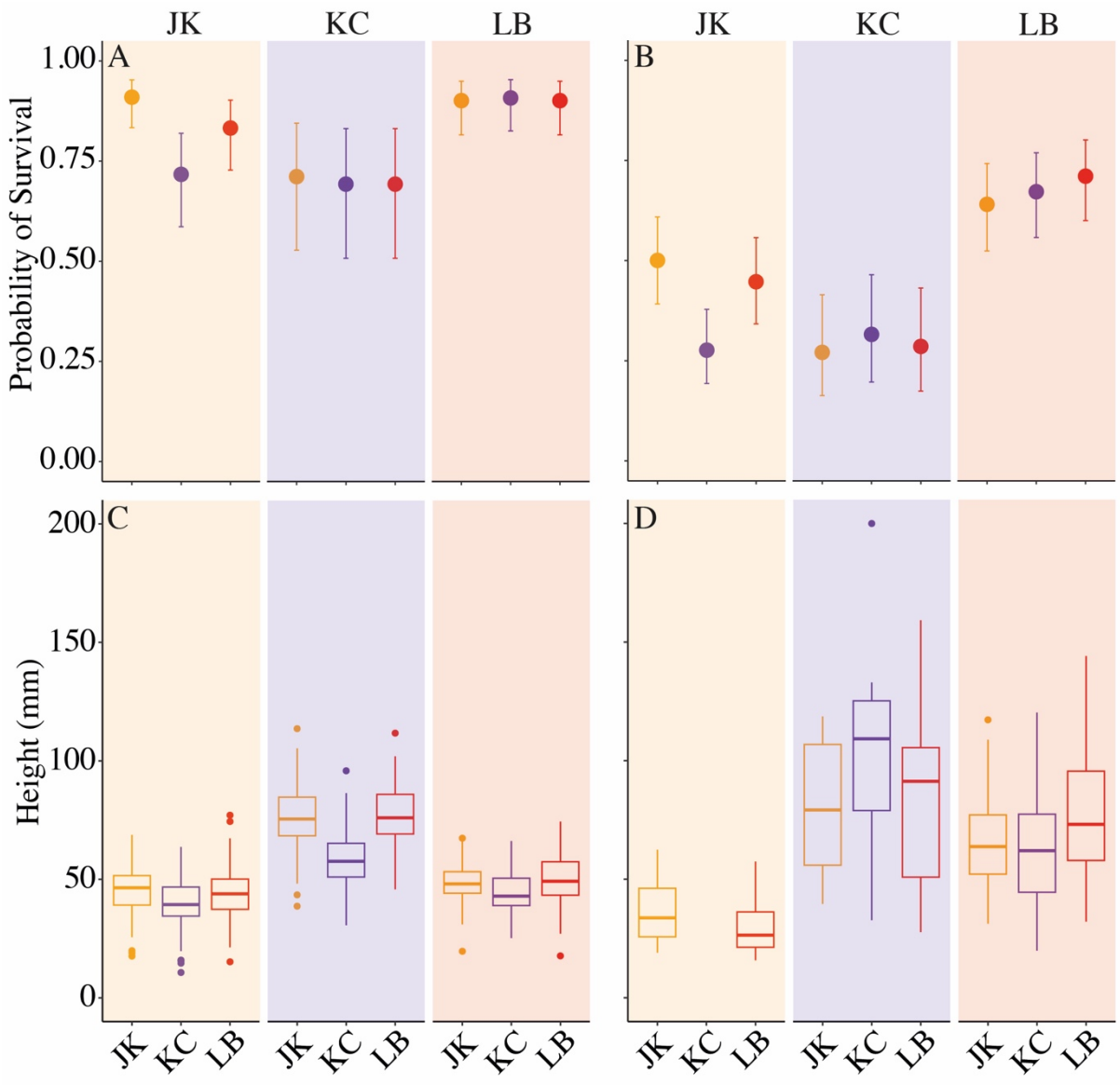

Figure 3.4. **Reciprocal translocation:** The probably of survival in (A) 2023 and (B) 2024, and height (mm) at the end of (C) 2023 and (D) 2024 between the three reciprocal translocation sites, Jonaskop (JK), Kleinmond Coast (KC), and Limietberg (LB). Generalized linear mixed models were used to model the effects of site, ecotype and their interaction on survival and height (mm) in 2023 and 2024. The sites are represented by the bands through the figure. The circles in A and B represent the predicted survival with asymmetric error bars.

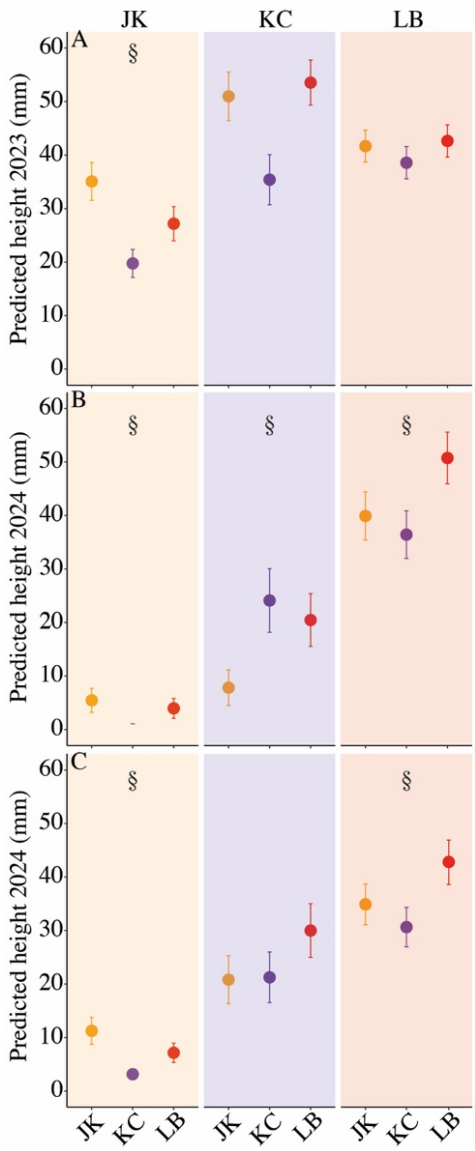

Figure 3.5. **Reciprocal translocation:** Predicted mean height (mm) of the (A) 2023 aster model, (B) the 2024 aster model and (C) the full 2023 and 2024 model. The 2023 and 2024 models only take into account the survival and height (mm) within their respective years. The full model takes into account survival and height in both years. All three models show the predicted height for ecotypes at the three reciprocal translocation sites, Jonaskop (JK), Kleinmond Coast (KC), and Limietberg (LM). The sites are represented by the bands through the figure. The circles represent the expected mean height with standard error. The '§' indicates the native ecotype has a fitness advantage based on foreign vs local criteria for local adaptation.

SUPPLEMENTARY MATERIALS

Table S3.1. Sample sizes for common garden experiments testing for differential fitness between Jonaskop (JK), Kleinmond Coast (KC), and Limietberg (LB) seedlings on each of their respective soils and a control soil.

		GLMM		aster
Soil type	**Ecotype**	**Survival 2024**	**Height 2024 (mm)**	
JK	JK	30	30	30
JK	KC	30	29	30
JK	LB	30	29	30
KC	JK	30	26	30
KC	KC	30	30	30
KC	LB	30	25	30
LB	JK	30	29	30
LB	KC	30	29	30
LB	LB	30	23	30
Control	JK	30	-	-
Control	KC	30	-	-
Control	LB	30	-	-

Table S3.2. Sample sizes for the reciprocal translocation experiments testing for differential fitness between Jonaskop (JK), Kleinmond Coast (KC), and Limietberg (LB) seedlings at each of their respective native sites.

		GLMM			aster
Site	**Ecotype**	**Survival 2023 & 2024**	**Height 2023 (mm)**	**Height 2024 (mm)**	
JK	JK	160	119	12	75
JK	KC	160	88	0	99
JK	LB	160	96	15	82
KC	JK	64	36	6	47
KC	KC	64	33	12	43
KC	LB	64	44	13	54
LB	JK	128	100	67	110
LB	KC	128	96	73	106
LB	LB	128	94	77	108

Table S3.3. The mean and standard error of soil layers from Cramer *et al.* (2019) for *Gladiolus carneus* ecotypes.

Ecotype	Electrical conductivity (mS/m)	Ext Potassium ($cmol^+/kg$)	Ext Sodium ($cmol^+/kg$)	Ext Phosphorus (mg/kg)	pH	Total Carbon (%)	Total Nitrogen (%)
albidus	11.93 ± 7.51	0.45 ± 0.18	0.28 ± 0.14	13.51 ± 5.61	4.57 ± 0.49	2.07 ± 0.80	0.18 ± 0.06
blandus	14.28 ± 8.55	0.09 ± 0.03	0.1 ± 0.06	3.48 ± 2.44	5.19 ± 0.55	1.18 ± 0.93	0.19 ± 0.04
callistus	22.67 ± 19.12	0.13 ± 0.09	0.23 ± 0.11	5.56 ± 2.82	5.02 ± 0.78	1.77 ± 0.80	0.19 ± 0.04
high-altitude	8.42 ± 1.78	0.1 ± 0.08	0.08 ± 0.04	4.74 ± 3.76	3.71 ± 0.31	4.76 ± 1.23	0.32 ± 0.11
langeberg	6.82 ± 1.52	0.18 ± 0.10	0.14 ± 0.07	5.80 ± 3.40	3.75 ± 0.32	2.25 ± 1.63	0.24 ± 0.10
macowanianus	17.47 ± 20.32	0.18 ± 0.14	0.18 ± 0.07	7.52 ± 5.38	4.44 ± 1.00	3.52 ± 2.13	0.35 ± 0.28
prismatosiphon	7.59 ± 2.36	0.14 ± 0.06	0.19 ± 0.07	0.50 ± 0.39	5.04 ± 0.85	1.14 ± 0.86	0.12 ± 0.06

Table S3.4. Pairwise comparisons between the *Gladiolus carneus* ecotypes soil properties. Significant pairings are highlighted in bold.

Comparison	EC (mS/m)	Ext Potassium ($cmol^+/kg$)	Ext Sodium ($cmol^+/kg$)	Ext Phosphorus (mg/kg)	pH	Total Carbon (%)	Total Nitrogen (%)
albidus – blandus	0.1061	**<0.0001**	**<0.0001**	**<0.0001**	**0.0073**	**<0.0001**	1.0000
albidus – callistus	**0.0001**	**<0.0001**	**<0.0001**	**<0.0001**	**0.0326**	0.3930	1.0000
albidus – high-altitude	0.0870	**<0.0001**	**<0.0001**	**<0.0001**	**<0.0001**	**<0.0001**	**<0.0001**
albidus – langeberg	**<0.0001**	**<0.0001**	**<0.0001**	**<0.0001**	**0.0002**	1.0000	**0.0497**
albidus – macowanianus	**0.0109**	**<0.0001**	**<0.0001**	**<0.0001**	0.5598	**<0.0001**	**<0.0001**
albidus – prismatosiphon	**0.0005**	**<0.0001**	0.0876	**<0.0001**	1.0000	**<0.0001**	**0.0164**
blandus – callistus	1.0000	1.0000	**<0.0001**	**0.0303**	**<0.0001**	**0.0043**	1.0000
blandus – high-altitude	**0.0008**	1.0000	1.0000	1.0000	**<0.0001**	**<0.0001**	**0.0221**
blandus – langeberg	**<0.0001**	**0.0169**	0.1135	0.1070	**<0.0001**	**0.0033**	1.0000
blandus – macowanianus	1.0000	**0.0216**	**<0.0001**	**<0.0001**	1.0000	**<0.0001**	0.4069
blandus – prismatosiphon	**<0.0001**	0.2758	**<0.0001**	0.0642	**<0.0001**	1.0000	**0.0104**
callistus – high-altitude	**<0.0001**	1.0000	**<0.0001**	0.9271	**<0.0001**	**<0.0001**	**0.0017**
callistus – langeberg	**<0.0001**	0.2683	**0.0007**	1.0000	**<0.0001**	1.0000	1.0000
callistus – macowanianus	0.0997	0.5099	0.0686	1.0000	1.0000	**<0.0001**	**0.0175**
callistus – prismatosiphon	**<0.0001**	1.0000	1.0000	**<0.0001**	1.0000	**0.0286**	**0.0038**
high-altitude – langeberg	0.3400	**0.0103**	**0.0038**	1.0000	1.0000	**<0.0001**	0.5813
high-altitude – macowanianus	**0.0002**	**0.0110**	**<0.0001**	**0.0131**	**<0.0001**	**0.0015**	0.3736
high-altitude – prismatosiphon	1.0000	0.2004	**<0.0001**	**0.0014**	**<0.0001**	**<0.0001**	**<0.0001**
langeberg – macowanianus	**<0.0001**	1.0000	0.0815	1.0000	**<0.0001**	**0.0006**	1.0000
langeberg – prismatosiphon	1.0000	1.0000	0.2197	**<0.0001**	**<0.0001**	**0.0179**	**0.0001**
macowanianus – prismatosiphon	**<0.0001**	1.0000	1.0000	**<0.0001**	**0.0013**	**0.0179**	**<0.0001**

Table S3.5. The mean and standard error of soil measurements taken at Jonaskop (JK), Kleinmond coast (KC), and Limietberg (LB).

Site	Potassium (mg/kg)	Sodium (mg/kg)	Phosphorus (mg/kg)	pH	Carbon (%)	NH_4 Nitrogen (%)
JK	28.00 ± 1.34	9.00 ± 0.63	13.60 ± 0.68	4.64 ± 0.02	0.71 ± 0.04	0.03 ± 0.01
KC	86.40 ± 2.93	283.60 ± 9.68	107.60 ± 5.07	5.52 ± 0.04	7.19 ± 0.21	0.41 ± 0.01
LB	95.20 ± 2.35	38.00 ± 3.26	18.60 ± 1.17	4.50 ± 0.00	0.62 ± 0.01	0.17 ± 0.01

Table S3.6. Pairwise comparisons between the soil measurements at Jonaskop (JK), Kleinmond coast (KC), and Limietberg (LB).

Comparisons	Potassium (mg/kg)	Sodium (mg/kg)	Phosphorus (mg/kg)	pH	Carbon (%)	NH_4 Nitrogen (%)
JK - KC	**<0.0001**	**0.0006**	**0.0006**	**<0.0001**	**0.0591**	**<0.0001**
JK - LB	**<0.0001**	0.1141	0.1320	**0.0071**	0.3409	**<0.0001**
KC - LB	0.058	0.1141	0.1048	**<0.0001**	**0.0016**	**<0.0001**

Table S3.7. Pairwise comparisons for the survival and height (mm) of Jonaskop (JK), Kleinmond Coast (KC), and Limietberg (LB) seedlings on each soil type. Soil type includes the native soil of all respective ecotypes and a control soil. The control soil was used to test whether any ecotypes were suffering from transplant shock, therefore, only the survival is presented. Significant differences are highlighted in bold.

Soil type	Ecotype comparison	Survival 2024	Height 2024 (mm)
JK	JK - KC	1.00	**0.0441**
JK	JK - LB	1.00	1.00
JK	KC - LB	1.00	0.31
KC	JK - KC	1.00	1.00
KC	JK - LB	1.00	1.00
KC	KC - LB	1.00	0.91
LB	JK - KC	1.00	1.00
LB	JK - LB	1.00	0.77
LB	KC - LB	1.00	**0.0009**
Control	JK - KC	1.00	-
Control	JK - LB	1.00	-
Control	KC - LB	1.00	-

Table S3.8. The survival rate (%) of all ecotypes at all translocation sites in 2023 and 2024. All survival rates presented are the percentage of seedlings that survived from the beginning of the experiment.

Site	Ecotype	Survival 2023 (%)	Survival 2024 (%)
JK	JK	89	50
JK	KC	70	29
JK	LB	81	45
KC	JK	77	33
KC	KC	75	38
KC	LB	75	34
LB	JK	88	61
LB	KC	88	64
LB	LB	88	68

Table S3.9. Pairwise comparisons between Jonaskop (JK), Kleinmond Coast (KC), and Limietberg (LB) seedlings at all the reciprocal translocation sites. Generalized linear mixed models were used to test for differences in survival and height at the end of 2023 and 2024.

Site	Ecotype comparison	Survival 2023	Survival 2024	Height 2023 (mm)	Height 2024 (mm)
JK	JK – KC	**0.0007**	**0.0028**	**0.0006**	1.0000
JK	JK – LB	1.0000	1.0000	1.0000	1.0000
JK	KC – LB	0.5551	0.0760	**0.0221**	1.0000
KC	JK – KC	1.0000	1.0000	**< 0.0001**	1.0000
KC	JK – LB	1.0000	1.0000	1.0000	1.0000
KC	KC – LB	1.0000	1.0000	**< 0.0001**	0.0929
LB	JK – KC	1.0000	1.0000	0.1731	1.0000
LB	JK – LB	1.0000	1.0000	1.0000	0.3629
LB	KC – LB	1.0000	1.0000	**0.0170**	**0.0033**

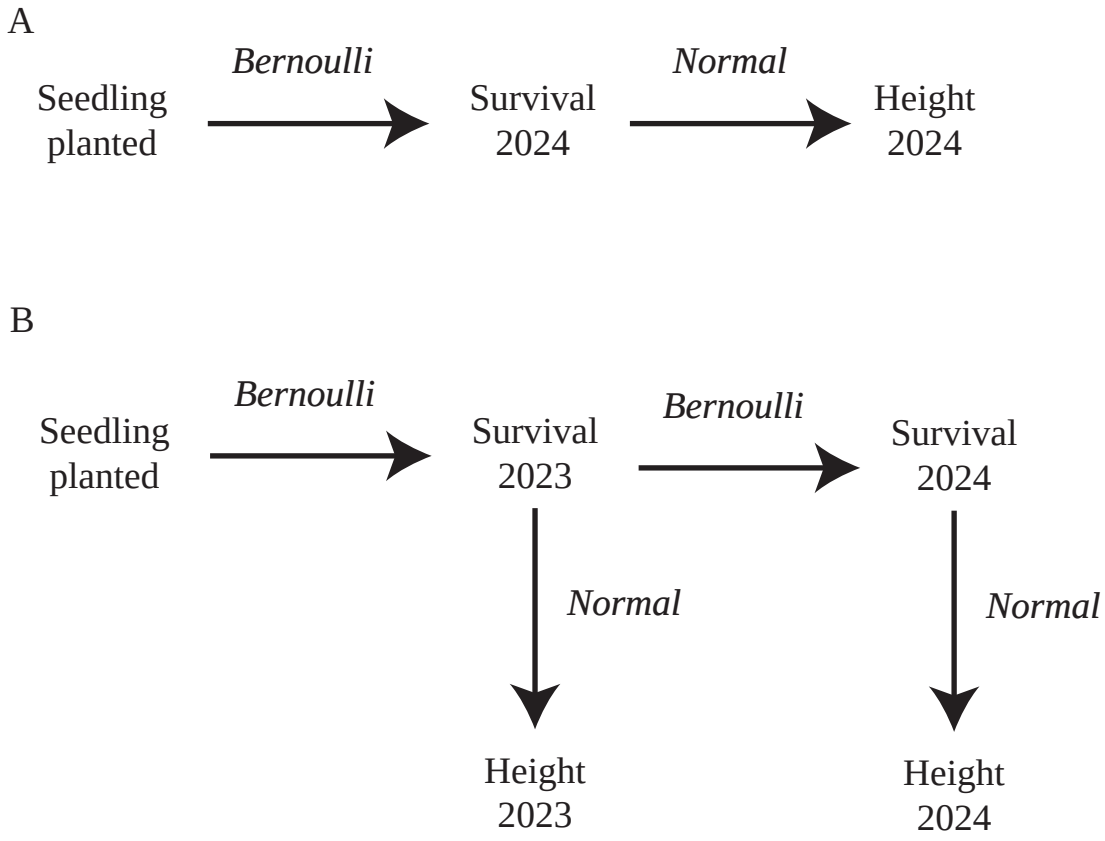

Figure S3.1. Aster model dependency structure used in the (A) common garden and (B) full 2023 and 2024 reciprocal translocation.

CHAPTER 4:

The role of niche differentiation and local adaptation in driving incipient speciation in the Cape Floristic Region

THESIS OVERVIEW

In this thesis, I used the *Gladiolus carneus* species complex as a model system to better understand how ecological shifts mediate speciation events in the Cape Floristic Region (CFR). In Chapter 2, I demonstrated that in the *G. carneus* species complex, phenotypic shifts often accompany ecological shifts, and that those shifts, particularly abiotic niche shifts, were ubiquitous across the species complex. These shifts in ecology, apart from a few exceptions, resulted in near complete premating reproductive isolation within the species complex. In Chapter 3, I showed that different ecotypes of *G. carneus* occupying the most divergent soil niches were locally adapted to their edaphic niche. I further found that the ecotypes were locally adapted to their abiotic niche across an elevational gradient. Overall, I found that ecological shifts, in particular those that were abiotic in nature, frequently lead to local adaptation and strong premating reproductive isolation in the *G. carneus* species complex.

THE ROLE OF ECOLOGICAL SHIFTS IN DRIVING THE DIVERSIFICATION OF THE *GLADIOLUS CARNEUS* SPECIES COMPLEX

Abiotic niche shifts

Within the CFR, population genetic (Prunier *et al.*, 2017), phylogenetic (van der Niet and Johnson, 2009, Bouchenak-Khelladi and Linder, 2017), and trait-by-environment associations (Carlson *et al.*, 2011, Mitchell *et al.*, 2015, Carlson *et al.*, 2016) have provided evidence of frequent abiotic niche shifts between closely related taxa. However, there are only a few examples that comprehensively test whether abiotic niche shifts result in local adaptation or reproductive isolation (Latimer *et al.*, 2009, Newman and Johnson, 2024). I found evidence that all seven *G. carneus* ecotypes occupied distinct abiotic niches which resulted in strong

ecogeographic isolation. Using reciprocal translocations, I found further evidence that the three *G. carneus* populations representing distinct ecotypes were locally adapted to their abiotic niche. These results indicate that habitat shifts, as quantified by the species distribution models (SDMs), are potentially indicative of local adaptation and reproductive isolation between ecotypes. The combination of niche modelling and reciprocal translocations provides comprehensive evidence that abiotic shifts are playing an important role in driving the diversification of the species complex.

Edaphic shifts

Despite the CFR having a suite of heterogenous edaphic niches (Cramer *et al.*, 2014), the extent to which they drive the diversification of plant linages has been questioned (Ellis *et al.*, 2014). This is mainly due to edaphic conditions imposing ecological filters, restricting some plant linages to only a single soil type, and reducing the scope for edaphically-driven ecological speciation (Linder, 2003, Verboom *et al.*, 2017). Additionally, the frequency of edaphic shifts among lineages is variable and have been documented as either the most (Schnitzler *et al.*, 2011) or least frequent ecological shift (van der Niet and Johnson, 2009, Forest *et al.*, 2014) between sister taxa in the CFR. In contrast to the previous literature, my results indicated that there have been frequent edaphic shifts in the *G. carneus* species complex. I further isolated the contribution of edaphic conditions to local adaptation using a common garden experiment and found that the ecotypes occupying edaphic niches with the most extreme nutrient compositions, have a fitness advantage on their native soils. These results contribute to the current evidence that edaphic shifts can cause local adaptation and likely mediates the diversification of plant lineages in the CFR. Furthermore, these findings provide comprehensive evidence that edaphic shifts contribute to the diversification of the Blandus series in *Gladiolus,* and possibly the broader Iridaceae occurring in the CFR, the diversification

of which has often been attributed to frequent pollinator rather than edaphic shifts (Manning and Goldblatt, 2005, Valente *et al.*, 2012, Forest *et al.*, 2014).

Phenological shifts

In Chapter 2, I found that there were frequent phenological shifts between the *G. carneus* ecotypes leading to moderate phenological isolation. I specifically documented whether there were broad-scale differences in the flowering phenology between the ecotypes, however, in ecotypes with long flowering times, such as *macowanianus*, there are likely to be further population-level differences that may lead to stronger phenological isolation between populations. In other lineages in the CFR, phenological shifts have been frequently documented (van der Niet and Johnson, 2009, Linder, 2020) and are important in preventing gene flow (Ellis *et al.*, 2014). As phenological shifts have been shown to be under selection by both biotic and abiotic factors (Elzinga *et al.*, 2007, Munguia-Rosas *et al.*, 2011), it is challenging to associate phenological shifts with any single driver in the CFR. Rather, phenological shifts may be frequent due to selection by heterogenous biotic as well as abiotic factors.

Pollinator shifts

Despite pollinator shifts being frequently documented across lineages in the CFR (Schnitzler *et al.*, 2011), and specifically within the Iridaceae (Manning and Goldblatt, 2005, Forest *et al.*, 2014) and *Gladioli* (Valente et al., 2012), I found little evidence of pollinator shifts between ecotypes in the *G. carneus* species complex. I rather found that *G. carneus* populations were associated with a single highly effective pollinator, and that floral and pollinator morphology were highly correlated at the population level. This set of results suggests that although pollinators are likely not driving ecotypic divergence, they are likely driving population-level divergence within the species complex. This population level diversity has been documented

in other species in the CFR such as *Nerine humilis*, *Tritoniopsis revoluta*, *Erica junonia* and *Erica plukenetii* (Anderson *et al.*, 2014, Van der Niet *et al.*, 2014, Newman *et al.*, 2015, Newman and Johnson, 2021), but has rarely been linked to local adaptation (*but see* Newman *et al.*, 2015) or reproductive isolation.

CONCLUSION

This thesis provides comprehensive evidence that niche differentiation, and particularly abiotic factors, causes local adaptation and strong premating reproductive isolation in the *Gladiolus carneus* species complex. I have also provided the first comprehensive evidence of local adaptation to edaphic niches in the CFR. Overall, I found that ecological heterogeneity likely plays a large role in the early stages of divergence between taxa in the CFR. However, further research is needed to document ecologically-driven population level divergence caused by biotic, abiotic and interacting factors below the ecotypic level in this system. This population level divergence should be documented along ecological gradients (Wadgymar *et al.*, 2017) using a variety of techniques including measuring phenotypic selection, local adaptation, genetic divergence and reproductive isolation. Furthermore, these techniques should be used to explore how multifarious selection mediates divergence in highly heterogenous environments such as the CFR (Wadgymar *et al.*, 2022).

LITERATURE CITED

Anderson B, Ros P, Wiese TJ, Ellis AG. 2014. Intraspecific divergence and convergence of floral tube length in specialized pollination interactions. *Proceedings of the Royal Society B: Biological Sciences,* **281**: 20141420.

Bouchenak-Khelladi Y, Linder HP. 2017. Frequent and parallel habitat transitions as driver of unbounded radiations in the Cape flora. *Evolution,* **71**: 2548-2561.

Carlson JE, Adams CA, Holsinger KE. 2016. Intraspecific variation in stomatal traits, leaf traits and physiology reflects adaptation along aridity gradients in a South African shrub. *Annals of Botany,* **117**: 195-207.

Carlson JE, Holsinger KE, Prunier R. 2011. Plant responses to climate in the Cape Floristic Region of South Africa: evidence for adaptive differentiation in the Proteaceae. *Evolution,* **65**: 108-124.

Cramer MD, West AG, Power SC, Skelton R, Stock WD. 2014. Plant ecophysiological diversity. In: Allsopp N, Colville JF, Verboom GA, eds. *Fynbos: ecology, evolution and conservation of a megadiverse region.* Oxford: Oxford University Press.

Ellis AG, Verboom GA, van der Niet T, Johnson SD, Linder HP. 2014. Speciation and extinction in the greater Cape Floristic Region. In: Allsopp N, Colville JF, Verboom GA, eds. *Fynbos: ecology, evolution and conservation of a megadiverse region.* Oxford: Oxford University Press.

Elzinga JA, Atlan A, Biere A, Gigord L, Weis AE, Bernasconi G. 2007. Time after time: flowering phenology and biotic interactions. *Trends in Ecology & Evolution,* **22**: 432-439.

Forest F, Goldblatt P, Manning JC, *et al.* 2014. Pollinator shifts as triggers of speciation in painted petal irises (*Lapeirousia*: Iridaceae). *Annals of Botany,* **113**: 357-371.

Latimer AM, Silander Jr. JA, Rebelo AG, Midgley GF. 2009. Experimental biogeography: the role of environmental gradients in high geographic diversity in Cape Proteaceae. *Oecologia,* **160**: 151-162.

Linder HP. 2003. The radiation of the Cape flora, southern Africa. *Biological Reviews,* **78**: 597–638.

Linder HP. 2020. The evolution of flowering phenology: an example from the wind-pollinated African Restionaceae. *Annals of Botany*, **126**: 1141-1153.

Manning JC, Goldblatt P. 2005. Radiation of pollination systems in the Cape genus *Tritoniopsis* (Iridaceae: Crocoideae) and the development of bimodal pollination strategies. *International Journal of Plant Sciences*, **166**: 459-474.

Mitchell N, Moore TE, Mollmann HK, *et al.* 2015. Functional traits in parallel evolutionary radiations and trait-environment associations in the Cape Floristic Region of South Africa. *The American Naturalist*, **185**: 525-537.

Munguia-Rosas MA, Ollerton J, Parra-Tabla V, De-Nova JA. 2011. Meta-analysis of phenotypic selection on flowering phenology suggests that early flowering plants are favoured. *Ecology Letters*, **14**: 511-521.

Newman E, Johnson SD. 2021. A shift in long-proboscid fly pollinators and floral tube length among populations of *Erica junonia* (Ericaceae). *South African Journal of Botany*, **142**: 451-458.

Newman E, Johnson SD. 2024. Pollinator-mediated isolation promotes coexistence of closely related food-deceptive orchids. *Journal of Evolutionary Biology*, **38**: 190-201.

Newman E, Manning J, Anderson B. 2015. Local adaptation: mechanical fit between floral ecotypes of *Nerine humilis* (Amaryllidaceae) and pollinator communities. *Evolution*, **69**: 2262-2275.

Prunier R, Akman M, Kremer CT, *et al.* 2017. Isolation by distance and isolation by environment contribute to population differentiation in *Protea repens* (Proteaceae L.), a widespread South African species. *American Journal of Botany*, **104**: 674-684.

Schnitzler J, Barraclough TG, Boatwright JS, *et al.* 2011. Causes of plant diversification in the Cape biodiversity hotspot of South Africa. *Systematic Biology*, **60**: 343-357.

Valente LM, Manning JC, Goldblatt P, Vargas P. 2012. Did pollination shifts drive diversification in southern African *Gladiolus*? Evaluating the model of pollinator-driven speciation. *The American Naturalist,* **180**: 83-98.

van der Niet T, Johnson SD. 2009. Patterns of plant speciation in the Cape Floristic Region. *Molecular Phylogenetics and Evolution,* **51**: 85-93.

Van der Niet T, Pirie MD, Shuttleworth A, Johnson SD, Midgley JJ. 2014. Do pollinator distributions underlie the evolution of pollination ecotypes in the Cape shrub *Erica plukenetii*? *Annals of Botany,* **113**: 301-315.

Verboom GA, Stock WD, Cramer MD. 2017. Specialization to extremely low-nutrient soils limits the nutritional adaptability of plant lineages. *The American Naturalist,* **189**: 684-699.

Wadgymar SM, DeMarche ML, Josephs EB, Sheth SN, Anderson JT. 2022. Local adaptation: Causal agents of selection and adaptive trait divergence. *Annual Review of Ecology, Evolution, and Systematics,* **53**: 87-111.

Wadgymar SM, Lowry DB, Gould BA, *et al.* 2017. Identifying targets and agents of selection: innovative methods to evaluate the processes that contribute to local adaptation. *Methods in Ecology and Evolution,* **8**: 738-749.